



POLITECHNIKA POZNAŃSKA



Wydział Inżynierii Materiałowej i Fizyki Technicznej  
Instytut Fizyki  
Zakład Fizyki Molekularnej

**Damian Łukawski**

*Modyfikacja właściwości fizykochemicznych drewna, bawełny  
i ich pochodnych za pomocą nanomateriałów węglowych*

---

Rozprawa doktorska

Promotor

prof. dr hab. Alina Dudkowiak

Promotor pomocniczy

dr inż. Agnieszka Łękawa-Raus

POZNAŃ 2020

Badania zostały sfinansowane w latach 2016-2019 ze środków Narodowego Centrum Nauki, projekt PRELUDIUM 2015/19/N/ST8/02184, pt. „*Preparatyka i charakteryzacja właściwości pokryć nanorurek węglowych na powierzchni drewna*”.



NATIONAL SCIENCE CENTRE  
POLAND

## PODZIĘKOWANIA

---

*Serdecznie dziękuję mojemu Promotorowi  
Pani prof. Alinie Dudkowiak oraz  
Promotorowi pomocniczemu Pani dr inż.  
Agnieszce Łękawie-Raus za cenne pomysły  
oraz wszystkie uwagi i wskazówki, bez  
których ta praca by nie powstała.*

*Dziękuję również pracownikom i  
doktorantom Zakładu Fizyki Molekularnej  
za miłą atmosferę i godziny dyskusji na  
tematy naukowe i nie tylko.*

*Dziękuję także wszystkim osobom, z którymi  
miałem okazję współpracować podczas  
prowadzonych badań.*

## PODZIĘKOWANIA

---

*Szczególne dziękuję rodzicom, Mariuszowi i Beacie oraz narzeczonej Sonii za bezustanne wsparcie podczas całej mojej dotychczasowej kariery naukowej.*

## Spis skrótów i oznaczeń

- CNM – nanomateriały węglowe (ang. *carbon nanomaterials*)
- CNT – nanorurki węglowe (ang. *carbon nanotubes*)
- CNT/PMMA – pokrycie zawierające nanorurki węglowe w matrycy PMMA
- CNT/SDBS – pokrycie zawierające nanorurki węglowe stabilizowane SDBS
- DB acetate – octan eteru monobutylowego glikolu dietylenowego (ang. *diethylene glycol monobutyl ether acetate*)
- EDS – spektrometria dyspersji energii promieniowania rentgenowskiego (ang. *energy-dispersive X-ray spectroscopy*)
- GO – tlenek grafenu (ang. *graphene oxide*)
- Gr – grafen płatkowy (ang. *graphene flakes*)
- GNP – nanopłytki grafenu (ang. *graphene nanoplatelets*)
- HDF – płyta pilśniowa wysokiej gęstości z włókien drzewnych (ang. *high density fiberboard*)
- LSM – skanujący laserowy mikroskop konfokalny (ang. *laser scanning microscope*)
- MDF – płyta pilśniowa średniej gęstości z włókien drzewnych (ang. *medium density fiberboard*)
- MWCNT – wielościenne CNT (ang. *multi-walled carbon nanotubes*)
- OSB – płyta o wiórach orientowanych (ang. *oriented strand board*)
- PHRR – maksymalna szybkość wydzielania ciepła (ang. *peak heat release rate*)
- PMMA – polimetakrylan metylu (ang. *poly(methyl methacrylate)*)
- R – rezystancja elektryczna
- rGO – zredukowany tlenek grafenu (ang. *reduced graphene oxide*)
- SC – zdolność sorpcyjna (ang. *sorption capacity*)
- SDBS – dodecylobenzenosulfonian sodu (ang. *sodiumdodecylbenzenesulphonate*)
- SEM – skaningowa mikroskopia elektronowa (ang. *scanning electron microscopy*)
- T – temperatura
- WPC – kompozyt polimerowo-drzewny (ang. *wood plastic composite*)
- WSA – kąt rozprysku wody (ang. *water shedding angle*)

## Spis treści

Streszczenie .....	7
Abstract.....	9
1. Wstęp.....	11
2. Forma pracy doktorskiej oraz wkład doktoranta .....	14
3. Badane materiały oraz techniki badawcze .....	16
3.1. Materiały .....	16
3.2. Charakteryzacja powierzchni .....	17
3.3. Badania zwilżalności i zdolności sorpcyjnej.....	17
3.4. Badania palności i właściwości mechanicznych.....	18
3.5. Badania elektryczne i elektrotermiczne .....	18
4. Krótki opis badań zawartych w rozprawie doktorskiej .....	20
5. Podsumowanie i wnioski .....	28
Literatura .....	30
Spis norm.....	34
Dorobek naukowy .....	35
Załączniki.....	39
Przedruk publikacji [Łukawski, POC 2018] .....	48
Przedruk opisu patentowego [Łukawski, UPRP 2017] .....	70
Przedruk publikacji [Łukawski, FiP 2018] .....	78
Przedruk publikacji [Łukawski, Drewno 2019] .....	91
Przedruk publikacji [Łukawski, POC 2018] .....	104

## Streszczenie

Prezentowana rozprawa doktorska opisuje wyniki prac badawczych nad modyfikacją właściwości fizykochemicznych drewna, materiałów drewnopochodnych i pokrewnych materiałów celulozowych, pokrywanych nanomateriałami węglowymi (ang. *carbon nanomaterials* – CNM). Przeprowadzone badania miały na celu określenie możliwości zastosowania takich pokryć: (i) do wytworzenia powłok i sączków hydrofobowych lub (ii) wykorzystania jako uniepalniacze oraz (iii) w nowych obszarach badawczo-rozwojowych na przykład jako zintegrowanych z drewnem elementów grzewczych i czujników. Uzyskane wyniki zostały szczegółowo opisane w czterech artykułach naukowych z listy Journal Citation Reports (JCR) oraz patencie.

W pierwszym etapie badań wykonano dwa rodzaje pokryć CNM na powierzchni drewna, stosując zawiesiny CNM w związku organicznym oraz w wodzie z dodatkiem surfaktantu. Na podstawie obrazów uzyskanych za pomocą mikroskopów fluorescencyjnego i elektronowego oraz pomiarów kąta zwilżania, potwierdzono możliwość wytworzenia jednorodnego pokrycia drewna za pomocą CNM i uzyskania powierzchni o właściwościach hydrofobowych. Wykonując badania dla różnych gatunków drewna pokazano, że hydrofobizację powierzchni drewna uzyskuje się niezależnie od jego gatunku, chropowatości i składu chemicznego. Jednocześnie zauważono, że pomimo wysokiej wartości kąta zwilżania (przekraczającej  $130^\circ$ ), kropla wody wykazuje silną adhezję do powierzchni drewna pokrytego CNM. Otrzymane wyniki umożliwiły zaproponowanie modelu zwilżalności drewna bazującego na modelu „płatka róży”.

Opracowane metody nanoszenia CNM wykorzystano następnie do hydrofobizacji włókien i wiórów drzewnych, bawełny i innych materiałów celulozowych. Dla uzyskanych w ten sposób materiałów określono zdolność sorpcyjną i zaproponowano zastosowanie ich jako hydrofobowych sączków do usuwania substancji oleistych (i innych związków organicznych) z powierzchni wody.

Badając palność wiórów drzewnych pokrytych CNM, stwierdzono nieznaczne obniżenie szybkości ubytku ich masy. Może być to spowodowane przyspieszeniem wytwarzania warstwy zwęglonej drewna poprzez obecność CNM. Dodatkowo pokazano, że wytworzenie płyty z wiórów zmodyfikowanych CNM, nie wpływa na zmianę jej parametrów mechanicznych.

Ponadto, wyznaczono przewodność elektryczną warstw CNM wytworzonych na drewnie i zbadano jej zależność od czynników zewnętrznych. Na podstawie otrzymanych wyników pokazano, że w zależności od wyboru odpowiednich modyfikatorów, uzyskana warstwa CNM na powierzchni drewna może być wykorzystana jako czujnik zalania wodą lub temperatury. Przedstawiono również rozwiązanie pozwalające na wytworzenie czujnika siły nacisku. Wykazano, że pod wpływem przepływającego prądu możliwy jest znaczący wzrost temperatury warstw CNM oraz przeanalizowano proces transferu ciepła pomiędzy nimi a materiałami drewnopochodnymi. W konsekwencji, zaproponowano wykorzystanie warstw CNM jako elementów grzewczych, mogących znaleźć zastosowanie w ogrzewaniu podłogowym lub osuszaniu drewna.

## Abstract

The following dissertation describes the influence of coating of wood, cotton and related materials with carbon nanomaterials (CNM), on physicochemical properties of the based materials. The focus of research was to determine the possibility of using CNM layers: (i) as a hydrophobic coatings and hydrophobic sorbents, (ii) as flame-retardant agents, and (iii) in the new research and development areas e.g., as electrical components integrated with wood, such as heaters or sensors. The results were described in detail in four scientific articles published in journals listed in the Journal Citation Reports (JCR), and in one patent specification.

In the first phase of the research, two methods of the formation of CNM coatings on wood were used. CNM were dispersed in an organic solvent as well as in aqueous solutions with the addition of surfactant. Analysing images obtained by means of fluorescence and electron microscopy, it has been shown that CNM may form a uniform thin film on the surface of wood. The results of water contact angle measurements proved also that this coating is hydrophobic. Experiments performed on various types of wood showed that the hydrophobic properties are present regardless of species, roughness, or chemical composition of wood. Although wood coated with CNM showed a very high value of water contact angle (exceeding  $130^\circ$ ) the droplet of water showed also significant adhesion to the surface. Those results led to the development of a wetting model based on the 'rose petal effect'.

The developed methods of coating were also used for hydrophobization of wood fibers, wood chips, and other cellulose-based fibrous materials. Sorption capacity of the obtained materials was estimated and their application as hydrophobic sorbents used for removal of oil spills from the surface of water was proposed.

The investigation on the flammability of CNM coated wood chips showed a decrease in the speed of their decomposition after the application of CNM coating. This phenomenon may be attributed to the accelerated char generation. Additionally, it was shown that it is possible to form chipboard out of CNM coated wood chips without impeding its mechanical performance.

Finally, the electrical conductivity of CNM coating on wood and its dependence on external factors was investigated. Based on the obtained results, it was shown that with the use of CNM modifiers selected for particular purpose, it is possible to prepare flood and temperature sensors integrated with the surface of the wood. Additionally, a design

of composite pressure sensor was proposed. Next, it was demonstrated that the electroconductive CNM coating on wood may be used as heater, which may be further applied as a floor heater or a wood drying element. Finally, the heat transfer between CNM heaters and wood-based materials was investigated.

## 1. Wstęp

Drewno będące naturalnym, tanim i łatwo dostępnym materiałem wykorzystywane jest jako główny surowiec do produkcji mebli oraz jako jeden z najpopularniejszych materiałów konstrukcyjnych. Analizy przeprowadzone przez Pajchrowskiego i innych [1] wykazały, że zastosowanie drewna zamiast innych materiałów budowlanych powoduje poprawę bilansu dwutlenku węgla w atmosferze oraz wpływa na zmniejszenie ilości odpadów i obniża zużycie energii. Jednocześnie ekologiczne walory tego materiału sprawiły, że w ostatnich latach wzrosło zainteresowanie innowacyjnymi rozwiązaniami w zakresie technologii drewna, w tym kompozytami polimerowo-drzewnymi (ang. *wood plastic composite* – WPC) [2], elastycznym drewnem [3] czy przezroczystym drewnem [4].

Interesującym materiałem jest także lignoceluloza będąca produktem odpadowym między innymi w procesie przetwórstwa drewna. Główną frakcją tego produktu jest celuloza – składnik budulcowy drewna oraz włókien naturalnych np. lnu, juty czy bawełny. Jest również najpopularniejszym biopolimerem wykorzystywanym w przemyśle (m. in. tekstylnym, papierniczym, budowlanym) oraz potencjalnym kandydatem do wielu nowych zastosowań, np. w czujnikach, systemach oczyszczania wody, aerożelach i innych [5–7].

Pomimo wielu zalet, drewno i materiały celulozowe posiadają kilka istotnych wad, ograniczających niektóre możliwości ich wykorzystania. Materiały te są łatwopalne, hydrofilowe oraz higroskopijne, a także podatne na czynniki biologiczne i promieniowanie UV. Koncepcja zaproponowana w rozprawie doktorskiej dotyczy możliwego połączenia odpowiednich walorów drewna i materiałów drewnopochodnych oraz nanomateriałów węglowych (ang. *carbon nanomaterials* – CNM), takich jak nanorurki węglowe (ang. *carbon nanotubes* – CNT), tlenek grafenu (ang. *graphene oxide* – GO), grafen płatkowy (Gr) i nanopłytki grafenu (ang. *graphene nanoplatelets* – GNP). CNT i materiały grafenowe są obiektem zainteresowania jako składniki wielofunkcyjnych pokryć i kompozytów [8–10], ze względu na ich niezwykle właściwości: przewodnictwo elektryczne [11,12], wytrzymałość mechaniczną [13], aktywność chemiczną [14], stabilność termiczną [15], superhydrofobowość [16]. Dzięki rozwojowi i optymalizacji metod syntezy, CNM mogą być produkowane na skalę przemysłową, w tym w ekologiczny sposób, wykorzystując np. gazy cieplarniane, takie jak metan [17–19]. Dostępność CNM oraz ich właściwości sprawiają, że są one

interesujące z punktu widzenia wykorzystania ich w badaniach nad ochroną drewna i materiałów drewnopochodnych, a jednocześnie rozwijania ich nowych zastosowań. Odpowiednia modyfikacja powierzchni drewna i jego pochodnych, z wykorzystaniem CNM, może nie tylko zniwelować ograniczenia ich wykorzystania, ale wprowadzić dodatkowe elektrycznie aktywne elementy (np. grzałki lub czujniki), otwierając zupełnie nowe możliwości aplikacyjne.

Pierwszym istotnym problemem ograniczającym funkcjonalność drewna, podjętym w niniejszej rozprawie, jest jego hydrofilowość. Zwilżenie drewna powoduje jego nasiąknięcie wodą, a w konsekwencji pęcznienie (wzrost objętości) i znaczące pogorszenie jego parametrów mechanicznych [20]. Ponadto, może sprzyjać rozwojowi pleśni i grzybów [21]. Lau i in. [22] wykazali, że pokrycie z pionowo ułożonych CNT wykazuje właściwości superhydrofobowe, dzięki odpowiedniej nanostrukturze i niskiej energii powierzchniowej. Stwarza to możliwości wykorzystania ich jako materiałów hydrofobizujących. Dotychczas opisano sposób hydrofobizacji powierzchni metali [23], polimerów [24] i tekstyliów [25,26] poprzez pokrycie ich CNT lub Gr. Natomiast, pokryte zredukowanym tlenkiem grafenu (rGO) aerożele i sączi bawełniane okazały się bardzo interesującymi hydrofobowymi absorbentami do wykorzystania np. przy usuwaniu oceanicznych rozlewów ropy [27–29]. Jednakże, do tej pory nie przeprowadzono badań wskazujących na możliwość wykorzystania CNM jako środka hydrofobizującego drewno i materiały drewnopochodne.

CNM mogą być potencjalnie wykorzystane do obniżenia palności materiałów, np. kompozytów polimerowych poprzez domieszkowanie ich GNP lub GO [30]. Efekt ten został także zaobserwowany i opisany przez Kashiwagi i in. [31] dla polimerów domieszkowanych CNT. Spalanie jest procesem dynamicznym zależnym od wielu czynników, dlatego nie można wskazać jednoznacznie w jaki sposób CNM wpływają na zwiększenia zdolności uniepalniających materiału. Najbardziej prawdopodobnym wyjaśnieniem jest przyspieszenie wytworzenia oraz wzmacnianie warstwy zwęglonej (naturalnie ograniczającej proces spalania), zwiększenie transferu ciepła czy tworzenie bariery dla łatwopalnych lotnych związków organicznych, wydzielanych podczas pirolizy polimerów [31,32]. Farsheh i in. [33] pokazali, że domieszkowanie polipropylenu GO powoduje obniżenie palności kompozytu WPC (polipropylenu z mączką drzewną). Wyniki te były inspiracją do przeprowadzenia badań dotyczących wpływu pokrycia drewna CNM na jego palność.

Wysokie przewodnictwo elektryczne oraz aktywność chemiczna CNT, pochodnych grafenu, w tym GNP lub Gr, stwarzają ciekawą perspektywę ich zastosowania. Pokazano, że możliwe jest wykorzystanie CNM, m. in. do wytwarzania elementów grzewczych [34,35], czujników [36–38] czy powierzchni antystatycznych [39]. Dotychczas, w literaturze nie opisano jednak możliwości wytwarzania aktywnych pokryć z CNM na powierzchni drewna. Na podstawie wyników badań przeprowadzonych w ramach rozprawy doktorskiej, po raz pierwszy zaproponowano wykorzystanie elektrycznie przewodzących warstw CNM do uzyskania warstw aktywnych, w tym elementów grzewczych i wielofunkcyjnych czujników zintegrowanych z drewnem.

W badaniach prowadzonych w ramach niniejszej rozprawy doktorskiej określono wpływ pokrycia CNM na zmianę właściwości fizykochemicznych drewna, bawełny i ich pochodnych. Przeprowadzone badania pozwoliły na pokazanie możliwości wykorzystania niezwykłych właściwości CNM, takich jak hydrofobowość, stabilność termiczna, wysokie przewodnictwo elektryczne i aktywność chemiczna, w odniesieniu do materiałów drewnopochodnych, w ich praktycznych i codziennych zastosowaniach oraz w technologii drewna. Proponowane rozwiązania mogą nie tylko zniwelować podstawowe problemy technologiczne, jakimi są łatwopalność czy zdolność do wchłaniania wody, lecz dodatkowo wprowadzić całkowicie nowe funkcjonalności, które wcześniej nie były rozważane w kontekście tych materiałów.

## 2. Forma pracy doktorskiej oraz wkład doktoranta

Na pracę doktorską pt. „*Modyfikacja właściwości fizykochemicznych drewna, bawełny i ich pochodnych za pomocą nanomateriałów węglowych*” składają się cztery oryginalne artykuły opublikowane w recenzowanych czasopismach naukowych indeksowanych w bazie *Journal Citation Reports* oraz patent zarejestrowany w Urzędzie Patentowym Rzeczypospolitej Polskiej:

1. [Łukawski, POC 2018] D. Łukawski, A. Lekawa-Raus, F. Lisiecki, K. Koziol, A. Dudkowiak, Towards the development of superhydrophobic carbon nanomaterial coatings on wood, *Progress in Organic Coatings* 125 (2018) 23–31.
2. [Łukawski, UPRP 2017] D. Łukawski, A. Dudkowiak, A. Lekawa-Raus, *Sączek hydrofobowy selektywnie pochłaniający oleje i związki organiczne przeznaczony do oczyszczania wód oraz sposób wytworzenia sączka* (P.423094/2017).
3. [Łukawski, FP 2018] D. Łukawski, F. Lisiecki, A. Dudkowiak, Coating cellulosic materials with graphene for selective absorption of oils and organic solvents from water, *Fibers and Polymers* 19 (2018) 524–530.
4. [Łukawski, Drewno 2019] D. Łukawski, W. Grześkowiak, D. Dukarska, B. Mazela, A. Lekawa-Raus, A. Dudkowiak, The influence of surface modification of wood particles with carbon nanotubes on properties of particleboard glued with phenol-formaldehyde resin, *Drewno* 203 (2019) 93–105.
5. [Łukawski, Composites A 2019] D. Łukawski, A. Dudkowiak, D. Janczak, A. Lekawa-Raus, Preparation and applications of electrically conductive wood layered composites, *Composites Part A: Applied Science and Manufacturing* 127 (2019) 105656: 1–10.

Zgodnie z załączonymi oświadczeniami współautorów, wkład doktoranta w powstanie publikacji był następujący:

Publikacja [Łukawski, POC 2018] – doktorant wykonał przegląd aktualnej literatury dotyczącej pokryć hydrofobowych oraz brał udział w planowaniu badań. Następnie, opracował metodę pokrywania drewna CNM (CNT, Gr oraz sadzą techniczną) i przygotował pokrycia. Doktorant zaprojektował, skonstruował i wykorzystał do badań układ do pomiaru kąta zwilżania. Przeprowadził także badania pokryć wykorzystując metodę mikroskopii fluorescencyjnej oraz pomiary chropowatości i wykonał testy odporności na ścieranie. Ponadto, był odpowiedzialny za wstępną analizę wyników

i przygotowanie pierwszej wersji manuskryptu oraz uczestniczył w tworzeniu modelu zwilżalności.

Patent [**Łukawski, UPRP 2017**] – doktorant opracował pomysł dotyczący wykorzystania hydrofobizowanych za pomocą nanomateriałów węglowych wiórów i włókien drzewnych do usuwania rozlewów oleistych z powierzchni wody. Następnie przedstawił przykładowe sposoby realizacji prototypu i wykonał próby walidujące jego działanie. Ponadto, wykonał przegląd aktualnego stanu techniki i we współpracy z rzecznikiem patentowym opracował treść patentu.

Publikacja [**Łukawski, FP 2018**] – w celu wytworzenia hydrofobowych sączków, doktorant zaproponował rozwinięcie badań przedstawionych w publikacji [**Łukawski, POC 2018**]. Wykonał przegląd aktualnej literatury oraz zaplanował eksperyment. Następnie, przygotował próbki celulozowe modyfikowane Gr. Wykonał pomiary metodą mikroskopii konfokalnej oraz określił właściwości sorpcyjne wszystkich próbek. Doktorant odpowiadał także za analizę i interpretację wyników oraz przygotowanie manuskryptu.

Publikacja [**Łukawski, Drewno 2019**] – doktorant uczestniczył w planowaniu eksperymentu oraz dokonał przeglądu aktualnej literatury. Stosując metodę homogenizacji ultradźwiękowej, przygotował zawiesinę CNT w roztworze wodnym, którą wykorzystał do wykonania pokrycia wiórów drzewnych. Był odpowiedzialny za kompleksową analizę wyników palności i badań mechanicznych, a także za redagowanie i korektę manuskryptu oraz kontakt z edytorem czasopisma jako autor korespondencyjny.

Publikacja [**Łukawski, Composites A 2019**] – doktorant brał udział w planowaniu eksperymentu oraz przygotował część próbek. Ponadto, był odpowiedzialny za wykonanie badań przewodnictwa elektrycznego pokryć CNT na powierzchni drewna, wpływu czynników zewnętrznych (wody, nacisku, temperatury) na przewodnictwo elektryczne oraz badań termoelektrycznych. Doktorant wykonał wszystkie wykresy, grafiki i tabele przedstawione w pracy, brał udział w analizie wyników oraz przygotowaniu manuskryptu.

### 3. Badane materiały oraz techniki badawcze

#### 3.1. Materiały

W ramach rozprawy doktorskiej badano komercyjnie dostępne nanomateriały węglowe, skupiając się na tych, których produkcja jest możliwa w skali przemysłowej – wielościennych CNT (*ang. multi-wall carbon nanotubes* – MWCNT) firmy *Nanocyl* (NC700) oraz Gr firmy *Cambridge Nanosystems* (Camgraph G1). Dodatkowo, jako materiały referencyjne wykorzystano sadzę techniczną (N-550), GNP oraz MWCNT firmy *Carbon Nanotubes Plus* (Tabela 1).

Tabela 1 Parametry wykorzystywanych nanomateriałów węglowych (dane uzyskane od producentów).

Nazwa komercyjna	Producent	Odmiana alotropowa węgla	Średnia średnica płatka/ długość nanorurki [ $\mu\text{m}$ ]	Średnia grubość płatka/ średnica nanorurki [nm]	BET [ $\text{m}^2/\text{g}$ ]	Zawartość węgla [%]
<u>NC7000</u>	Nanocyl SA	MWCNT	1,5	9,5	250-300	90
<u>Camgraph G1</u>	Cambridge Nanosystems Ltd.	Gr	0,3	< 1	313±19	> 99,8
-	Cheaptubes Inc.	GNP	>2	8-15	500-700	97
-	Carbon Nanotubes Plus	MWCNT	0,5-2	8-15	-	95
-	Carbon Nanotubes Plus	MWCNT	50	8-15	-	98
N-550	Konimpex Ltd.	Sadza techniczna	-	-	40±5	-

W pracy [Łukawski, POC 2018] jako podłoża dla CNM wykorzystano różne gatunki drewna: balsem, sosnę, dąb, brzozę, buk oraz topolę. Badania te rozszerzono stosując rozwłóknione drewno i wióry drzewne oraz materiały celulozowe o różnym stopniu uporządkowania, średnicy i długości włókien celulozowych [Łukawski, FP 2018]. Wióry drzewne pokryte CNM zostały także wykorzystane do wytworzenia modyfikowanej płyty wiórowej i były obiektem badań przedstawionych w pracy [Łukawski, Drewno 2019]. Natomiast, w pracy [Łukawski, Composites A 2019] badania przeprowadzono dla drewna litego (sosny) oraz płyt drewnopochodnych (płyty

pilśniowej o średniej (ang. *medium density fiberboard* – MDF) i wysokiej (ang. *high density fiberboard* – HDF) gęstości włókien drzewnych, płyty o wiórach orientowanych (ang. *oriented strand board* – OSB), płyty wiórowej i sklejki).

Wszystkie zawiesiny CNM zostały przygotowane wykorzystując homogenizator ultradźwiękowy. Podczas homogenizacji próbki były umieszczane w wodzie z lodem, w celu efektywnego odprowadzania ciepła. W badaniach w ramach rozprawy doktorskiej wykorzystano trzy rodzaje zawiesin CNM:

- (1) wodna z dodatkiem surfaktantu jonowego - dodecylobenzenosulfonianu sodu (ang. *sodiumdodecylbenzenesulphonate* – SDBS) pozwalającego na stabilizację CNM,
- (2) w lotnym związku organicznym (aceton, dichlorometan) bez dodatku substancji stabilizującej,
- (3) z dodatkiem polimeru stabilizującego, polimetakrylanu metylu (ang. *poly(methyl methacrylate)* – PMMA) w octanie eteru monobutyłowego glikolu dietylenowego (ang. *diethylene glycol monobutyl ether acetate* – DB acetate).

W zależności od rodzaju zawiesiny zastosowano różne techniki nanoszenia warstw: nanoszenie zanurzeniowe, nanoszenie z kropli, nanoszenie natryskowe lub sitodruk.

### 3.2. Charakteryzacja powierzchni

Do badań struktury powierzchni drewna pokrytego CNM, wykorzystano mikroskopie fluorescencyjną, konfokalną (ang. *laser scanning microscope* – LSM) oraz elektronową (ang. *scanning electron microscopy* – SEM). Pozwoliły one na zbadanie morfologii warstw. Ocenę skuteczności usuwania SDBS z powierzchni drewna pokrytego CNM określono na podstawie analizy widma uzyskanego metodą spektrometrii dyspersji energii promieniowania rentgenowskiego (ang. *energy-dispersive X-ray spectroscopy* – EDS). Pomiary chropowatości zostały wykonane z wykorzystaniem LSM, a reflaktancja wybranych próbek została wyznaczona za pomocą spektrofotometru absorpcyjnego.

### 3.3. Badania zwilżalności i zdolności sorpcyjnej

Dla wytworzonych warstw CNM wykonano pomiary kąta zwilżania za pomocą dedykowanego układu oraz wykorzystano oprogramowanie ImageJ (wtyczka Dropsnake) do precyzyjnego określenia kąta. Ponadto, przeprowadzono pomiary kąta rozprysku

wody (ang. *water shedding angle* – WSA) metodą opisaną w pracy [40] oraz pomiary nasiąkliwości dla rozwłóknionego drewna i wiórów drzewnych, a także dla włókien celulozowych. Zdolność sorpcyjną (ang. *sorption capacity* – SC) włókien celulozowych pokrytych CNM dla wody oraz wybranych związków organicznych o różnej lepkości i gęstości (tj. eteru naftowego, heksanu, chloroformu, toluenu, oleju lnianego, parafiny ciekłej, oleju silnikowego) obliczono na podstawie równania:

$$SC = \frac{m_f - m_0}{m_0}, \quad (1)$$

gdzie  $m_f$  – masa próbki po zanurzeniu w cieczy,  $m_0$  – masa suchej próbki.

Wyznaczono także selektywność (S) pochłaniania związków organicznych (jako przykładowy związek wykorzystano chloroform) w stosunku do pochłaniania wody wykorzystując równanie:

$$S = \frac{m_f - m_0}{(m_{org} - m_0) + (m_w - m_0)}, \quad (2)$$

gdzie  $m_w$  – masa próbki po zanurzeniu w wodzie,  $m_{org}$  – masa próbki po zanurzeniu w związku organicznym.

### 3.4. Badania palności i właściwości mechanicznych

Badania palności wiórów drzewnych i płyty wiórowej zostały wykonane w Pracowni Ochrony i Konserwacji Drewna Wydziału Technologii Drewna Uniwersytetu Przyrodniczego w Poznaniu (WTD UP). Pomiary szybkości spalania wiórów drzewnych pokrytych CNM, metodą rury do spalań wg. Metza, przeprowadzono zgodnie z normą ASTM E69. Ponadto, w Zakładzie Tworzyw Drzewnych WTD UP, wykonano płytę wiórową z wiórów drzewnych zmodyfikowanych CNM oraz zbadano jej właściwości mechaniczne zgodnie z normami EN 310 (wytrzymałość materiału na zginanie i rozciąganie), EN 319 (wytrzymałości na rozciąganie w kierunku prostopadłym do płaszczyzn płyty) oraz nasiąkliwość zgodnie z normą EN 317. Określono również palność płyty wiórowej za pomocą kalorymetru ubytku masy, zgodnie z normą ISO 13927.

### 3.5. Badania elektryczne i elektrotermiczne

W celu wykonania pomiaru oporu elektrycznego warstw MWCNT, wytworzonych na drewnie lub płytach drewnopochodnych, na podłoże naniesiono elektrody srebrne. Pomiary wykonano za pomocą precyzyjnego multimetru. Zmiany

rezystancji warstw CNM pod wpływem czynników zewnętrznych takich jako woda, nacisk itp. rejestrowano wykorzystując miernik rezystancji podłączony do komputera. Pomiary termoelektryczne dla warstw MWCNT wykonano za pomocą podłączonej do komputera kamery termowizyjnej i pirometru sprzężonego z zasilaczem prądu stałego.

#### 4. Krótki opis badań zawartych w rozprawie doktorskiej

Początkowo przeprowadzone badania skupiły się na analizie morfologii cienkiej warstwy CNM naniesionej na powierzchnię drewna i określeniu jej wpływu na zwilżalność warstwy [Łukawski, POC 2018]. Badania rozpoczęto wykorzystując balsę, jako drewno silnie hydrofilowe o jednorodnej strukturze. Wykonano pokrycia CNM metodą nanoszenia z kropli, a następnie warstwy charakteryzowano metodami mikroskopowymi [Łukawski, POC 2018 – Rysunek 1, 2 i 3]. Zauważono, że z powodu wygaszania fluorescencji przez CNM, mikroskopia fluorescencyjna jest efektywną metodą do badania dystrybucji CNM na powierzchni drewna, dającą znacznie wyższą rozdzielczość niż tradycyjna mikroskopia optyczna. Na podstawie rozkładu emisji fluorescencji stwierdzono, że w skali mikroskopowej CNM jednorodnie osadzają się na powierzchni balsy, aglomerując tylko częściowo w obszarach związanych z nierównościami struktury drewna. Analizując obrazy SEM zaobserwowano, że Gr oraz MWCNT osadzone na powierzchni drewna tworzą jednorodne warstwy, natomiast w przypadku osadzania sadzy technicznej powstają aglomeraty. Zauważono także, że MWCNT tworzą sieci pomiędzy nierównościami w strukturze drewna, co może powodować znaczącą modyfikację właściwości warstwy na granicy drewno-CNM.

Pomiary kąta zwilżania [Łukawski, POC 2018 – Rysunek 5] pokazały, że w przypadku pokryć drewna przez CNT i Gr, wartość kąta zwilżania przekracza  $130^\circ$  i nie zmienia się w funkcji czasu, co oznacza, że uzyskujemy silnie hydrofobową powierzchnię. Dla porównania kropla woda osadzana na czystej powierzchni balsy po 60 s całkowicie wsiąka w jej strukturę. Pokrycie drewna sadzą techniczną powodowało tylko nieznaczne zwiększenie właściwości hydrofobowych powierzchni, a wyznaczona wartość kąta zwilżania zmieniała się w miarę upływu czasu.

Po uzyskaniu hydrofobowych warstw na powierzchni balsy, postanowiono kontynuować badania dla innych gatunków drewna pokrywając je Gr. Na podstawie obrazów uzyskanych za pomocą mikroskopii fluorescencyjnej obserwowano znaczące różnice w ilości osadzonych Gr na powierzchni drewna, w przypadku występowania w strukturze drewna wyraźnego podziału słoje na drewno wczesne i późne (np. dla sosny). CNM osadzały się w większej ilości na drewnie wczesnym, w związku z jego mniejszą gęstością i większą chropowatością. Jednak, badania przeprowadzone dla różnych gatunków drewna pokrytych Gr, nie potwierdziły istnienia korelacji pomiędzy wartością

kąta zwilżania a gatunkiem drewna, w tym jego chropowatością, składem chemicznym, czy średnią wielkością porów.

W związku z obiecującymi wynikami powyższych badań zastosowano również inne metody nanoszenia CNT i Gr, gdyż nanoszenie z kropli nie jest metodą optymalną do zastosowań w przemyśle. W tym celu, do wykonania pokryć na powierzchni drewna, przygotowano zawiesinę wodną zawierającą CNT oraz surfaktant jonowy SDBS i zastosowano metodę zanurzeniową. Obecność surfaktantu spowodowała, że powierzchnia drewna pokryta CNT wykazywała właściwości superhydrofilowe. Wykorzystując metodę zaproponowaną w pracy [25], usunięto SDBS z pokrycia poprzez wielokrotne przepłukiwanie i suszenie próbki. Skuteczność metody zweryfikowano na podstawie analizy widm EDS i identyfikacji pasma dla siarki (występującej w strukturze SDBS) [Łukawski, POC 2018 – Rysunek 4]. Efektywne usunięcie surfaktantu zostało także potwierdzone pomiarami kąta zwilżania, którego wartość wynosiła  $0^\circ$  (przed wypłukiwaniem) i wzrosła do ponad  $139^\circ$  i  $145^\circ$  (po wypłukaniu), odpowiednio dla pokryć drewna Gr i CNT. Wykonane pomiary WSA wykazały, że najlepsze właściwości hydrofobizujące wykazują pokrycia z CNT, co potwierdzają również wyniki pomiarów kąta zwilżania.

Kompleksowa analiza wyników badań pozwoliła na zaproponowanie modelu zwilżania powierzchni drewna pokrytej CNM, analogicznego do zjawiska „płatka róży”, obserwowanego w naturze [41]. Poprzez połączenie CNM ze strukturą drewna uzyskuje się powierzchnię o wysokiej chropowatości zarówno w skali nano jak i mikro. Dodatkowo, biorąc pod uwagę niską energię powierzchniową CNM, dla idealnie pokrytego drewna można byłoby uzyskać powierzchnię superhydrofobową. Jednakże, zanieczyszczenia na powierzchni drewna powodują miejscowo słabszą adhezję CNM, dlatego warstwa ta nie jest w pełni jednorodna i pojawiają się miejsca, gdzie możliwy jest kontakt wody z drewnem. W ten sposób powstaje powierzchnia charakteryzująca się bardzo wysoką wartością kąta zwilżania, a jednocześnie silną zdolnością do adhezji wody [Łukawski, POC 2018 – Rysunek 7].

Opracowana metoda zanurzeniowa, nanoszenia CNM na powierzchnię drewna, została zastosowana także do wytworzenia pokryć włókien i wiórów drzewnych, powodując zmniejszenie ich nasiąkliwości wodą. Efekt ten wykorzystano, proponując zastosowanie włókien drzewnych hydrofobizowanych za pomocą CNM do wytworzenia

hydrofobowego sączka, mogącego służyć do usuwania np. oceanicznych rozlewów zanieczyszczeń oleistych. Sączek taki, w założeniu miałby absorbować w swojej objętości wyłącznie związki organiczne, nie pochłaniając wody, co umożliwiłoby efektywne usunięcie np. ropy naftowej z powierzchni wody i jej odzyskanie do ponownego przetworzenia. Rozwiązanie to zostało opatentowane [Łukawski, UPRP 2017] w Urzędzie Patentowym Rzeczypospolitej Polskiej.

Badania dotyczące modyfikacji zdolności sorpcyjnej drewna postanowiono kontynuować wykorzystując materiały celulozowe pokryte CNM. Do badań opisanych w pracy [Łukawski, FP 2018] wybrano pięć różnych materiałów składających się z włókien celulozowych, będących głównym składnikiem drewna. Strukturę badanych materiałów zobrazowano wykorzystując metodę mikroskopii fluorescencyjnej. Materiały celulozowe o różnym stopniu uporządkowania włókien celulozowych, średnicy i długości, pokryto Gr (stosując odpowiednio jeden i sześć cykli nanoszenia). Na podstawie obrazów SEM stwierdzono, że po kilku cyklach nanoszenia Gr możliwe jest wytworzenie jednorodnego pokrycia na powierzchni pojedynczego włókna celulozowego.

Następnie przeprowadzono badania zwilżalności materiałów celulozowych (czystych i pokrytych Gr). Ze względu na dużą chropowatość powierzchni badanych materiałów, utrudniającą określenie wartości kąta zwilżania, wykonano pomiary zdolności sorpcyjnej (SC) wody [Łukawski, FP 2018 – Rysunek 4]. Otrzymane wyniki potwierdziły uzyskanie nieznacznej hydrofobizacji powierzchni sączków pokrytych jedną warstwą Gr (po pierwszym cyklu nanoszenia) oraz znaczący wzrost właściwości hydrofobowych sączków po sześciu cyklach nanoszenia. Przykładowo, dla włókien celulozowych splecionych w formie gazy SC w odniesieniu do wody spadła z 11,0 g/g dla czystych próbek do poniżej 0,07 g/g dla próbek pokrytych 6-krotnie Gr.

Oprócz silnej hydrofobizacji powierzchni (niskiej wartości SC względem wody) kluczowe jest otrzymanie sączka o wysokiej zdolności do absorbowania różnych związków organicznych. Badania sorpcji związków organicznych sączków celulozowych pokrytych Gr pokazały, że wysoką wartość SC sączków można uzyskać niezależnie od stopnia hydrofobizacji powierzchni [Łukawski, FP 2018 – Rysunek 5]. Na podstawie badań przeprowadzonych dla eteru naftowego, heksanu, chloroformu, toluenu, oleju lnianego, parafiny ciekłej, oleju silnikowego, stwierdzono, że materiałem

o najwyższej zdolności do sorpcji wszystkich badanych absorbatów jest zesłana bawelniiana pokryta Gr (po sześciu cyklach nanoszenia). Przykładowo, jej SC dla oleju silnikowego była równa 30,6 g/g, przy niskiej sorpcji wody tj. na poziomie 0,12 g/g. Selektowność absorbowania związków organicznych w stosunku do wody wynosiła ponad 99%, co oznacza, że na 99 g pochłoniętego związku organicznego wchłonięty zostanie jedynie 1 g wody. Wykazano także, że hydrofobizacja sączków nie zmienia się znacząco, po wykonaniu kilku cykli zanurzania absorbentu w badanych związkach organicznych, co świadczy o silnej adhezji Gr do powierzchni włókien celulozowych [Łukawski, FP 2018 – Tabela 1].

Po przeprowadzeniu badań związanych z modyfikacją zwilżalności drewna i materiałów celulozowych wykorzystując CNM postanowiono określić wpływ CNM na palność drewna. Proces spalania jest zjawiskiem zachodzącym w objętości, dlatego badania palności przeprowadzono dla wiórów drzewnych pokrytych CNT (jednocześnie częściowo nimi impregnowanych) [Łukawski, Drewno 2019 – Rysunek 1] i płyty drewnopochodnej wykonanej ze zmodyfikowanych wiórów. Wyniki dotyczące palności wiórów drzewnych pokrytych CNT pokazały spowolnienie procesu ich spalania, co prawdopodobnie jest spowodowane zwiększeniem efektywności wytwarzania warstwy zwęglonej w wyniku obecności CNM na ich powierzchni. Wydaje się, że wysoka absorpcja promieniowania cieplnego przez CNT oraz ich wysokie przewodnictwo cieplne może powodować bardziej efektywny transport ciepła do zewnętrznej części wiórów drzewnych, przyspieszając generowanie warstwy zwęglonej, będącej naturalną barierą termiczną powodującą ograniczenie spalania.

Wióry drzewne pokryte CNT wykorzystano następnie do wytworzenia płyty wiórowej. Płyta została wytworzona poprzez sprasowanie zmodyfikowanych wiórów z żywicą fenolowo-formaldehydową w temperaturze 200°C i pod ciśnieniem 2,5 N/mm<sup>2</sup>. Zastosowane podejście umożliwiło umieszczenie CNT w całej objętości płyty wiórowej, bez konieczności stosowania np. żywicy zmodyfikowanej CNM. Badania palności płyty wiórowej modyfikowanej CNT, wykonane za pomocą kalorymetru ubytku masy, pokazały nieznaczne przyspieszenie procesu jej spalania. Dla płyty wiórowej zawierającej CNT, czas do zapłonu był o 4 s krótszy niż dla płyty referencyjnej, a czas do osiągnięcia maksymalnej szybkości wydzielania ciepła (ang. *peak heat release rate* – PHRR) o 25 s krótszy. Jednakże, niezmiennymi zostały kluczowe parametry rejestrowane

podczas procesu spalania, takie jak wartość PHRR oraz całkowity ubytek masy, co oznacza istnienie tylko nieznacznego wpływu CNT na proces spalania.

Dla płyty wytworzonej z wiórów pokrytych CNT przeprowadzono także badania mające na celu określenie jej właściwości mechanicznych [Łukawski, Drewno 2019 – Tabela 1]. Otrzymane wyniki testów wytrzymałościowych (badanie wytrzymałości materiału na zginanie i rozciąganie oraz rozciąganie w kierunku prostopadłym do płaszczyzn płyty) oraz nasiąkliwości płyty, wskazują na brak istotnego wpływu CNT zawartych w objętości płyty na jej właściwości mechaniczne i zdolności do absorbowania wody. Na podstawie analizy uzyskanych wyników wydaje się, że nowym interesującym kierunkiem dalszych badań mającym na celu zwiększenie wytrzymałości mechanicznej płyty, będzie raczej domieszkowanie CNM żywicy spajającej wióry niż modyfikowanie powierzchni wiórów.

Dotychczasowe badania dotyczyły wpływu pokryć CNM na drewno i materiały drewnopochodne w odniesieniu do poprawy ich odporności na czynniki zewnętrzne. Kolejnym etapem badań w ramach niniejszej rozprawy doktorskiej było wytworzenie funkcjonalnych pokryć CNM na powierzchni drewna. Do ich uzyskania wykorzystano zawiesiny CNT (Tabela 2) w związku organicznym oraz wodzie z dodatkiem surfaktantu. W pracy [Łukawski, Composites A 2019] zastosowano również pasty (zawiesiny CNT w związku organicznym stabilizowanym polimerem) opracowane w Zakładzie Mikrotechnologii i Nanotechnologii Politechniki Warszawskiej [42]. Stosując wybrane zawiesiny CNM możliwe było wytworzenie pokryć o różnych właściwościach (Tabela 2). Ponadto, uzyskane pokrycia z CNT były elektroprowadzące, dlatego sprawdzono ich potencjał aplikacyjny jako czujników lub elementów grzewczych.

**Tabela 2 Zestawienie zawiesin CNT wykorzystywanych do wytwarzania pokryć elektroprowadzących oraz ich charakterystyka**

Zawiesina CNT w	Charakterystyka otrzymanego pokrycia
związku organicznym (czyste CNT)	Superhydrofobowe, stosunkowo niejednorodne, nanoszone metodą natryskową
związku organicznym stabilizowanym polimerem (CNT/PMMA)	Hydrofobowe lub hydrofilowe, często nie przepuszczające wody, jednorodne, nanoszone sitodrukiem
wodzie z dodatkiem surfaktantu (CNT/SDBS)	Superhydrofilowe, jednorodne, nanoszone metodą natryskową

W wyniku przeprowadzonych badań określono przewodność elektryczną pokryć w zależności od ilości CNT naniesionych na powierzchnię drewna [Łukawski, Composites A 2019 – Rysunek 2]. Pokazano, że rezystancja elektryczna warstwy utworzonej z CNT/SDBS maleje logarytmicznie wraz z ilością CNT osiągając wartość  $140 \pm 15 \Omega/\text{sq}$  dla pokrycia CNT wynoszącego  $324 \pm 36 \mu\text{g}/\text{cm}^2$ . Podobną zależność zaobserwowano dla warstw z CNT/SDBS i czystych CNT. Zauważono również korelację, pomiędzy przewodnością elektryczną, a reflaktancją warstwy. Wysoko-przewodzące pokrycia CNT absorbują większość promieniowania widzialnego, powodując uzyskanie czarnej barwy.

Czarne zabarwienie warstw CNM może być mało atrakcyjne w wielu praktycznych zastosowaniach, dlatego postanowiono warstwę CNM przykryć warstwą dekoracyjną (przyklejoną do drewna) i zbadać jej wpływ na przewodność warstwy CNM. Pomiarów elektrycznych przed i po przyklejeniu warstwy dekoracyjnej pokazały, że relatywny wzrost oporu elektrycznego wyniósł  $(9 \pm 3)\%$ ,  $(27 \pm 5)\%$  i  $(3 \pm 4)\%$ , odpowiednio dla pokryć utworzonych z czystych CNT, CNT/SDBS i CNT/PMMA. Okazało się, że pokrycia o wysokim oporze elektrycznym (na granicy progu perkolacji) zwiększają opór elektryczny bardziej niż wysoko przewodzące pokrycia. Obecność kleju powoduje efekt przesunięcia progu perkolacji. Nieznaczne zmiany przewodności dla dobrze przewodzących warstw sugerują, że wytworzone warstwy CNM mogą być także wykorzystywane po przyklejeniu do nich warstwy dekoracyjnej.

Dla zaprojektowania i wytworzenia czujników np. zalania, temperatury, siły nacisku i innych, istotne znaczenie ma zależność przewodności elektrycznej warstw CNM od czynników zewnętrznych. W tym celu przeprowadzono badania pozwalające na określenie wpływu zalania wodą i związkami organicznymi, a także zmian temperatury i przyłożenia zewnętrznego nacisku, na przewodność elektryczną warstw CNT, wytworzonych na powierzchni drewna.

Wpływ wody na przewodność elektryczną warstw w głównej mierze zależy od zwilżalności warstwy. Zgodnie z wynikami badań opisanymi w pracy [Łukawski, POC 2018], pokrycia z CNT (czystych CNT) powodują silną hydrofobizację drewna, natomiast obecność surfaktantu SDBS (CNT/SDBS) zmienia właściwości pokrycia i pozwala uzyskać powierzchnie całkowicie hydrofilowe. Pośrednia sytuacja występuje dla pokryć otrzymywanych z wykorzystaniem CNT/PMMA. W konsekwencji,

przewodność elektryczna warstw z czystych CNT i CNT/PMMA nie zmienia się w wyniku kontaktu z wodą, natomiast dla warstw z CNT/SDBS obserwuje się wyraźny wzrost jej oporu elektrycznego [Łukawski, *Composites A* 2019 – Rysunek 3]. Przeprowadzone badania jednoznacznie pokazują, że jedynie warstwa CNT/SDBS naniesiona na powierzchnię drewna może być wykorzystana jako czuły czujnik zalania wodą.

Analogiczne badania przeprowadzono wykorzystując dwa związki organiczne (niepolarny heksan i polarny aceton). Naniesienie kropli acetonu na warstwę powoduje wyraźny wzrost przewodności elektrycznej dla każdego typu pokrycia, natomiast efekt ten jest znacząco słabszy dla heksanu. Zaobserwowano także, że po usunięciu związków organicznych poprzez wygrzanie próbki, opór elektryczny wraca do wartości początkowych. Ponadto zauważono, że po naniesieniu związków organicznych zakres zmian przewodności elektrycznej dla CNT/SDBS jest wyraźnie mniejszy niż dla wody.

Następnie, postanowiono zbadać możliwość wytworzenia na powierzchni drewna czujnika nacisku. W tym celu określono wpływ naprężeń spowodowanych obciążeniem zewnętrznym na przewodność elektryczną warstw CNM na drewnie. Okazało się, że dla wszystkich badanych warstw nie zaobserwowano istotnej zmiany rezystancji w wyniku przyłożonego obciążenia. W związku z tym, zaproponowano wytworzenie kompozytowego czujnika naprężeń, składającego się ze stykających się ze sobą warstw CNT naniesionych na dwie powierzchnie drewna [Łukawski, *Composites A* 2019 – Rysunek 4]. Czujnik przetestowano obciążając go kolejno ciężarkami o masie 0,1 kg (0.6 kPa), 1 kg (6 kPa), 5 kg (30 kPa) i 65 kg (390 kPa). Położenie najmniejszej masy (0,1 kg) nie wywołało istotnej zmiany oporu elektrycznego, natomiast sukcesywne obciążanie czujnika aż do 65 kg spowodowało spadek oporu o 25%. Podczas wykonania 5 niezależnych cykli obciążania czujnika uzyskiwano te same wyniki.

Określono także wpływ zmiany temperatury na właściwości elektryczne warstw CNM na drewnie. Pokazano, że dla warstwy CNT/PMMA zmiana oporu elektrycznego pod wpływem zmiany temperatury wykazuje silnie nieliniową zależność, związaną prawdopodobnie z wewnętrzną przebudową struktury polimerów. Natomiast, dla pokrycia drewna CNT/SDBS obserwowano liniową i powtarzalną w kolejnych cyklach zmianę, co umożliwia wykorzystanie warstwy z CNT/SDBS jako czujnika temperatury drewna.

Zastosowanie elektrycznie aktywnych warstw CNT na drewnie jako czujników jest jednym z możliwych rozwiązań aplikacyjnych. Drugim, zaproponowanym na podstawie badań przeprowadzonych w ramach pracy doktorskiej, jest ich wykorzystanie jako elementów grzewczych. Przyłączenie zewnętrznego napięcia do warstwy CNM umożliwia podgrzanie pokrycia, a w konsekwencji drewna, dlatego postanowiono wykonać badania mające na celu określenie właściwości elektrotermicznych warstwy CNT na powierzchni drewna. Badania przeprowadzono dla litego drewna oraz płyt drewnopochodnych (MDF, OSB, płyta wiórowa) o różnych wartościach chropowatości. Wykazano, że zastosowanie pokrycia CNT/PMMA pozwala na wytworzenie jednorodnie nagrzewającej się warstwy na wszystkich badanych podłożach, nawet na płycie OSB o najwyższej chropowatości. Natomiast, pokrycia nie zawierające polimeru (czyste CNT i CNT/SDBS) umożliwiają uzyskanie takiej warstwy jedynie na powierzchni charakteryzującej się najniższą chropowatością (płyce MDF) [Łukawski, *Composites A* 2019 – Rysunek 5].

W przypadku wielu zastosowań (np. panele podłogowe) element grzewczy powinien znajdować się pod płytą drewnopochodną. W związku z tym, zbadano możliwość transferu ciepła pomiędzy warstwą CNM a płytą drewnopochodną (HDF) o różnych grubościach (3 mm, 7,3 mm oraz 19 mm) [Łukawski, *Composites A* 2019 – Rysunek 7]. Warstwę CNT nagrzano do temperatury ok. 90°C i po upływie 20 min, za pomocą kamery termowizyjnej określono temperaturę powierzchni płyty, znajdującej się po przeciwnej stronie płyty (ponad warstwą grzewczą). Wykazano, że relatywnie cienka płyta (3 mm) nagrzewa się do temperatury zbliżonej do temperatury warstwy (78°C), podczas gdy najgrubsza płyta osiąga temperaturę tylko 35°C. Ponadto, dla płyty 3 mm pokazano możliwość sterowania temperaturą poprzez zmianę natężenia prądu płynącego przez warstwę CNT i wykazano, że zmiany natężenia są dobrze skorelowane ze zmianą temperatury warstwy i następują bez istotnego opóźnienia.

Efektywne nagrzewanie drewna za pomocą zintegrowanej z nim warstwy grzewczej z CNT, daje możliwość np. znacznego przyspieszenia procesu suszenia wilgotnych płyt. W celu sprawdzenia efektywności takiego zastosowania, silnie higroskopijne płyty pilśniowe umieszczono w pojemniku, utrzymując w nim wilgotność względną 90%. Po siedmiu dniach masa płyt wzrosła do 108,5% masy początkowej. Następnie jedną z płyt pozostawiono w temperaturze pokojowej, a drugą podgrzano wykorzystując naniesione wcześniej warstwy grzewcze z CNT. Udowodniono, że po

100 min, masa płyty ogrzewanej zmniejszyła się, osiągając 102%, a płyty nieogrzewanej – 106% masy początkowej [Łukawski, Composites A 2019 – Rysunek 8]. Przeprowadzony eksperyment pokazał, że zastosowanie zintegrowanej z powierzchnią drewna warstwy grzewczej z CNT wpływa na przyspieszenie procesu suszenia wilgotnej płyty, co może mieć istotne znaczenie dla ograniczenia narostu grzybów i pleśni.

## 5. Podsumowanie i wnioski

Badania w ramach niniejszej pracy doktorskiej koncentrowały się na określeniu właściwości fizykochemicznych drewna, bawełny i ich pochodnych, pokrywanych wybranymi materiałami węglowymi. Następnie, konsekwentnie zostały rozwinięte o badania dotyczące właściwości elektrycznie aktywnych pokryć CNM na powierzchni drewna, w celu określenia ich potencjalnych zastosowań jako czujników (zalania, temperatury i siły nacisku) oraz elementów grzewczych zintegrowanych z powierzchnią drewna. Zakres badań obejmował wybór metod nanoszenia i wykonanie pokryć z CNM, charakteryzację powierzchni metodami mikroskopowymi, określenie zwilżalności powierzchni, palności materiałów zmodyfikowanych CNM oraz wyznaczenie właściwości elektrycznych i elektrotermicznych warstw CNM na podłożach z drewna i materiałów drewnopochodnych.

Najważniejszymi osiągnięciami uzyskanymi na podstawie analizy wyników są:

- pokazanie możliwości wytworzenia jednorodnej, wytrzymałej mechanicznie warstwy CNM na powierzchni drewna, bez użycia polimerów wiążących,
- wykazanie, że mikroskopia fluorescencyjna pozwala na obrazowanie jednorodności pokrycia CNM na powierzchni drewna,
- udowodnienie, że jednorodna warstwa CNM hydrofobizuje powierzchnię drewna, a kąt zwilżania takiej powierzchni może osiągnąć wartość powyżej 140°,
- zaproponowanie modelu zwilżalności drewna pokrytego CNM oraz pokazanie sposobu hydrofobizacji powierzchni różnych gatunków drewna, bez względu na ich chropowatość czy skład chemiczny,
- wykorzystanie metodyki opracowanej dla hydrofobizacji drewna do wytworzenia hydrofobowych sączków z wiórów i włókien drzewnych oraz innych materiałów celulozowych pokrytych CNM,

- określenie zdolności sorpcyjnej hydrofobowych sączków celulozowych w odniesieniu do związków organicznych i pokazanie, że można je wykorzystać jako sorbenty np. oceanicznych rozlewów ropy naftowej,
- wykazanie, że pokrycie wiórów drzewnych warstwą CNT powoduje częściowe obniżenie ich palności,
- zaproponowanie metody i sposobu wytworzenia płyty wiórowej zawierającej CNT,
- wyznaczenie właściwości elektrycznych warstw CNT wytworzonych na drewnie i materiałach drewnopochodnych oraz zbadanie wpływu substancji wiążącej/dyspergującej CNM na te właściwości,
- określenie wpływu czynników zewnętrznych (woda, siła nacisku, temperatura) na przewodność elektryczną warstwy CNT na podłożu drewna i materiałów drewnopochodnych oraz zaproponowanie konstrukcji odpowiednich czujników,
- wytworzenie czujnika zalania wodą i związkami organicznymi oraz czujnika temperatury i zbadanie ich właściwości,
- wytworzenie kompozytowego czujnika siły nacisku,
- wytworzenie elementów grzewczych na bazie pokryć CNT zintegrowanych z powierzchnią drewna oraz przeanalizowanie procesu transferu ciepła pomiędzy warstwą CNT (stosowaną jako element grzewczy) a materiałem drewnopochodnym,
- wykorzystanie elementu grzewczego do osuszania wilgotnych płyt drewnopochodnych np. w celu ograniczenia narostu grzybów i pleśni.

Wyniki badań opisane w niniejszej rozprawie doktorskiej pozwoliły po raz pierwszy poznać właściwości drewna i materiałów drewnopochodnych pokrytych nanomateriałami węglowymi oraz zaproponować sposób wykorzystania wybranych materiałów w nowych, potencjalnych rozwiązaniach aplikacyjnych, jako elementów elektrycznie aktywnych.

## Literatura

- [1] G. Pajchrowski, A. Noskowiak, A. Lewandowska, W. Strykowski, Wood as a building material in the light of environmental assessment of full life cycle of four buildings, *Constr. Build. Mater.* 52 (2014) 428–436.  
<https://doi.org/10.1016/j.conbuildmat.2013.11.066>.
- [2] A. Ashori, Wood-plastic composites as promising green-composites for automotive industries!, *Bioresour. Technol.* 99 (2008) 4661–4667.  
<https://doi.org/10.1016/j.biortech.2007.09.043>.
- [3] C. Chen, Y. Li, J. Song, Z. Yang, Y. Kuang, E. Hitz, C. Jia, A. Gong, F. Jiang, J.Y. Zhu, B. Yang, J. Xie, L. Hu, Highly Flexible and Efficient Solar Steam Generation Device, *Adv. Mater.* 29 (2017) 1–8. <https://doi.org/10.1002/adma.201701756>.
- [4] M. Zhu, J. Song, T. Li, A. Gong, Y. Wang, J. Dai, Y. Yao, W. Luo, D. Henderson, L. Hu, Highly Anisotropic, Highly Transparent Wood Composites, *Adv. Mater.* 28 (2016) 5181–5187. <https://doi.org/10.1002/adma.201600427>.
- [5] J. Shi, L. Lu, W. Guo, Y. Sun, Y. Cao, An environment-friendly thermal insulation material from cellulose and plasma modification, *J. Appl. Polym. Sci.* 130 (2013) 3652–3658. <https://doi.org/10.1002/app.39615>.
- [6] F. Jiang, Y. Lo Hsieh, Cellulose nanofibril aerogels: Synergistic improvement of hydrophobicity, strength, and thermal stability via cross-linking with diisocyanate, *ACS Appl. Mater. Interfaces.* 9 (2017) 2825–2834. <https://doi.org/10.1021/acsami.6b13577>.
- [7] H. Qi, B. Schulz, T. Vad, J. Liu, E. Mäder, G. Seide, T. Gries, Novel Carbon Nanotube/Cellulose Composite Fibers As Multifunctional Materials, *ACS Appl. Mater. Interfaces.* 7 (2015) 22404–22412. <https://doi.org/10.1021/acsami.5b06229>.
- [8] A.C. Ferrari, F. Bonaccorso, V. Falko, K.S. Novoselov, S. Roche, P. Bøggild, S. Borini, *et al.*, Science and technology roadmap for graphene, related two-dimensional crystals, and hybrid systems, *Nanoscale* 7 (2014) 4598–4810.  
<https://doi.org/10.1039/C4NR01600A>.
- [9] M.J. Nine, M.A. Cole, D.N.H. Tran, D. Losic, Graphene: a multipurpose material for protective coatings, *J. Mater. Chem. A.* 3 (2015) 12580–12602.  
<https://doi.org/10.1039/C5TA01010A>.
- [10] S. Park, M. Vosguerichian, Z. Bao, A review of fabrication and applications of carbon nanotube film-based flexible electronics., *Nanoscale.* 5 (2013) 1727.  
<https://doi.org/10.1039/c3nr33560g>.
- [11] S. Frank, Carbon Nanotube Quantum Resistors, *Science* 280 (1998) 1744–1746.  
<https://doi.org/10.1126/science.280.5370.1744>.
- [12] A.K. Geim, K.S. Novoselov, The rise of graphene, *Nat. Mater.* 6 (2007) 183–191.

- <https://doi.org/10.1038/nmat1849>.
- [13] E.T. Thostenson, Z. Ren, T.-W. Chou, Advances in the science and technology of carbon nanotubes and their composites: a review, *Compos. Sci. Technol.* 61 (2001) 1899–1912. [https://doi.org/10.1016/S0266-3538\(01\)00094-X](https://doi.org/10.1016/S0266-3538(01)00094-X).
- [14] T. Lin, V. Bajpai, T. Ji, L. Dai, Chemistry of carbon nanotubes, *Aust. J. Chem.* 56 (2003) 635–651. <https://doi.org/10.1071/CH02254>.
- [15] J. Zhang, F.L. Huang, C.Y. Wang, Y.N. Qi, X. Meng, Q.Z. Jiao, L.X. Sun, F. Xu, X.F. Lan, H.Y. Ru, L.N. Yang, Thermal stability of carbon nanotubes, *J. Therm. Anal. Calorim.* 102 (2010) 785–791. <https://doi.org/10.1007/s10973-010-0793-x>.
- [16] Y.Y. Liu, R.H. Wang, H.F. Lu, L. Li, Y.Y. Kong, K.H. Qi, J.H. Xin, Artificial lotus leaf structures from assembling carbon nanotubes and their applications in hydrophobic textiles, *J. Mater. Chem.* 17 (2007) 1071–1078. <https://doi.org/10.1039/B613914k>.
- [17] G.Y. Xiong, Y. Suda, D.Z. Wang, J.Y. Huang, Z.F. Ren, Effect of temperature, pressure, and gas ratio of methane to hydrogen on the synthesis of double-walled carbon nanotubes by chemical vapour deposition, *Nanotechnology* 16 (2005) 532–535. <https://doi.org/10.1088/0957-4484/16/4/033>.
- [18] K. Lee, W. Yeoh, S. Chai, S. Ichikawa, K. Lee, W. Yeoh, S. Chai, Optimization of Carbon Nanotubes Synthesis via Methane Decomposition over Alumina-Based Catalyst Optimization of Carbon Nanotubes Synthesis via Methane Decomposition over Alumina-Based Catalyst, *Fullerenes, Nanotub. Carbon Nanostructures.* 18 (2010) 273–284. <https://doi.org/10.1080/15363831003782999>.
- [19] A. Malesevic, R. Vitchev, K. Schouteden, A. Volodin, L. Zhang, G. Van Tendeloo, A. Vanhulsel, C. Van Haesendonck, Synthesis of few-layer graphene via microwave plasma-enhanced chemical vapour deposition, *Nanotechnology.* 19 (2008) 305604. <https://doi.org/10.1088/0957-4484/19/30/305604>.
- [20] M.A. Khan, K.M.I. Ali, Swelling Behavior of Wood and Wood-Plastic Composite (WPC), *Polym. Plast. Technol. Eng.* 31 (1992) 299–307. <https://doi.org/10.1080/03602559208017750>.
- [21] J. Gallup, P. Kozak, L. Cummins, S. Gillman, Indoor mold spore exposure: characteristics of 127 homes in Southern California with endogenous mold problems, in: G.Boehm, R.M. Leuschner (Eds.), *Adv. Aerobiol. Proc. 3rd Internat. Conf. Aerobiol., CIP-Kurztitelaufnahme der Deutschen Bibliothek, basel, 1987: pp. 140–142.*
- [22] K.K.S. Lau, J. Bico, K.B.K. Teo, M. Chhowalla, G.A.J. Amaratunga, W.I. Milne, G.H. McKinley, K.K. Gleason, Superhydrophobic Carbon Nanotube Forests, *Nano Lett.* 3 (2003) 1701–1705. <https://doi.org/10.1021/nl034704t>.
- [23] C. Lee, S. Baik, Vertically-aligned carbon nano-tube membrane filters with superhydrophobicity and superoleophilicity, *Carbon* 48 (2010) 2192–2197.

- <https://doi.org/10.1016/j.carbon.2010.02.020>.
- [24] D.D. Nguyen, N.-H. Tai, S.-B. Lee, W.-S. Kuo, Superhydrophobic and superoleophilic properties of graphene-based sponges fabricated using a facile dip coating method, *Energy Environ. Sci.* 5 (2012) 7908. <https://doi.org/10.1039/c2ee21848h>.
- [25] T. Makowski, D. Kowalczyk, W. Fortuniak, D. Jeziorska, S. Brzezinski, A. Tracz, Superhydrophobic properties of cotton woven fabrics with conducting 3D networks of multiwall carbon nanotubes, MWCNTs, *Cellulose* 21 (2014) 4659–4670. <https://doi.org/10.1007/s10570-014-0422-0>.
- [26] M. Shateri-Khalilabad, M.E. Yazdanshenas, Preparation of superhydrophobic electroconductive graphene-coated cotton cellulose, *Cellulose* 20 (2013) 963–972. <https://doi.org/10.1007/s10570-013-9873-y>.
- [27] N.T. Hoai, N.N. Sang, T.D. Hoang, Thermal reduction of graphene-oxide-coated cotton for oil and organic solvent removal, *Mater. Sci. Eng. B.* 216 (2016) 1–6. <https://doi.org/10.1016/j.mseb.2016.06.007>.
- [28] N.D. Tissera, R.N. Wijesena, J.R. Perera, K.M.N. De Silva, G.A.J. Amaratunge, Hydrophobic cotton textile surfaces using an amphiphilic graphene oxide (GO) coating, *Appl. Surf. Sci.* 324 (2015) 455–463. <https://doi.org/10.1016/j.apsusc.2014.10.148>.
- [29] L. Xu, G. Xiao, C. Chen, R. Li, Y. Mai, G. Sun, D. Yan, Superhydrophobic and superoleophilic graphene aerogel prepared by facile chemical reduction, *J. Mater. Chem. A.* 3 (2015) 7498–7504. <https://doi.org/10.1039/C5TA00383K>.
- [30] A.L. Higginbotham, J.R. Lomeda, A.B. Morgan, J.M. Tour, Graphite oxide flame-retardant polymer nanocomposites, *ACS Appl. Mater. Interfaces.* 1 (2009) 2256–2261. <https://doi.org/10.1021/am900419m>.
- [31] T. Kashiwagi, F. Du, J.F. Douglas, K.I. Winey, R.H. Harris, J.R. Shields, Nanoparticle networks reduce the flammability of polymer nanocomposites, *Nat. Mater.* 4 (2005) 928–933. <https://doi.org/10.1038/nmat1502>.
- [32] T. Kashiwagi, M. Mu, K. Winey, B. Cipriano, S.R. Raghavan, S. Pack, M. Rafailovich, Y. Yang, E. Grulke, J. Shields, R. Harris, J. Douglas, Relation between the viscoelastic and flammability properties of polymer nanocomposites, *Polymer* 49 (2008) 4358–4368. <https://doi.org/10.1016/j.polymer.2008.07.054>.
- [33] A.T. Farsheh, M. Talaeipour, A.H. Hemmasi, H. Khademislam, I. Ghasemi, Investigation on the mechanical and morphological properties of foamed nanocomposites based on wood flour/PVC/multi-walled carbon nanotube, *BioResources* 6 (2011) 841–852.
- [34] D. Janas, K.K. Koziol, Rapid electrothermal response of high-temperature carbon nanotube film heaters, *Carbon* 59 (2013) 457–463. <https://doi.org/10.1016/j.carbon.2013.03.039>.

- [35] T.J. Kang, T. Kim, S.M. Seo, Y.J. Park, Y.H. Kim, Thickness-dependent thermal resistance of a transparent glass heater with a single-walled carbon nanotube coating, *Carbon* 49 (2011) 1087–1093. <https://doi.org/10.1016/j.carbon.2010.11.012>.
- [36] M. Jian, K. Xia, Q. Wang, Z. Yin, H. Wang, C. Wang, H. Xie, M. Zhang, Y. Zhang, Flexible and Highly Sensitive Pressure Sensors Based on Bionic Hierarchical Structures, *Adv. Funct. Mater.* 27 (2017). <https://doi.org/10.1002/adfm.201606066>.
- [37] D.J. Lipomi, M. Vosgueritchian, B.C.K. Tee, S.L. Hellstrom, J.A. Lee, C.H. Fox, Z. Bao, Skin-like pressure and strain sensors based on transparent elastic films of carbon nanotubes, *Nat. Nanotechnol.* 6 (2011) 788–792. <https://doi.org/10.1038/nnano.2011.184>.
- [38] R. Zhang, H. Deng, R. Valenca, J. Jin, Q. Fu, E. Bilotti, T. Peijs, Carbon nanotube polymer coatings for textile yarns with good strain sensing capability, *Sensors Actuators, A Phys.* 179 (2012) 83–91. <https://doi.org/10.1016/j.sna.2012.03.029>.
- [39] D. Li, M.B. Müller, S. Gilje, R.B. Kaner, G.G. Wallace, 1012Processable aqueous dispersions of graphene nanosheets., *Nat. Nanotechnol.* 3 (2008) 101–105. <https://doi.org/10.1038/nnano.2007.451>.
- [40] J. Zimmermann, S. Seeger, F. a. Reifler, Water Shedding Angle: A New Technique to Evaluate the Water-Repellent Properties of Superhydrophobic Surfaces, *Text. Res. J.* 79 (2009) 1565–1570. <https://doi.org/10.1177/0040517509105074>.
- [41] L. Feng, Y. Zhang, J. Xi, Y. Zhu, N. Wang, F. Xia, L. Jiang, Petal effect: A superhydrophobic state with high adhesive force, *Langmuir* 24 (2008) 4114–4119. <https://doi.org/10.1021/la703821h>.
- [42] P. Kopyt, B. Salski, P. Zagrajek, D. Janczak, M. Sloma, M. Jakubowska, M. Olszewska-Placha, W. Gwarek, Electric Properties of Graphene-Based Conductive Layers from DC Up to Terahertz Range, *IEEE Trans. Terahertz Sci. Technol.* 6 (2016) 480–490. <https://doi.org/10.1109/TTHZ.2016.2544142>.

**Spis norm**

**ASTM E69** Standard test method for combustible properties of treated wood by the fire-tube apparatus

**EN 310:1993** Wood based panels. Determination of modulus of elasticity in bending and of bending strength. European Committee for Standardization, Brussels

**EN 317:1993** Particleboards and fiberboards. Determination of swelling in thickness after immersion in water. European Committee for Standardization, Brussels

**EN 319:1993** Determination of tensile strength perpendicular to the plane of the board. European Committee for Standardization, Brussels

**EN 1087-1:1995** Particleboards – Determination of moisture resistance – Boil test

**ISO 13927:2015** Plastics – Simple heat release test using a conical radiant heater and a thermopile detector

**ISO 5660** Cone calorimeter, heat release and smoke production

**Dorobek naukowy**

Publikacje naukowe (\* – autor korespondencyjny, IF – pięcioletni Impact Factor):

1. A. Lekawa-Raus, Ł. Kurzepa, G. Kozłowski, S.C. Hopkins, M. Wozniak, **D. Łukawski**, B.A. Glowacki, K.K. Koziol\*,  
*Influence of atmospheric water vapour on electrical performance of carbon nanotube fibres,*  
Carbon 87 (2015) 18–28 [IF=7,251].
2. K. Rytel\*, M. Widelicka, **D. Łukawski**, F. Lisiecki, K. Kędziński, D. Wróbel,  
*Ultrasonication induced  $sp^3$  hybridization defects in Langmuir-Schaefer layers of turbostratic graphene,*  
Physical Chemistry Chemical Physics 20 (2018) 12777-12784 [IF=3,963].
3. **D. Łukawski**, F. Lisiecki, A. Dudkowiak\*,  
*Coating cellulosic materials with graphene for selective absorption of oils and organic solvents from water,*  
Fibers and Polymers 19 (2018) 524–530 [IF=1,468].
4. **D. Łukawski**, A. Lekawa-Raus, F. Lisiecki, K. Koziol, A. Dudkowiak\*,  
*Towards the development of superhydrophobic carbon nanomaterial coatings on wood,* Progress in Organic Coatings 125 (2018) 23–31 [IF=3,334].
5. **D. Łukawski**\*, W. Grześkowiak, D. Dukarska, B. Mazela, A. Lekawa-Raus, A. Dudkowiak,  
*The influence of surface modification of wood particles with carbon nanotubes on properties of particleboard glued with phenol-formaldehyde resin;*  
Drewno 203 (2019) 93-105 [IF=0,570].
6. G. Stando, G., **D. Łukawski**, F. Lisiecki, D. Janas\*,  
*Intrinsic hydrophilic character of carbon nanotube networks,*  
Applied Surface Science 463 (2019) 227-233 [IF=4,281].
7. **D. Łukawski**, A. Dudkowiak, D. Janczak, A. Lekawa-Raus\*,  
*Preparation and applications of electrically conductive wood layered composites,* Composites Part A: Applied Science and Manufacturing 127 (2019) 105656 (11 pp) [IF=6,050].
8. J. Chen, A. Lekawa-Raus, J. Trevarthen, T. Gizewski, **D. Łukawski**, K. Hazra, S.S. Rahatekar\*, K.K. Koziol\*,  
*Carbon nanotube films spun from a gas phase reactor for manufacturing carbon nanotube film/carbon fibre epoxy hybrid composites for electrical applications,* Carbon, 158 (2020) 282-290 [IF=7,251].

Rozdziały w monografiach naukowych:

1. **D. Łukawski**, K. Rytel, W. Grześkowiak, F. Lisiecki, A. Dudkowiak, *Grafen, nanorurki węglowe i ich zastosowanie w ochronie przed ogniem*, Innowacje w polskiej nauce w obszarze nauk technicznych, J. Doskocz i T. Janiczek (red.), Wydawnictwo Nauka i Biznes (2016), ISBN: 978-83-947095-4-9.

Patenty

1. **D. Łukawski**, A. Dudkowiak, A. Lekawa-Raus, *Sączek hydrofobowy selektywnie pochłaniający oleje i związki organiczne przeznaczony do oczyszczania wód oraz sposób wytworzenia sączka* (P.423094/2017).

Zgłoszenia patentowe

1. A. Lekawa-Raus, K.K. Koziol, **D. Łukawski**, M. Jakubowska, J. Krzemiński, *Multifunctional wood coatings* (GB2548394/2017 oraz WO2017158349/2017).
2. A. Lekawa-Raus, M. Jakubowska, D. Janczak, **D. Łukawski**, A. Dudkowiak, T. Bohun, *Zastosowanie nanomateriałów węglowych do wytwarzania inteligentnych produktów drzewnych* (P.427380).

Inne osiągnięcia naukowe:**a) Kierowanie grantami badawczymi**

1. Preludium, NCN, 2015/19/N/ST8/02184, *Preparatyka i charakteryzacja właściwości pokryć nanorurek węglowych na powierzchni drewna*, 07/2016-12/2019.
2. DS-MK, MNiSW, 06/62/DSMK/0200, *Badanie wpływu ultra-cienkich warstw nanorurek węglowych na palność polimerów*, 03/2016-12/2016.
3. DS-MK, MNiSW, 06/62/DSMK/6201, *Pokrycia celulozy nanomateriałami węglowymi dla selektywnego pochłaniania związków organicznych*, 03/2017-12/2017.

**b) Uczestnictwo w grantach badawczych**

1. ERC Starting Grant, 259061, *High performance and ultralight carbon nanotube wires for power transmission*, 01/2015-07/2015.
2. OPUS, NCN, nr 2017/27/B/ST8/01838, *Analiza procesów fizycznych towarzyszących zapłonowi paliw wzbogaconych nanorurkami węglowymi*, 06/2019-obecnie.

**c) Staże naukowe**

1. IHP GmbH Innovation for High Performance Microelectronics, 2013 (3 miesiące).
2. Department of Materials Science and Metallurgy, University of Cambridge, 2014 (3 miesiące), 2015 (5 miesięcy).
3. Wydział Technologii Drewna, Uniwersytet Przyrodniczy w Poznaniu, 2016 (3 miesiące).

**d) Wystąpienia na konferencjach /sympoziach/ warsztatach naukowych**

1. **D. Łukawski**, K. Rytel, A. Dudkowiak,  
*Wpływ ultra-cienkowarstwowych pokryć polimerów na ich palność,*  
Grafen i inne materiały 2D, Szczecin 2016, wystąpienie ustne.
2. **D. Łukawski**, F. Lisiecki, A. Dudkowiak,  
*Sączki celulozowe pokryte grafenem jako selektywne pochłaniacze związków organicznych,*  
Grafen i inne materiały 2D, Szczecin 2017, wystąpienie ustne.
3. **D. Łukawski**, A. Łękawa-Raus, F. Lisiecki, K. Koziol, A. Dudkowiak,  
*Superhydrophobic wood coatings based on carbon nanomaterials,*  
European Materials Research Society Fall Meeting, Warszawa 2017, wystąpienie ustne.
4. **D. Łukawski**, A. Dudkowiak, D. Janczak, A. Lekawa-Raus,  
*Preparation and applications of electrically conductive wood layered composites,*  
Polish Scientific Networks, Poznań 2019, wystąpienie ustne.
5. **D. Łukawski**, A. Łękawa-Raus, A. Dudkowiak,  
*Graphene-based coatings for wood,*  
NanoTech Poland, Poznań 2016, plakat.
6. **D. Łukawski**, K. Rytel, W. Grzeskowiak, F. Lisiecki, A. Dudkowiak,  
*Wpływ nanomateriałów węglowych na właściwości palne polimerów,*  
Innowacyjni naukowcy, Wrocław 2016, plakat.
7. **D. Łukawski**, A. Łękawa-Raus, F. Lisiecki, K. Koziol, A. Dudkowiak,  
*Hydrofobowe pokrycia drewna na bazie grafenu i innych materiałów węglowych,*  
Grafen i inne materiały 2D, Szczecin 2017, plakat.
8. **D. Łukawski**, F. Lisiecki, A. Dudkowiak,  
*Selective filters based on cellulose/carbon nanomaterials,*  
European Materials Research Society Fall Meeting, Warszawa 2017, plakat.
9. **D. Łukawski**, A. Lekawa-Raus, W. Grzeskowiak, F. Lisiecki, A. Dudkowiak,

*Towards the development of multifunctional wood coatings based on carbon nanotubes,*

19<sup>th</sup> International conference on the science and application of nanotubes and low-dimensional materials, Pekin 2018, plakat

10. **D. Łukawski**, A. Lekawa-Raus, F. Lisiecki, A. Dudkowiak,

*Multifunctional nanocarbon coating on wood,*

InterNano Poland, Katowice 2019, plakat

11. **D. Łukawski**, M. Widelicka, F. Lisiecki, A. Dudkowiak

*Zastosowanie nanopłatków grafenu do wytworzenia hydrofobowych sączków oleju na bazie celulozy*

I Poznańskie mikrosymposium grafenowe, Poznań 2019, plakat

## **Załączniki**

prof. dr hab. Alina Dudkowiak

## OŚWIADCZENIE

Jako współautor prac:

1. D. Łukawski, A. Lekawa-Raus, F. Lisiecki, K. Koziol, A. Dudkowiak, Towards the development of superhydrophobic carbon nanomaterial coatings on wood, *Progress in Organic Coatings* 125 (2018) 23–31
2. D. Łukawski, A. Dudkowiak, A. Lekawa-Raus, Sączek hydrofobowy selektywnie pochłaniający oleje i związki organiczne przeznaczony do oczyszczania wód oraz sposób wytworzenia sączka (P.423094/2017).
3. D. Łukawski, F. Lisiecki, A. Dudkowiak, Coating cellulosic materials with graphene for selective absorption of oils and organic solvents from water, *Fibers and Polymers* 19 (2018) 524–530
4. D. Łukawski, W. Grześkowiak, D. Dukarska, B. Mazela, A. Lekawa-Raus, A. Dudkowiak, The influence of surface modification of wood particles with carbon nanotubes on properties of particleboard glued with phenol-formaldehyde resin, *Drewno* 203 (2019) 93–105.
5. D. Łukawski, A. Dudkowiak, D. Janczak, A. Lekawa-Raus, Preparation and applications of electrically conductive wood layered composites, *Composites Part A: Applied Science and Manufacturing* 127 (2019) 105656: 1–10.

oświadczam, iż mój własny wkład merytoryczny w przygotowanie, przeprowadzenie i opracowanie badań oraz przedstawienie prac w formie publikacji polegał na:

- Ad. 1 Analizie i dyskusji końcowej wersji manuskryptu oraz pracach redakcyjnych.
- Ad. 2 Konsultacjach i pomocy w pracach redakcyjnych.
- Ad. 3 Współtworzeniu planu badań, dyskusji wyników i redakcji końcowej wersji manuskryptu.
- Ad. 4 Konsultacjach oraz pomocy w pracach redakcyjnych.
- Ad. 5 Analizie końcowej wersji manuskryptu.

Jednocześnie wyrażam zgodę na przedłożenie ww. prac przez mgr. inż. **Damiana Łukawskiego** jako część rozprawy doktorskiej w formie spójnego tematycznie zbioru artykułów opublikowanych w czasopiśmie naukowym.



.....  
(podpis współautora)

dr inż. Agnieszka Łekawa-Raus

## OŚWIADCZENIE

Jako współautor prac:

1. D. Łukawski, A. Dudkowiak, D. Janczak, A. Lekawa-Raus, Preparation and applications of electrically conductive wood layered composites, *Composites Part A: Applied Science and Manufacturing* 127 (2019) 105656: 1–10.
2. D. Łukawski, W. Grześkowiak, D. Dukarska, B. Mazela, A. Lekawa-Raus, A. Dudkowiak, The influence of surface modification of wood particles with carbon nanotubes on properties of particleboard glued with phenol-formaldehyde resin, *Drewno* 203 (2019) 93–105.
3. D. Łukawski, A. Lekawa-Raus, F. Lisiecki, K. Koziol, A. Dudkowiak, Towards the development of superhydrophobic carbon nanomaterial coatings on wood, *Progress in Organic Coatings* 125 (2018) 23–31.
4. D. Łukawski, A. Dudkowiak, A. Lekawa-Raus, Sączek hydrofobowy selektywnie pochłaniający oleje i związki organiczne przeznaczony do oczyszczania wód oraz sposób wytworzenia sączka (P.423094/2017).

oświadczam, iż mój własny wkład merytoryczny w przygotowanie, przeprowadzenie i opracowanie badań oraz przedstawienie prac w formie publikacji polegał na:

- Ad. 1 Sformułowaniu problemu badawczego i współtworzeniu planu badań, dyskusji wyników, ostatecznej analizie danych, redakcji końcowej wersji manuskryptu oraz przygotowaniu odpowiedzi dla recenzentów.
- Ad. 2 Przygotowaniu koncepcji badań, analizie wstępnych wyników, które doprowadziły do wykonania badań w ostatecznej formie przedstawionej w publikacji.
- Ad. 3 Zaproponowaniu planu badań, bieżącej dyskusji wyników i współtworzeniu modelu, współdziałanie w interpretacji danych i redakcji finalnej wersji manuskryptu, przygotowaniu odpowiedzi dla recenzentów.
- Ad. 4 Pomoc w realizacji pomysłu wykorzystania hydrofobizowanych materiałów drewnopochodnych.

Jednocześnie wyrażam zgodę na przedłożenie ww. prac przez mgr. inż. **Damiana Łukawskiego** jako część rozprawy doktorskiej w formie spójnego tematycznie zbioru artykułów opublikowanych w czasopiśmie naukowych.

Agnieszka Łekawa-Raus

.....  
(podpis współautora)

dr inż. Filip Lisiecki

## OŚWIADCZENIE

Oświadczam, że w niniejszych publikacjach

1. D. Łukawski, A. Lekawa-Raus, F. Lisiecki, K. Koziol, A. Dudkowiak, *Towards the development of superhydrophobic carbon nanomaterial coatings on wood*, **Progress in Organic Coatings** 125 (2018) 23–31
2. D. Łukawski, F. Lisiecki, A. Dudkowiak, *Coating Cellulosic Materials with Graphene for Selective Absorption of Oils and Organic Solvents from Water*, **Fibers and Polymers** 19 (2018) 524-530

mój udział polegał na wykonaniu pomiarów mikroskopii elektronowej.

Wyrażam zgodę na przedłożenie ww. pracy przez mgr. inż. **Damiana Łukawskiego** jako część rozprawy doktorskiej w formie zbioru opublikowanych i powiązanych tematycznie artykułów naukowych.

Lisiecki Filip

(podpis współautora)

Dr inż. Wojciech Grześkowiak  
Uniwersytet Przyrodniczy w Poznaniu

## OŚWIADCZENIE

Oświadczam, że w niniejszej publikacji

D. Łukawski, W. Grześkowiak, D. Dukarska, B. Mazela, A. Lekawa-Raus, A. Dudkowiak,  
*The influence of surface modification of wood particles with carbon nanotubes on properties of particleboard glued with phenol-formaldehyde resin*, **Drewno** 203 (2019) 93-105.

mój udział polegał na współudziale przy planowaniu eksperymentu, wykonaniu pomiarów odporności na ogień oraz współudziale przy redagowaniu części manuskryptu opisującej palność.

Wyrażam zgodę na przedłożenie ww. pracy przez mgr. inż. **Damiana Łukawskiego** jako część rozprawy doktorskiej w formie zbioru opublikowanych i powiązanych tematycznie artykułów naukowych.

.....  


(podpis współautora)

Poznań, dnia 18.02.2020

Dr hab. inż. Dorota Dukarska  
Uniwersytet Przyrodniczy

## OŚWIADCZENIE

Oświadczam, że w niniejszej publikacji

D. Łukawski, W. Grześkowiak, D. Dukarska, B. Mazela, A. Lekawa-Raus, A. Dudkowiak, *The influence of surface modification of wood particles with carbon nanotubes on properties of particleboard glued with phenol-formaldehyde resin*, **Drewno** 203 (2019) 93-105.

mój udział polegał na wytworzeniu płyt wiórowych wykorzystując zmodyfikowane wióry, zbadaniu ich właściwości wytrzymałościowych i wodoodporności oraz analizie uzyskanych w tym zakresie wyników badań.

Wyrażam zgodę na przedłożenie ww. pracy przez mgr. inż. **Damiana Łukawskiego** jako część rozprawy doktorskiej w formie zbioru opublikowanych i powiązanych tematycznie artykułów naukowych.

..........

(podpis współautora)

Poznań , dnia 20/02/2020

Prof. dr hab. Bartłomiej Mazela  
Uniwersytet Przyrodniczy

## OŚWIADCZENIE

Oświadczam, że w niniejszej publikacji

D. Łukawski, W. Grześkowiak, D. Dukarska, B. Mazela, A. Lekawa-Raus, A. Dudkowiak,  
*The influence of surface modification of wood particles with carbon nanotubes on properties of particleboard glued with phenol-formaldehyde resin*, **Drewno** 203 (2019) 93-105.

mój udział polegał na konsultacji założeń metodycznych oraz korekcie finalnej wersji publikacji.

Wyrażam zgodę na przedłożenie ww. pracy przez mgr. inż. **Damiana Łukawskiego** jako część rozprawy doktorskiej w formie zbioru opublikowanych i powiązanych tematycznie artykułów naukowych.



(podpis współautora)

dr inż. Daniel Janczak

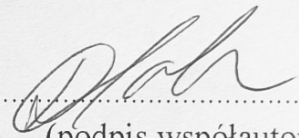
## OŚWIADCZENIE

Oświadczam, że w niniejszej publikacji

D. Łukawski, A. Dudkowiak, D. Janczak, A. Lekawa-Raus, *Preparation and applications of electrically conductive wood layered composites*, **Composites Part A: Applied Science and Manufacturing** 127 (2019) 105656: 1-10.

mój udział polegał na przygotowaniu warstw metodą sitodruku.

Wyrażam zgodę na przedłożenie ww. pracy przez mgr. inż. **Damiana Łukawskiego** jako część rozprawy doktorskiej w formie zbioru opublikowanych i powiązanych tematycznie artykułów naukowych.



.....  
(podpis współautora)

Poznań, dnia 13.02.2020

Prof. Krzysztof Koziol  
Cranfield University

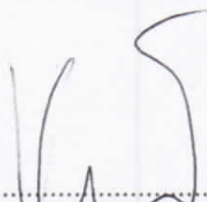
### OŚWIADCZENIE

Oświadczam, że w niniejszej publikacji

D. Łukawski, A. Lekawa-Raus, F. Lisiecki, K. Koziol, A. Dudkowiak, *Towards the development of superhydrophobic carbon nanomaterial coatings on wood*, **Progress in Organic Coatings** 125 (2018) 23–31

mój udział polegał na wsparciu merytorycznym przy planowaniu eksperymentu.

Wyrażam zgodę na przedłożenie ww. pracy przez mgr. inż. **Damiana Łukawskiego** jako część rozprawy doktorskiej w formie zbioru opublikowanych i powiązanych tematycznie artykułów naukowych.

  
.....  
(podpis współautora)  
K. Koziol

**Przedruk publikacji [Łukawski, POC 2018]**

D. Łukawski, A. Lekawa-Raus, F. Lisiecki, K. Koziol, A. Dudkowiak, Towards the development of superhydrophobic carbon nanomaterial coatings on wood, *Progress in Organic Coatings* 125 (2018) 23–31.



## Towards the development of superhydrophobic carbon nanomaterial coatings on wood



Damian Łukawski<sup>a</sup>, Agnieszka Lekawa-Raus<sup>b,e</sup>, Filip Lisiecki<sup>c</sup>, Krzysztof Koziol<sup>d,e</sup>, Alina Dudkowiak<sup>a,\*</sup>

<sup>a</sup> Faculty of Technical Physics, Poznan University of Technology, 60-965 Poznan, Poland

<sup>b</sup> Faculty of Mechatronics, Warsaw University of Technology, 02-525 Warsaw, Poland

<sup>c</sup> Institute of Molecular Physics, Polish Academy of Sciences, 60-179 Poznan, Poland

<sup>d</sup> Enhanced Composites & Structures Centre, Cranfield University, MK43 0AL Cranfield, UK

<sup>e</sup> Department of Materials Science and Metallurgy, University of Cambridge, Cambridge CB3 0FS, UK

### ARTICLE INFO

#### Keywords:

Carbon nanotubes  
Graphene  
Hydrophobic coating  
Rose petal effect  
Wood

### ABSTRACT

Carbon nanomaterials (CNMs) have recently been used to form superhydrophobic coatings on metals, synthetic polymers or textiles. Here we investigate the possibility of using carbon black (CB), graphene (Gr) and carbon nanotubes (CNTs), as water repellent agents on naturally hydrophilic wood. We show that it is possible to form homogeneous CNM coatings on any type of wood via simple methods of drop casting and dip coating, using CNMs dispersed in organic solvents or water. Contact angle measurements of wood coated with only 0.05 g/m<sup>2</sup> CNTs and 0.25 g/m<sup>2</sup> Gr gave the results exceeding 130°, indicating apparent hydrophobicity. Yet, high adhesion of the droplets was observed, simultaneously suggesting a “rose petal” type of superhydrophobic behavior. That may be explained by the formation of micro-nano architectures in which low surface energy CNMs deposited on microrough surface of wood cause superhydrophobicity. Yet, due to heterogeneity of wood, some part of hydrophilic surface is still uncovered, resulting in high adhesion of water. Finally, although Gr and CNT were only physically bond to wood surface, the hydrophobic properties of CNM coatings were maintained after sandpaper abrasion test. Moreover, wood fibers and particles covered with Gr showed the decrease of water absorption equal 98% and 87%, respectively.

### 1. Introduction

Although, wood has been successively replaced by concrete and steel, over the years, it is still one of the extremely widely used construction materials. On the contrary to the past trends modern world sees wood as an extremely valuable resource due to the fact that it is a fully natural, renewable and biodegradable material and has low carbon footprint. Unfortunately, wood still has several disadvantages, which have been the limiting factors before. One of them is low resistance to water which deteriorates its mechanical performance, increases construction mass [1] and enables the growth of mold [2]. Although many techniques of surface preservation has been recently developed [3–5], none of them can fully solve the hydrophobicity problem in every application of wood, therefore any new exploration in this area may be highly valuable. Here we propose, for the first time ever, that recent developments in nanotechnology area could help in this respect and offer inexpensive and easily up-scalable method of

hydrophobization of wood and its composites by the use of carbon nanomaterials (CNMs).

Due to unique properties and rapidly decreasing price, carbon nanomaterials, such as graphene (Gr) and carbon nanotubes (CNTs), have recently found interest in both science and industry. It has been observed that these carbon allotropes properly structured at micro-nanoscale may show superhydrophobic effect and form various types of water repellent materials and coatings. Particularly pronounced effect imitating water repellent properties of lotus leaves (also referred to as “lotus effect”) has been observed in CNT forests i.e. vertically aligned CNT arrays [6–9]. Lotus leaves exhibit high water contact angles – above 130° and low adhesion with sliding angles below 5°. Therefore, raindrops can easily roll off the surface, without wetting the leaves. This effect is caused by the unique micro-nanoscale hierarchical and rough architectures of the leaves surfaces [10]. Various types of water repellent behavior have been also found in other CNT, Gr architectures including graphene sponges [11], films [12,13], and foams [14,15],

\* Corresponding author.

E-mail address: [alina.dudkowiak@put.poznan.pl](mailto:alina.dudkowiak@put.poznan.pl) (A. Dudkowiak).

carbon black (CB) coatings [16] or nanoengineered CNTs [17].

Further studies showed that powders of CNMs may act as hydrophobic agents for other materials, including metal meshes [18,19], polymer sponges [20], textiles and cellulosic materials like cotton [21–26]. All of these substrates are characterized by micro-porous structure, which in combination with low surface energy of carbon allotropes is responsible for superhydrophobicity of the final product. Graphene has been used in cellulose nanocomposites [22,23], showing both increased hydrophobicity and enhanced mechanical performance.

In this paper, we test the possibility of using Gr and CNT and for comparison of CB which is a well-known high specific surface area hydrophobic carbon allotrope of amorphous structure as superhydrophobic agents in wood technology applications. Although wood is a cellulose rich material and its chemical composition is therefore somehow similar to cotton (90% cellulose content), yet wood consists of comparably significant amounts of lignin and hemicelluloses which together may exceed even 50% of woods mass. Moreover, wood comprises fatty acids, resin acids, waxes and terpenes [27]. Woods with higher extract content in general are more hydrophobic [28]. Therefore, it is a much more complex material than cotton and its interaction with CNMs might be considerably different from cotton-CNM ones. Additionally, wood has also its own specific surface microstructure which is influenced by processing such as sawing or polishing. All these aspects could influence the formation of CNM coatings and their wetting characteristics. Moreover, wood consists of nano, micro- and mesopores, which are specific to each wood species. The influence of roughness onto wetting of wood is not straightforward, but it was presented that while increasing the roughness of wood the contact angle at first slightly decreases, but for very rough surface it increases and wood becomes even more hydrophobic [28].

The purpose of this paper is fourfold. First, we demonstrate that most popular types of wood may be coated by CNMs using simple methods of dip coating and drop casting. We show that both organic solvent and water-based dispersions of CNMs may ensure the deposition of pure CNM materials on the surface of wood. Next, we analyze the morphology of coatings formed on bulk wood and wood-based products such as fibers and wood particles used for the production of popular wood composites such as fiberboards or particleboards, and prove their hydrophobic properties. Finally, the model of hydrophobicity of our coatings is proposed.

## 2. Experimental

### 2.1. Materials

The initial experiments were performed on balsa (*Ochroma pyramidale*), as a highly water absorptive wood, with a significant cellulose content and homogeneity [29]. The comparative tests were further carried out on scots pine (*Pinus sylvestris*), oak (*Quercus*), birch (*Betula*), beech (*Fagus*) and poplar (*Populus alba*) woods, characterized by different pore distribution and chemical composition [30,31]. Industrial grade, sphere-like CB (N-550) was obtained from Konimpex Ltd. Gr with average diameter of 300 nm and thickness below 1 nm was obtained from Cambridge Nanosystems Ltd. (Camgraph G1). Industrial grade, short and tangled multiwall carbon nanotubes (MWCNTs) (NC-7000) were ordered from Nanocyl SA. Sodium dodecylbenzenesulfonate (SDBS), technical grade, was purchased from Sigma Aldrich. Dichloromethane (DCM), spectroscopy grade, was ordered from Avantor Performance Materials Poland SA. Water was filtrated by Milli-Q® ultrapure water system.

### 2.2. Preparation of coatings

The procedure started from preparation of CNM dispersions in an organic solvent. At first, all CNMs were mixed with DCM in the concentrations of 1 mg/2 ml CB, 1 mg/30 ml and 1 mg/2 ml Gr and 1 mg/

60 ml MWCNT. Then the samples were sonicated for 10–20 mins (power 60 W per 40 ml of mixture) to obtain uniform dispersions. These CNM dispersions were further deposited onto wood via drop-casting and the samples were dried at 40 °C on a hot plate. Due to very high vapor pressure of DCM, the applied heating should be sufficient to remove any DCM trapped between CNM and wood surface. The droplets were applied slowly in order to let DCM to evaporate before next droplet was casted. Due to capillary forces in wood pores the suspension was naturally distributed onto the surface, but no CNMs were found inside wood.

The amount of deposited dispersion was set to obtain two selected values of mass per square meter. Thus, in order to obtain 0.05 g/m<sup>2</sup> Gr (1.5 ml of 1 mg/30 ml) and CNT (3 ml of 1 mg/60 ml) were drop casted onto 10 cm<sup>2</sup> of balsa wood (BW). Whilst for 0.25 g/m<sup>2</sup> (0.5 ml of 1 mg/2 ml) CB and Gr was deposited on 10 cm<sup>2</sup> of BW. Gr was chosen for CNM deposition on various wood types, due to good stability of highly concentrated dispersion. Gr was deposited by dip-coating in 1 mg/2 ml Gr repeated 10 times. The same procedure was applied for wood fibers and wood particles.

Although the use of organic solvent such as DCM enables investigation of CNM deposition on wood, it is not convenient in potential industrial applications. Thus, the aqueous dispersion was tested as well. The aqueous dispersions were prepared using 0.3 g of SDBS and 0.3 g of CNM per 100 ml of ultrapure water. The concentration was relatively high in order to obtain more hydrophobic surface. Then, it was sonicated for 10–20 mins similarly as for organic solvent dispersions. CNMs were deposited on wood surface via dip-coating, followed by drying at 90 °C. Afterwards, the samples were washed 3 times in order to remove the outer layer of the surfactant and again immersed in CNM dispersion. The procedure was repeated three times, to obtain 3 layers of CNMs. Then, according to Makowski et al. [24] SDBS was removed by several washing and drying cycles.

### 2.3. Surface imaging

CNMs were dispersed via Hielscher 400 St (400 W) ultrasonic horn. The SEM images were taken by FEI Nova NanoSEM 650 and the EDS by Bruker XFlash® 5010 detector. Due to excessive charging under SEM, wood coated with CB was covered with 10 nm thick layer of platinum (Pt) which enabled successful imaging of the surface. The fluorescence microscopy images were taken by Zeiss Laser Scanning Microscope (LSM) 510, using a mercury lamp HXP 120 and a filter set 38. Each image was taken with the exposure time of 300 ms. The roughness, calculated as quadratic mean deviation of all profile height values ( $R_{qa}$ ), was measured using the confocal mode of Zeiss LSM 510.

### 2.4. Roughness and robustness measurements

The roughness of wood was measured by Zeiss LSM 510. The measurement and calculations were performed according to [32,33]. Briefly, topography map was obtained by LSM, using argon laser (458 nm) and EC Epiplan-Nefluar 20 × lens. Then, the roughness was calculated by ZEN2011 software, as the arithmetic mean of total surface height values  $RS_a$ , according to DIN EN ISO 428. The topography map was taken in five random spots on each wood type and the average value is presented in manuscript. The standard deviation of the mean was used as measurement uncertainty.

To demonstrate the robustness of CNM coated wood we performed sandpaper abrasion test (P100 grit) according to Chen et al. [34]. Briefly, 3 cm<sup>2</sup> wood coated with CNM were placed onto sandpaper facedown under a weight of 17 g (approximately 550 Pa). Then, the sample was dragged thirty times 10 cm longitudinally and transversely in each direction.

## 2.5. Wetting measurements

Contact angle ( $\theta$ ) was measured with a CCD camera (Nikon D300s). Droplets of  $13.0 \pm 0.5 \mu\text{l}$  were deposited using a Hamilton microsyringe ( $25 \mu\text{l}$ ). The volume was increased as compared to the standard contact angle measurements due to very high roughness of wood surface.

The angles were measured with the aid of Dropsnake plugin to ImageJ software [35]. The contact angles on each surface were measured for three droplets and the result is presented as a mean value of all three measurements with a standard deviation of the mean. Water shedding angle (WSA) was measured according to the Zimmerman procedure [36]. The droplets of  $13.0 \pm 0.5 \mu\text{l}$  were deposited on the surface under the set angle. The angle was controlled by a precise goniometer to the accuracy of  $1^\circ$ . The starting level was  $50^\circ$  and, when all the droplets fell from the surface, rolled off or bounced away, the inclination was decreased by  $5^\circ$ . The distance between the end of the needle and the surface was constant and equal to  $20 \pm 1 \text{ mm}$ . The procedure was repeated until at least one drop would not completely roll off the surface.

The water absorption (WA) was measured according to the following procedure. First, wood-based products were weighed and placed in a glass container. Next, the container was filled with deionized water. After one minute, samples were collected using a strainer. The excessive amount of water was gently removed via cellulose wipe and the samples were weighed again. The WA was calculated as the amount of water soaked up into a 1 g of the sample. The WA of wood and wood particles was measured for 3 different sets, each weighing 0.2 g.

## 3. Results and discussion

### 3.1. Characterization of CNM covered wood

Covering of wood with various CNMs caused darkening of the surface (Fig. 1A). Thus, a bare eye inspection gave a rough estimation of the uniformity of the coatings and their thickness proving that at macroscale the coatings are quite homogeneous independent of the

thickness. However, the same darkening obstructed a microscale characterization of the samples via classical optical microscopy. To overcome this problem well-known fluorescent properties of wood [37] and fluorescence quenching of CNMs were utilized [38]. High contrast between fluorescing wood and dark CNMs allowed sufficient qualitative microanalysis of the coated samples and their simple comparison (Fig. 1B). The comparison of BW (Fig. 1C) and BW coated with Gr (Gr/BW) (Fig. 1B) leads to a few conclusions. First, it is noticeable that the fluorescence image of Gr/BW is less intensive over the whole surface, which confirms that Gr is deposited on the entire area of BW. However, it is also observable that the image of Gr/BW is not just the less intensive version of BW, but it has some additional darker spots which may be attributed to the presence of nanomaterial agglomerates, placed in favorable spots of the rough surface. This hypothesis was confirmed for higher magnification ( $\times 20$ ) images (Fig. 1D). Generally, the fluorescence images of CNT coated BW (CNT/BW) and CB coated BW (CB/BW) showed a similar coverage and it is impossible to distinguish CNMs using only fluorescence microscopy (Supplementary materials, Figs. S1, S2).

In order to perform further analysis, some SEM images were also taken. The lower magnification images show the homogeneity of CNM deposition (Fig. 2A,C,E), while the higher magnification images present the structure of CB/BW (Fig. 2B), Gr/BW (Fig. 2D) and CNT/BW (Fig. 2F), respectively. It may be observed that CB structures are agglomerated into sub- or micrometer clusters (Fig. 2A,B). CB clusters are randomly distributed over the surface of wood and do not create macroscale agglomerates. Overall, CB provided very poor coverage, as compared to further materials (Fig. 2A). Grs formed mostly a multilayer structure on wood surface (Fig. 2D) with sponge-like morphology for most of the surface. Although a few uncoated or simple Gr flake coated places were also found they did not large fraction of the surface area. Grs were found to deposit both on flat surface and on irregularities and it was found that they do not completely fill the holes in the porous wood structure (Supplementary materials, Figs. S3, S4).

Since CNTs were deposited in smaller amounts, CNT coatings did not form any sponge-like structures (Fig. 2F). Although CNTs were highly entangled and coatings were not homogeneous, they covered

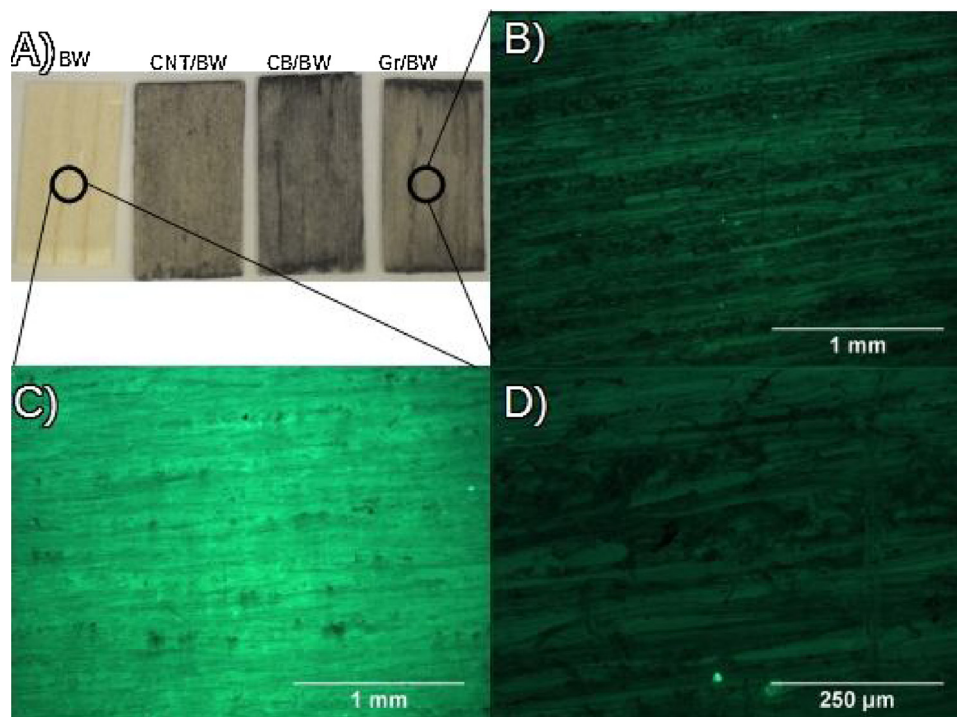


Fig. 1. A) Camera images of BW, and BW covered with CNT, CB and Gr. Fluorescence microscopy image of C) BW; B) and D) Gr/BW.

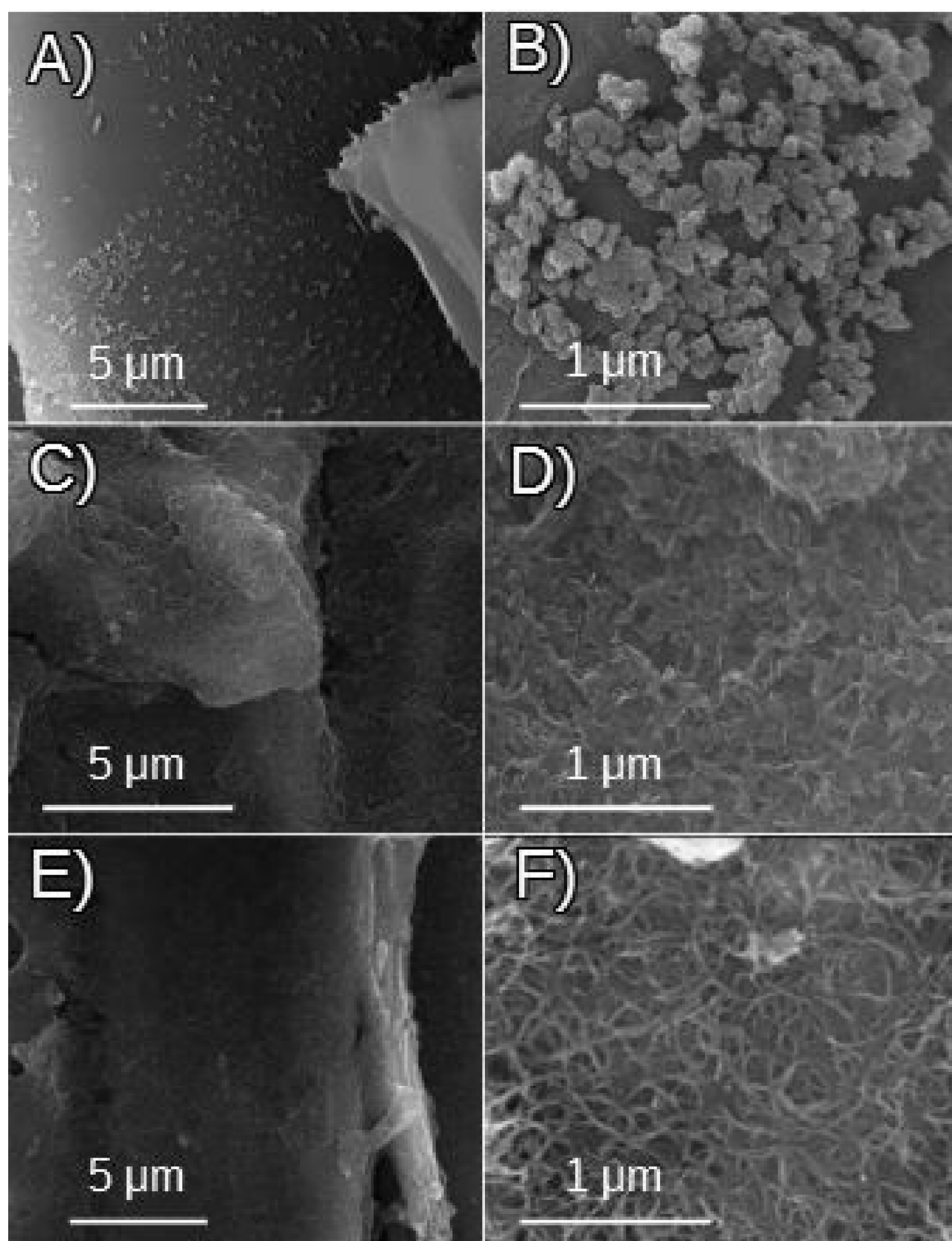


Fig. 2. SEM images of A) and B) CB/BW, C) and D) Gr/BW, E) and F) CNT/BW.

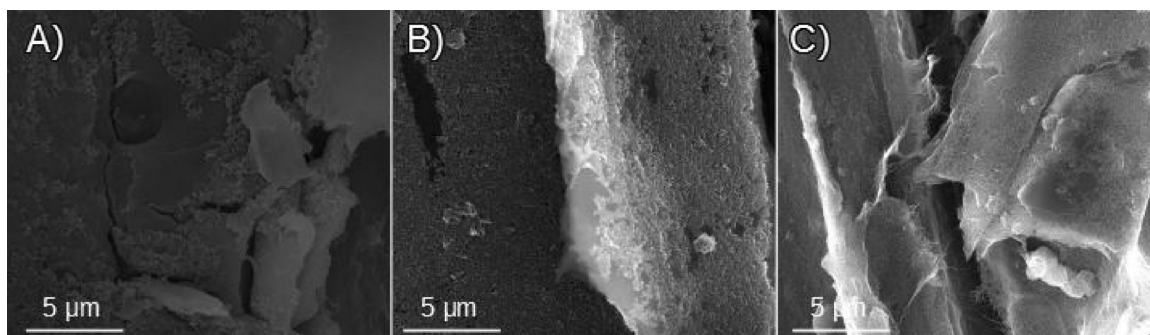


Fig. 3. SEM images of A) CB/H<sub>2</sub>O/BW B) Gr/H<sub>2</sub>O/BW, C) CNT/H<sub>2</sub>O/BW.

most of the surface. Additionally, CNTs created nets between wood irregularities, which may have prevented further CNTs from entering and filling the hidden parts of wood. Therefore, some small parts of wood surface fraction may be unprotected. Yet, despite a small amount of the

material (0.25 g/m<sup>2</sup> and 0.05 g/m<sup>2</sup> for Gr and CNT, respectively) in general, both Gr/BW and CNT/BW had very high CNM coverage fraction. On the basis of SEM images it was expected that CNTs and Grs may create a waterproofing layer, whilst the hydrophobic character of CB/

BW would be highly unlikely.

Although the results of deposition CNMs onto the surface of wood are sufficient in the research, it would be inconvenient to use organic solvents on industrial scale. Thus, analogous BW samples were also coated with the aid of aqueous dispersions of CNMs, using SDBS as a surfactant (CNM/H<sub>2</sub>O/BW) and via the industrially popular dip-coating. All CNMs i.e. CB, Gr and CNT (CB/H<sub>2</sub>O/BW, Gr/H<sub>2</sub>O/BW and CNT/H<sub>2</sub>O/BW, respectively) were used for these tests. The SEM images were taken to investigate the quality of aqueous surfactant coating.

The SEM image showed again that CB was not deposited homogeneously on the wood surface. Many agglomerates exceeding 5 μm were found, yet analysis of a few SEM images showed that the coverage fraction did not exceed 50% (Fig. 3A). This may have been caused by two factors. First, CB shows an increased propensity to form agglomerates when deposited from high concentrated dispersions (Fig. 3A). Secondly, it was found that CB was partly washed from the surface of wood during rinsing process, which may be caused by lower adhesive force between CB and wood, than in case of Grs and CNTs.

SEM images of Gr/H<sub>2</sub>O/BW showed a uniform coverage of almost all the surface of wood with a multilayer of Gr (Fig. 3B). Similarly to Gr, CNT/H<sub>2</sub>O/BW exhibits a very uniform coating over the whole surface (Fig. 3C). However, for CNTs some micrometer sized agglomerates were also found. These may be caused by trapped surfactant, CNT bundling, metal impurities or wood imperfections.

Due to the fact that the trapped surfactant may influence the wetting behavior of the CNM coated surfaces we performed EDS measurements before and after SDBS removal procedures. It is visible that for Gr/H<sub>2</sub>O/BW samples the rinsing process decreases the EDS signal of sulfur and sodium (Fig. 4). Therefore, sulfur and sodium are rinsed out of Gr/H<sub>2</sub>O/BW. As, neither sodium nor sulfur should be found in wood or CNMs, the EDS spectra proves the effectiveness of SDBS rinsing, which agrees with the previous research result [24]. Similar EDS measurement was performed for CB/H<sub>2</sub>O/BW and CNT/H<sub>2</sub>O/BW and showed slightly less intensive than for Gr/H<sub>2</sub>O/BW but still a very significant decrease in the signals assigned to S and Na (Supplementary materials, Figs. S6, S7) indicating that in both cases most of SDBS is successfully removed enabling the formation of pure CNT and Gr coatings.

Finally, the above coating methods were also tested on other wood species to check whether the deposition was dependent on wood characteristics such as chemical composition or pore size distribution. The tests were performed on both soft woods and hard woods, with different surface roughness, morphology and chemical structure (Table 1). The materials chosen were pine which is an example of a softwood; poplar, beech, oak and birch which are hardwoods with different sizes of pores, varying overall surface roughness, and cellulose and lignin content. Moreover, each wood type show specific roughness also dependent on the smoothing procedure. The roughness of wood

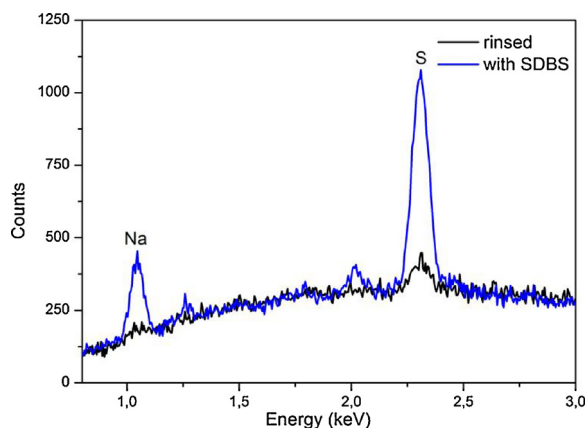


Fig. 4. EDS spectra of Gr/H<sub>2</sub>O/BW, before and after rinsing.

Table 1

The roughness and chemical composition of various wood species and water contact angle of wood and Gr/wood obtained by the dip coating method.

Type of wood	RS <sub>a</sub> (μm)	Characteristic pore radius <sup>a</sup> [31] (μm)	Cellulose content [30] (%)	Lignin content [30] (%)	θ <sub>0</sub> [°]	
					Pure wood	Gr/wood
balsa	10 ± 2	–	40	29	74 ± 3	137 ± 5
birch	11 ± 2	873	46	20	97 ± 5	127 ± 4
beech	5 ± 1	1571	48	19	50 ± 3	137 ± 4
oak	7 ± 1	178	47	22	59 ± 3	138 ± 2
pine	4 ± 1	4044	57	28	67 ± 5	104 ± 5
poplar	7 ± 1	–	48	19	42 ± 9	128 ± 2

<sup>a</sup> The results of mercury intrusion porosimetry.

samples were measured according to Section 2.4, and varied from 4.1 for pine to 10.9 for birch. Balsa, was an example of hardwood with an extremely large porosity, reaching 91% [29]. Due to easiness of Gr dispersion, it was chosen as the representative CNM for these tests.

The analysis of all these samples did not show any significant differences with regard to coating formation, uniformity or durability of these coatings. Only in the case of pine wood it was visible that CNM was not deposited uniformly (Supplementary materials, Figs. S8, S9), due to the clear coexistence of earlywood and latewood. In comparison to earlywood, the latewood shows higher density and mechanical strength, smaller cavities and thicker walls, which causes also different surface properties [31]. The measured roughness was equal 5 ± 1 μm and 2.4 ± 0.3 μm, for earlywood and latewood respectively. The higher roughness causes more favorable deposition onto earlywood and in consequence heterogeneity of CNM coating, and worse CNMs deposition. The visible heterogeneity may cause worse water repellent properties of CNM/pine than in the other CNM/wood samples.

In general, we may conclude that CNMs are deposited in a similar way using either organic solvent or water. Additional SDBS present in aqueous dispersions is effectively removed and should not influence the hydrophobic behavior of the surfaces. Yet, irrespective of the solvent, we observe that the quality of coating is dependent on the nanomaterial used. Grs and CNTs uniformly cover most of the surfaces, while CB forms separated agglomerates, which indicates that the hydrophobic effect may be dependent on the applied CNM. It was also proved that CNMs may be successfully deposited onto various types of wood, via the simple dip coating method. Finally, it was found that the morphology and chemical composition of wood has little influence on the coating formation.

### 3.2. Wetting of CNM covered wood

Further, wetting properties of all the samples were investigated experimentally, by deposition of water droplets on their surfaces and measurement of the change in contact angle over time, as shown by the examples in Fig. 5.

A simple visual analysis of Fig. 5 indicates that coating of wood with any of the carbon nanomaterials may increase contact angle of water as compared to pure BW, both straight after deposition (within 1 s) and after 60 s dwell time. The in-depth analysis of measurements performed for a set of samples (Table 1) gives some more insight into this matter. As expected, the uncoated BW showed a clear hydrophilicity. The initial contact angle amounted to θ<sub>0</sub> = 75 ± 3° and quickly decreased due to wetting of the wood surface and soaking of the droplet, becoming 0° after 60 s (θ<sub>60</sub> = 0°). Although the results showed some divergence due to heterogeneity of wood morphology, the hydrophilic character of the surface was observed for all the pure samples.

The measurements of CB dispersed in DCM and deposited by drop casting on BW surface with the area density of 0.25 g/m<sup>2</sup> show that the latter amount indeed enables the increase in the initial contact angle to

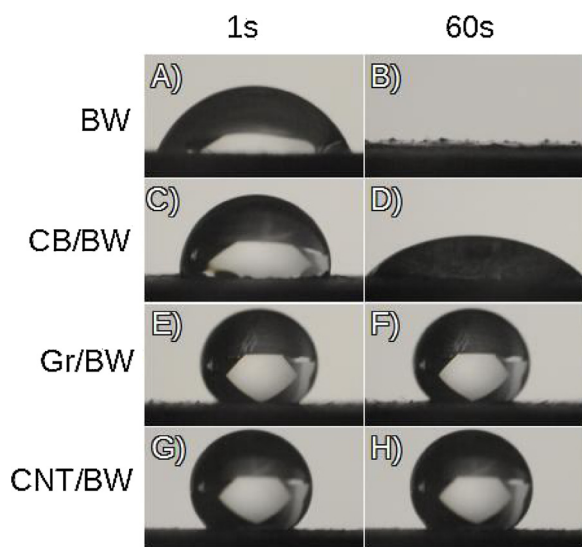


Fig. 5. Contact angle  $\theta$  measured immediately after water deposition (A, C, E, G) and after 60 s (B, D, F, H). A) and B) pure balsa wood, C) and D) CB/BW, E) and F) Gr/BW, G) and H) CNT/BW.

the hydrophobic level i.e. above  $90^\circ$  ( $\theta_0 = 104 \pm 2^\circ$ ). Unfortunately, this contact angle decreases quickly amounting to only  $\theta_{60} = 30^\circ$  after 60 s. Due to a weak effect of relatively thick coating ( $0.25 \text{ g/m}^2$ ), no research on other area density was made. The situation was quite different for Gr/BW. In this case two coatings with area density of  $0.05 \text{ g/m}^2$  and  $0.25 \text{ g/m}^2$  were deposited by drop casting from DCM dispersion. Already,  $0.05 \text{ g/m}^2$  significantly delayed soaking of water into the sample and increased the initial contact angle to  $\theta_0 = 120 \pm 7^\circ$  and  $\theta_{60} = 78 \pm 16^\circ$ . Increase in the amount of deposited Gr improved the results further and gave the initial contact angle of  $\theta_0 = 133 \pm 3^\circ$  which did not decrease below  $90^\circ$  after 60 s and reached to  $\theta_{60} = 125 \pm 5^\circ$ . This coating may be well considered superhydrophobic. However, even better results were obtained for CNT/BW for which only  $0.05 \text{ g/m}^2$  coating gave the initial contact angle of  $\theta_0 = 143 \pm 3^\circ$  with a decrease to  $130 \pm 4^\circ$  after 60 s.

As CNM coatings is bonded with wood only by physical interactions, it was important to determine their robustness. Therefore, sandpaper abrasion test was performed (Section 2.4). According to SEM images (see Supplementary materials, Figs. S10–S12) no significant difference between samples before and after sandpaper treatment were observed. CB/wood samples show many uncovered spots both before and after sandpaper abrasion test (see Supplementary materials, Fig. S10). Gr/wood and CNT/wood before abrasion tests showed full coverage of CNMs onto wood, but after sandpaper tests, some uncovered spots were noticed (see Supplementary materials, Figs. S11–S12). However, still, Gr/CNTs cover the majority of wood surface. Water contact angles of CB/BW, Gr/BW and CNT/BW measured after sandpaper test amounted to  $80 \pm 9^\circ$ ,  $129 \pm 4^\circ$  and  $136 \pm 6^\circ$ , respectively. The significant drop was observed for CB/BW, whilst for Gr/BW and CNT/BW the decline was almost statistically insignificant. This is because Gr and CNT have high surface areas, and the van der Waals interactions with wood are much stronger than for CB particles.

Similar contact angle tests were performed for CNM covered BW with the coatings produced from water dispersions via the dip coating method (Table 2). As might have been expected, the presence of surfactant made the coatings hydrophilic (Fig. 6D). However, after the removal of surfactant CNT/H<sub>2</sub>O/BW and Gr/H<sub>2</sub>O/BW became clearly superhydrophobic, with  $\theta_0$  exceeding  $130^\circ$  (Fig. 6A, Table 1). The contact angle of superhydrophobic surfaces was stable even ten minutes after droplet deposition, and for CNT/H<sub>2</sub>O/BW it was equal  $134^\circ$  (Fig. 6B). Yet, hydrophobicity was not observed for CB coatings which was probably due to insufficient amount of this CNM deposited upon

triple dip coating.

All the above presented results indicate that the coating of BW with CNTs and Gr introduces real superhydrophobicity into the normally hydrophilic wood surface. However, we have also noticed that although the observed contact angles were high and stable, the deposited droplets were also quite firmly attached to the surface (Fig. 6C) and did not easily roll off. To investigate the phenomenon further we performed some WSA measurements according to [32] (see also Experimental section) which takes into account that some of the surfaces hold the droplets even upside-down. This procedure allows the determination of an angle above which the droplets are bounced off or rolled off the surface without any water shedding.

Due to relatively high affinity of BW and CB/BW to water, their WSA exceeded  $50^\circ$ . The lowest WSA was observed for CNT/BW and CNT/H<sub>2</sub>O/BW, with the best individual sample of CNT/H<sub>2</sub>O/BW showing WSA =  $15^\circ$ , which is in agreement with the contact angle results (Table 2). The above results indicate that although we observe clear hydrophobicity with the contact angles similar to those mentioned in the introduction, CNT carpets, the high adhesion of water droplets point at a different mechanism responsible for the superhydrophobic effect of CNTs and Gr deposited on wood. This further indicates that the whole superhydrophobic effect could potentially be dependent on such parameters as chemical composition, wood porosity and roughness. In order to explore these issues further we investigated the wetting properties of other wood species coated with Gr.

Gr was deposited from highly concentrated dispersion ( $0.5 \text{ mg/ml}$ ) onto pine, oak, birch, beech and poplar wood, via the dipcoating method. It was proved that each wood covered with Gr (Gr/wood), besides pine, is highly hydrophobic (Table 1). The slightly inferior behavior of pine may be explained by the mentioned before nonuniform deposition of CNMs onto latewood and earlywood (Supplementary materials, Fig. S12). This effect may be diminished by using other deposition methods. It is visible that most of the results are similar to those obtained for balsa indicating that the hydrophobic effect is largely independent of the pore size distribution, roughness and chemical composition (Table 1). The result is highly important as it shows that any wood covered with CNMs creates unique micro-nano structure which increases the contact angle to approx.  $130^\circ$ . Moreover, that means, that Gr/CNTs either are small enough to fill the pores (see Supplementary materials, Figs. S13–S16) or large enough to cover the pores preventing (Fig. 3C) from water soaking.

However, it was also important to examine, whether the industrial processing, such as polishing may affect hydrophobicity. Thus, in order to determine whether the roughness of wood influence the deposition of CNMs, poplar wood sample was mechanically polished using micro grinder. Then Gr was deposited with the earlier described dip-coating procedure. It was found that although the roughness of the surface dropped from  $12 \pm 1 \mu\text{m}$  to  $8 \pm 1 \mu\text{m}$  after polishing, it did not give any statistically significant change in the measured angles equal  $138 \pm 3^\circ$  and  $135 \pm 3^\circ$ , respectively.

The samples were coated with Gr and tested in terms of water absorption according to Sections 2.1 and 2.3, respectively. For pure wood fibers, water absorption amounted to  $19 \pm 3 \text{ g/g}$  and decreased to  $0.3 \pm 0.3 \text{ g/g}$  after Gr deposition. In case of pure wood particles water absorption amounted to  $1.3 \pm 0.2 \text{ g/g}$  and decreased to  $0.17 \pm 0.03 \text{ g/g}$  for Gr covered particles, respectively. Thus, both wood fibers and wood particles became water repellent after Gr coating.

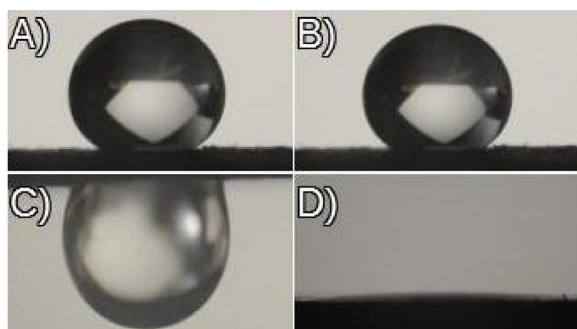
### 3.3. Model of wetting

It is well known from nature that superhydrophobic effect may be observed in the materials of specific nano-micro structure in which nanoelements are uniformly distributed over micro-rough surface such as in lotus leaves [10]. The explanation of this phenomenon may be described with the use of Wenzel's model [40] and Cassie's model [41].

**Table 2**

The wetting properties of balsa wood covered with carbon nanomaterials by the drop casting and dip coating methods in various configurations.

Sample	CNM in dispersion	Medium	Deposition	$\theta_0$ [°]	$\theta_{60}$ [°]	WSA [°]
BW	–	–	–	$75 \pm 3$	$0 \pm 4$	> 50
CB/BW	CB 1 mg/2 ml	DCM	Drop casting (0.25 g/m <sup>2</sup> )	$104 \pm 2$	$34 \pm 9$	> 50
Gr/BW	Gr 1 mg/30 ml	DCM	Drop casting (0.05 g/m <sup>2</sup> )	$120 \pm 7$	$78 \pm 16$	–
Gr/BW	Gr 1 mg/2 ml	DCM	Drop casting (0.25 g/m <sup>2</sup> )	$133 \pm 3$	$125 \pm 5$	35
CNT/BW	CNT 1 mg/60 ml	DCM	Drop casting (0.05 g/m <sup>2</sup> )	$143 \pm 3$	$130 \pm 4$	20
CB/H <sub>2</sub> O/BW	CB 0.3 g/100 ml	0.3% SDBS in H <sub>2</sub> O	3 × dip coating	$73 \pm 3$	$0 \pm 0$	> 50
Gr/H <sub>2</sub> O/BW	Gr 0.3 g/100 ml	0.3% SDBS in H <sub>2</sub> O	3 × dip coating	$139 \pm 4$	$136 \pm 3$	40
CNT/H <sub>2</sub> O/BW	CNT 0.3 g/100 ml	0.3% SDBS in H <sub>2</sub> O	3 × dip coating	$145 \pm 3$	$142 \pm 2$	30

**Fig. 6.** A droplet of water at CNT/H<sub>2</sub>O/BW: A) immediately after dropping, B) 10 min after dropping, C) with surface turned upside-down, D) without surfactant rinsing.

The Wenzel's model extends Young's model, describing wetting mechanism of flat surfaces [42], to rough surfaces. Water penetrates rough surface and contact angle is expected to change according to Eq. (1).

$$\cos\theta^* = r\cos\theta \quad (1)$$

where  $\theta$  is the contact angle on flat surface,  $r$  is roughness ratio, and  $\theta^*$  is the contact angle according to Wenzel's regime (on rough surfaces). Thus, the cosine of contact angle of the Wenzel model should be higher than the one calculated from Young's model. Therefore, the hydrophobic material with a rough surface may become superhydrophobic and the hydrophilic material with a rough surface may become superhydrophilic. This is observed inter alia for the lotus leaves. The interesting high contact angle and low sliding angle features of this structure stem from a high uniformity of the roughness and are described by Cassie's state [43].

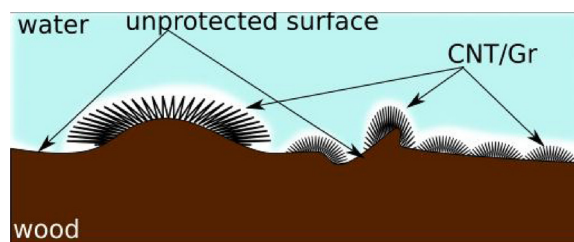
However, in contrast to the “lotus effect”, there are also structures similar to our CNM coated wood e.g. rose petals leaves which exhibit superhydrophobicity with high adhesion also called the “rose petal effect”. In that case, water droplet onto the surface of rose petal forms very high contact angle of about 150°, but the adhesive forces are so strong, that it can pin to a leaf even when the leaf is turned upside down [9]. The “rose petal effect” is described as Cassie's impregnating wetting state [42], where due to far distances between nanostructures, the interface between water and surface is larger. Thus, stronger adhesive forces are observed. In order to describe fully the “rose petal effect”, the Wenzel's model must be transformed into the Cassie's model [43]. In the latter model a very rough or irregular surface is considered and a water droplet is in contact only with the top of the rough surface according to Eq. (2).

$$\cos\theta^{**} = rf\cos\theta + f - 1 \quad (2)$$

where  $\theta$  is the contact angle taken from Young's equation,  $r$  is the roughness ratio,  $f$  is the fraction of solid surface area wetted by the liquid and  $\theta^{**}$  is the contact angle according to the Cassie's regime. In the “lotus effect” it is expected that  $f = 1$ , whilst in “rose petal effect”  $f < 1$ . In this paper “lotus effect” and “rose petal effect” surfaces will be referred to as superhydrophobic with low adhesion and superhydrophobic with high adhesion, respectively.

Considering all the above it is reasonable to propose that the combination of carbon nanostructures which have low surface energy and wood which has a micro-rough surface, (see also SEM and fluorescence images Fig. 2, Supplementary materials, Figs. S3–S5) may result in the formation of a specific micro-nano structure which leads to the superhydrophobic effect. However, the morphology irregularities of wood surface confirmed by SEM and fluorescence microscopy images (Fig. 2) may result in the nonuniform deposition of CNMs and existence of unprotected spots ( $f < 1$ ) which due to high hydrophilicity of pure wood enable pinning of water droplets into the surface and in consequence high adhesion like in the “rose petal effect”. Thus, we propose a model of CNM/wood wetting, where water is not in contact with the surface only next to nanostructures, whereas in the case of large or irregular distances between them, the surface is partly wetted by water (Fig. 7).

It is worth noticing here that this model implies that the most important feature of wood responsible for the superhydrophobic effect is the micro-roughness of the wood surface. The tests on different wood species which have varying chemical composition and pore sizes actually back up this theory as we, have not observed much difference in wetting angles independent of the type of wood we used. Although one could expect that in this case the polishing experiment should show some type of difference between rough and polished surface, but it has to be also taken into account that the polished sample is still in the same order of magnitude with regard to roughness sizes, which may in this case be of no importance to the effect.

**Fig. 7.** Cassie's impregnating state model for wood covered with CNMs.

#### 4. Conclusions

In this paper we have shown that carbon nanomaterials may be used to change the wetting properties of wood surfaces from naturally hydrophilic to superhydrophobic. The study performed on three types of carbon allotropes i.e. carbon black, graphene and carbon nanotubes has shown that all of these nanomaterials may increase water contact angle on the surface of wood, but the two former ones can produce particularly homogenous coatings resulting in a long-lasting superhydrophobic effect. Only 0.25 g of Gr and 0.05 g of CNTs were enough to obtain waterproofing layer. According to market price of industrial grade Gr powder (manufacturer: Cambridge Nanosystems, 1200 USD/1 kg) and MWCNTs (manufacturer: Nanocyl SA, 120 USD/1 kg), it may be estimated that the price of CNMs used to produce 1 m<sup>2</sup> of the coating (excluding solvents) may be equal 0.3 USD and 0.02 USD for Gr and CNTs, respectively. The coatings were prepared using simple methods of drop-casting and dip-coating from organic solvent and aqueous dispersions of CNMs. We have shown that the presence of a surfactant in the water-based suspension is not destructive for the superhydrophobic effect as the surfactant may be easily removed by several rinsing cycles.

It has been further shown that the production of uniform coatings and resultant superhydrophobic effect is largely independent of the type of wood or polishing. However, it may depend on the thickness of the nanomaterials layer and the type of nanomaterial. The optimized coatings have shown contact angles of approximately 130° for Gr coatings and 140° for CNT coatings. Yet, the droplets were not easily rolling off the surfaces showing water shading angles of over 15°. Although the sandpaper abrasion test slightly decreased the water contact angle of Gr and CNT coated wood, the apparent water resistance was maintained. Moreover, not only bulk wood may be coated with CNMs. Wood fibers and particles covered with Gr showed the decrease of water absorption equaling 98% and 87%, respectively.

On the basis of the obtained results a model of CNM/wood wetting related to “rose petal effect” theory has been proposed. The CNM-based water repellent coatings should prevent wood from swelling, mechanical weakening and the growth of mold. The proposed coating may be in use for raw wood, but also wood-based composites. Finally, wood covered with CNMs, with all the advantages of pure wood and lacking the wettability, may be highly interesting as a novel engineering material.

#### Acknowledgements

The authors would like to thank CambridgeNanosystems Ltd. and Konimpex Ltd. for materials provided. D.Ł. would like to thank the National Science Centre, Poland for sponsoring the study (project no. 2015/19/N/ST8/02184). A.D. thanks the Ministry of Science & Higher Education in Poland (06/62/DSPB/2181). A.L.-R. and K.K. thank the European Research Council (under the Seventh Framework Program FP7/2007-2013, ERC agreement no 259061) for funding this research. K. K. also thanks the Royal Society providing financial support.

#### Appendix A. Supplementary data

Supplementary material related to this article can be found, in the online version, at doi:<https://doi.org/10.1016/j.porgcoat.2018.08.025>.

#### References

- [1] M.A. Khan, K.M.I. Ali, Swelling behavior of wood and wood-plastic composite (WPC), *Polym. Plast. Technol. Eng.* 31 (1992) 299–307, <https://doi.org/10.1080/03602559208017750>.
- [2] J. Gallup, P. Kozak, L. Cummins, S. Gillman, Indoor mold spore exposure: characteristics of 127 homes in Southern California with endogenous mold problems, *Adv. Aerobiol. Proc. 3rd Internat. Conf. Aerobiol.* (1987) 140–142.
- [3] S.M. Shah, U. Zulfiqar, S.Z. Hussain, I. Ahmad, I. Habib-ur-Rehman, T. Hussain, Subhani, A durable superhydrophobic coating for the protection of wood materials, *Mater. Lett.* 203 (2017) 17–20, <https://doi.org/10.1016/j.matlet.2017.05.126>.
- [4] S. Jia, M. Liu, Y. Wu, S. Luo, Y. Qing, H. Chen, Facile and scalable preparation of highly wear-resistance superhydrophobic surface on wood substrates using silica nanoparticles modified by VTES, *Appl. Surf. Sci.* 386 (2016) 115–124, <https://doi.org/10.1016/j.apsusc.2016.06.004>.
- [5] W. Gan, L. Gao, W. Zhang, J. Li, X. Zhan, Fabrication of microwave absorbing CoFe<sub>2</sub>O<sub>4</sub> coatings with robust superhydrophobicity on natural wood surfaces, *Ceram. Int.* 42 (2016) 13199–13206, <https://doi.org/10.1016/j.ceramint.2016.05.112>.
- [6] B.L. Feng, S.H. Li, Y.S. Li, H.J. Li, L.J. Zhang, J. Zhai, Y.L. Song, B.Q. Liu, L. Jiang, L. Feng, S.H. Li, Y.S. Li, H.J. Li, L.J. Zhang, J. Zhai, Y.L. Song, B.Q. Liu, L. Jiang, D.B. Zhu, Super-hydrophobic surfaces: from natural to artificial, *Adv. Mater.* 14 (2002) 1857–1860, <https://doi.org/10.1002/adma.200290020>.
- [7] K.K.S. Lau, J. Bico, K.B.K. Teo, M. Chhowalla, G.A.J. Amarantunga, W.I. Milne, G.H. McKinley, K.K. Gleason, Superhydrophobic carbon nanotube forests, *Nano Lett.* 3 (2003) 1701–1705, <https://doi.org/10.1021/nl034704t>.
- [8] T. Sun, G. Wang, H. Liu, L. Feng, L. Jiang, D. Zhu, Control over the wettability of an aligned carbon nanotube film, *J. Am. Chem. Soc.* 125 (2003) 14996–14997, <https://doi.org/10.1021/ja038026o>.
- [9] K. Liu, X. Yao, L. Jiang, Recent developments in bio-inspired special wettability, *Chem. Soc. Rev.* 39 (2010) 3240–3255, <https://doi.org/10.1039/b917112f>.
- [10] W. Barthlott, C. Neinhuis, Purity of the sacred lotus, or escape from contamination in biological surfaces, *Planta* 202 (1997) 1–8, <https://doi.org/10.1007/s004250050096>.
- [11] X. Dong, J. Chen, Y. Ma, J. Wang, M.B. Chan-Park, X. Liu, L. Wang, W. Huang, P. Chen, Superhydrophobic and superoleophilic hybrid foam of graphene and carbon nanotube for selective removal of oils or organic solvents from the surface of water, *Chem. Commun.* 48 (2012) 10660–10662, <https://doi.org/10.1039/c2cc35844a>.
- [12] J. Rafiee, M.A. Rafiee, Z.Z. Yu, N. Koratkar, Superhydrophobic to superhydrophilic wetting control in graphene films, *Adv. Mater.* 22 (2010) 2151–2154, <https://doi.org/10.1002/adma.200903696>.
- [13] Z. Chen, L. Dong, D. Yang, H. Lu, Superhydrophobic graphene-based materials: surface construction and functional applications, *Adv. Mater.* 25 (2013) 5352–5359, <https://doi.org/10.1002/adma.201302804>.
- [14] Y. Lin, G.J. Ehlert, C. Bukowsky, H.A. Sodano, Superhydrophobic functionalized graphene aerogels, *J. Chem. Inf. Model.* 53 (2013) 1689–1699, <https://doi.org/10.1017/CBO9781107415324.004>.
- [15] E. Singh, Z. Chen, F. Houshmand, W. Ren, Y. Peles, H.M. Cheng, N. Koratkar, Superhydrophobic graphene foams, *Small* 9 (2013) 75–80, <https://doi.org/10.1002/sml.201201176>.
- [16] S. Naha, S. Sen, I.K. Puri, Flame synthesis of superhydrophobic amorphous carbon surfaces, *Carbon N. Y.* 45 (2007) 1702–1706, <https://doi.org/10.1016/j.carbon.2007.04.018>.
- [17] X. Gui, J. Wei, K. Wang, A. Cao, H. Zhu, Y. Jia, Q. Shu, D. Wu, Carbon nanotube sponges, *Adv. Mater.* 22 (2010) 617–621, <https://doi.org/10.1002/adma.200902986>.
- [18] C. Lee, S. Baik, Vertically-aligned carbon nano-tube membrane filters with superhydrophobicity and superoleophilicity, *Carbon* 48 (2010) 2192–2197, <https://doi.org/10.1016/j.carbon.2010.02.020>.
- [19] C.H. Lee, N. Johnson, J. Drelich, Y.K. Yap, The performance of superhydrophobic and superoleophilic carbon nanotube meshes in water-oil filtration, *Carbon* 49 (2011) 669–676, <https://doi.org/10.1016/j.carbon.2010.10.016>.
- [20] D.D. Nguyen, N.-H. Tai, S.-B. Lee, W.-S. Kuo, Superhydrophobic and superoleophilic properties of graphene-based sponges fabricated using a facile dip coating method, *Energy Environ. Sci.* 5 (2012) 7908–7912, <https://doi.org/10.1039/c2ee21848h>.
- [21] H.X. Sun, Z.Q. Zhu, W.D. Liang, B.P. Yang, X.J. Qin, X.H. Zhao, C.J. Pei, P.Q. La, A. Li, Reduced graphene oxide-coated cottons for selective absorption of organic solvents and oils from water, *RSC Adv.* 4 (2014) 30587–30591, <https://doi.org/10.1039/C4ra03208j>.
- [22] W. Shao, S. Wang, H. Liu, J. Wu, R. Zhang, H. Min, M. Huang, Preparation of bacterial cellulose/graphene nanosheets composite films with enhanced mechanical performances, *Carbohydr. Polym.* 138 (2016) 166–171, <https://doi.org/10.1016/j.carbpol.2015.11.033>.
- [23] M. Shateri-Khalilabad, M.E. Yazdanshenas, Preparation of superhydrophobic electroconductive graphene-coated cotton cellulose, *Cellulose* 20 (2013) 963–972, <https://doi.org/10.1007/s10570-013-9873-y>.
- [24] T. Makowski, D. Kowalczyk, W. Fortuniak, D. Jeziorska, S. Brzezinski, A. Tracz, Superhydrophobic properties of cotton woven fabrics with conducting 3D networks of multiwall carbon nanotubes, MWCNTs, *Cellulose* 21 (2014) 4659–4670, <https://doi.org/10.1007/s10570-014-0422-0>.
- [25] Y.Y. Liu, R.H. Wang, H.F. Lu, L. Li, Y.Y. Kong, K.H. Qi, J.H. Xin, Artificial lotus leaf structures from assembling carbon nanotubes and their applications in hydrophobic textiles, *J. Mater. Chem.* 17 (2007) 1071–1078, <https://doi.org/10.1039/B613914k>.
- [26] G. Li, H. Wang, H. Zheng, R. Bai, A facile approach for the fabrication of highly stable superhydrophobic cotton fabric with multi-walled carbon nanotubes-azide polymer composites, *Langmuir* 26 (2010) 7529–7534, <https://doi.org/10.1021/la904337z>.
- [27] D. Mohan, C.U. Pittman, P.H. Steele, Pyrolysis of wood/biomass for bio-oil: a critical review, *Energy Fuels* 20 (2006) 848–889, <https://doi.org/10.1021/ef0502397>.
- [28] E.A. Papp, C. Csiha, Contact angle as function of surface roughness of different wood species, *Surf. Interfaces* 8 (2017) 54–59, <https://doi.org/10.1016/j.surfint.2017.04.009>.
- [29] M. Borrega, P. Ahvenainen, R. Serimaa, L. Gibson, Composition and structure of

- balsa (*Ochroma pyramidale*) wood, *Wood Sci. Technol.* 49 (2015) 403–420, <https://doi.org/10.1007/s00226-015-0700-5>.
- [30] R. Pettersen, The chemical composition of wood, *Chem. Solid Wood* 2 (1984) 57–126, <https://doi.org/10.1021/ba-1984-0207>.
- [31] M. Plötze, P. Niemz, Porosity and pore size distribution of different wood types as determined by mercury intrusion porosimetry, *Eur. J. Wood Wood Prod.* 69 (2010) 649–657, <https://doi.org/10.1007/s00107-010-0504-0>.
- [32] T. Bezak, M. Kusy, M. Elias, M. Kopcek, Surface roughness determination using laser scanning confocal microscope Zeiss LSM 700, *METAL 2013 – 22nd International Conference on Metallurgy and Materials, Conference Proceedings*, (2013).
- [33] A. Bartkowiak, M. Rojewska, A. Biadasz, J. Lulek, K. Prochaska, Surface properties and morphology of selected polymers and their blends designed to mucoadhesive dosage forms, *React. Funct. Polym.* 118 (2017) 10–19, <https://doi.org/10.1016/j.reactfunctpolym.2017.06.011>.
- [34] B. Chen, J. Qiu, E. Sakai, N. Kanazawa, R. Liang, H. Feng, Robust and super-hydrophobic surface modification by a “paint + adhesive” method: applications in self-cleaning after oil contamination and oil-water separation, *ACS Appl. Mater. Interfaces* 8 (2016) 17659–17667, <https://doi.org/10.1021/acsami.6b04108>.
- [35] A.F. Stalder, G. Kulik, D. Sage, L. Barbieri, P. Hoffmann, A snake-based approach to accurate determination of both contact points and contact angles, *Colloids Surf. A: Physicochem. Eng. Asp.* 286 (2006) 92–103, <https://doi.org/10.1016/j.colsurfa.2006.03.008>.
- [36] J. Zimmermann, S. Seeger, F. Reifler, Water shedding angle: a new technique to evaluate the water-repellent properties of superhydrophobic surfaces, *Text. Res. J.* 79 (2009) 1565–1570, <https://doi.org/10.1177/0040517509105074>.
- [37] K.K. Pandey, Study of the effect of photo-irradiation on the surface chemistry of wood, *Polym. Degrad. Stab.* 90 (2005) 9–20, <https://doi.org/10.1016/j.polymdegradstab.2005.02.009>.
- [38] R.J. Stöhr, R. Kolesov, K. Xia, R. Reuter, J. Meijer, G. Logvenov, J. Wrachtrup, Super-resolution fluorescence quenching microscopy of graphene, *ACS Nano* 6 (2012) 9175–9181, <https://doi.org/10.1021/nn303510p>.
- [40] R.N. Wenzel, Surface roughness and contact angle, *J. Psychosom. Res.* 53 (1949) 1466–1467, [https://doi.org/10.1016/0022-3999\(86\)90018-8](https://doi.org/10.1016/0022-3999(86)90018-8).
- [41] B.D. Cassie, S. Baxter, Of porous surfaces, *Trans. Faraday Soc.* 40 (1944) 546–551, <https://doi.org/10.1039/tf9444000546>.
- [42] M.E. Schrader, Young-Dupre revisited, *Langmuir* 11 (1995) 3585–3589, <https://doi.org/10.1021/la00009a049>.
- [43] L. Feng, Y. Zhang, J. Xi, Y. Zhu, N. Wang, F. Xia, L. Jiang, Petal effect: a super-hydrophobic state with high adhesive force, *Langmuir* 24 (2008) 4114–4119, <https://doi.org/10.1021/la703821h>.

Supporting information for:

**Towards the development of superhydrophobic carbon nanomaterial coatings on wood**

*Damian Łukawski<sup>a</sup>, Agnieszka Lekawa-Raus<sup>b,e</sup>, Filip Lisiecki<sup>c</sup>, Krzysztof Koziol<sup>d,e</sup>, Alina Dudkowiak<sup>a\*</sup>*

*<sup>a</sup> Faculty of Technical Physics, Poznan University of Technology, 60-965 Poznan, Poland*

*<sup>b</sup> Faculty of Mechatronics, Warsaw University of Technology, 02-525 Warsaw, Poland*

*<sup>c</sup> Institute of Molecular Physics, Polish Academy of Sciences, 60-179 Poznan, Poland*

*<sup>d</sup> Enhanced Composites & Structures Centre, Cranfield University, MK43 0AL Cranfield, UK*

*<sup>e</sup> Department of Materials Science and Metallurgy, University of Cambridge, Cambridge CB3 0FS, UK*

*\*corresponding author, tel: +48 665 31 81, fax: +48 61 665 3201, email: [alina.dudkowiak@put.poznan.pl](mailto:alina.dudkowiak@put.poznan.pl)*

## 1. Results



**Fig. S1** Florescence microscopy image of CB/BW (size of image 2.78 mm x 2.09 mm).

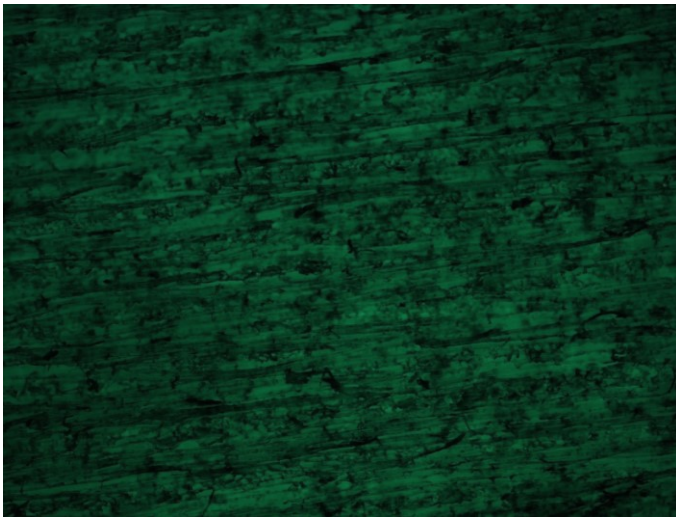


**Fig. S2** Florescence microscopy image of CNT/BW (size of image 2.78 mm x 2.09 mm).

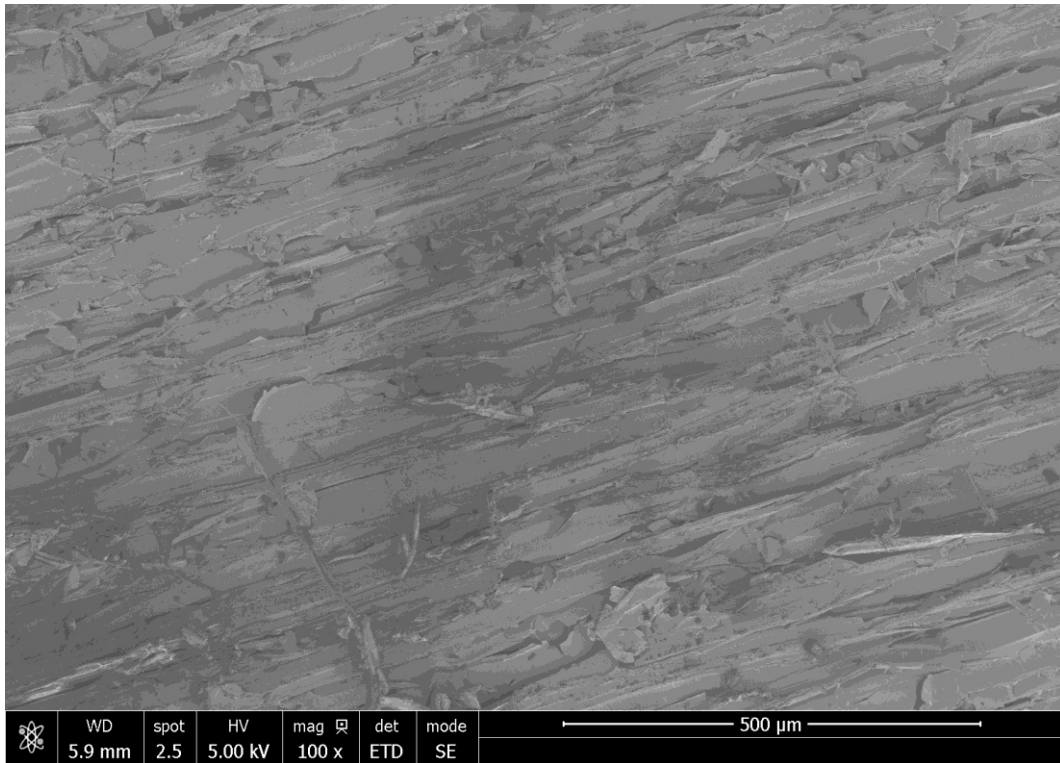


**Fig. S3** SEM image BW coated with thin gold layer (size of image 1.25 μm x 1.25 mm).

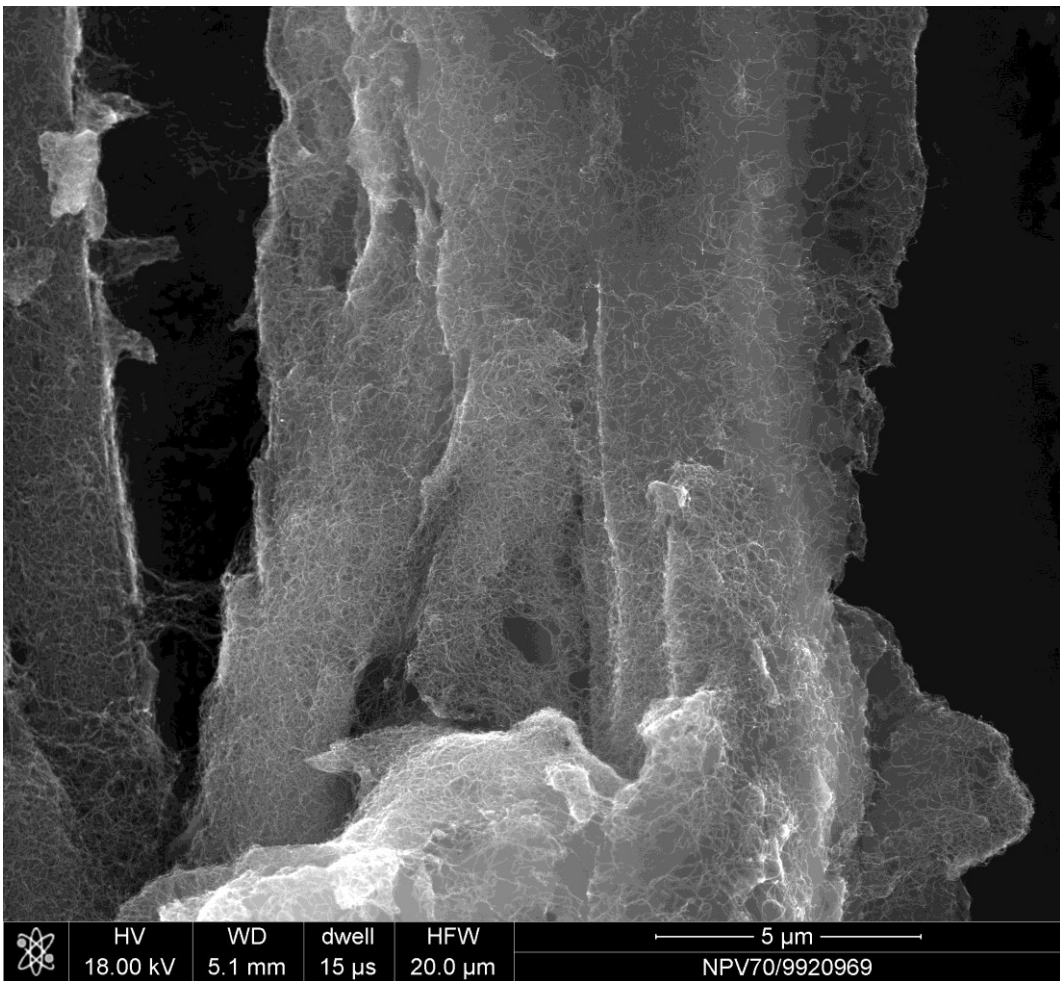


**Fig. S4** SEM image CNT/BW (size of image 20 μm x 20 μm).

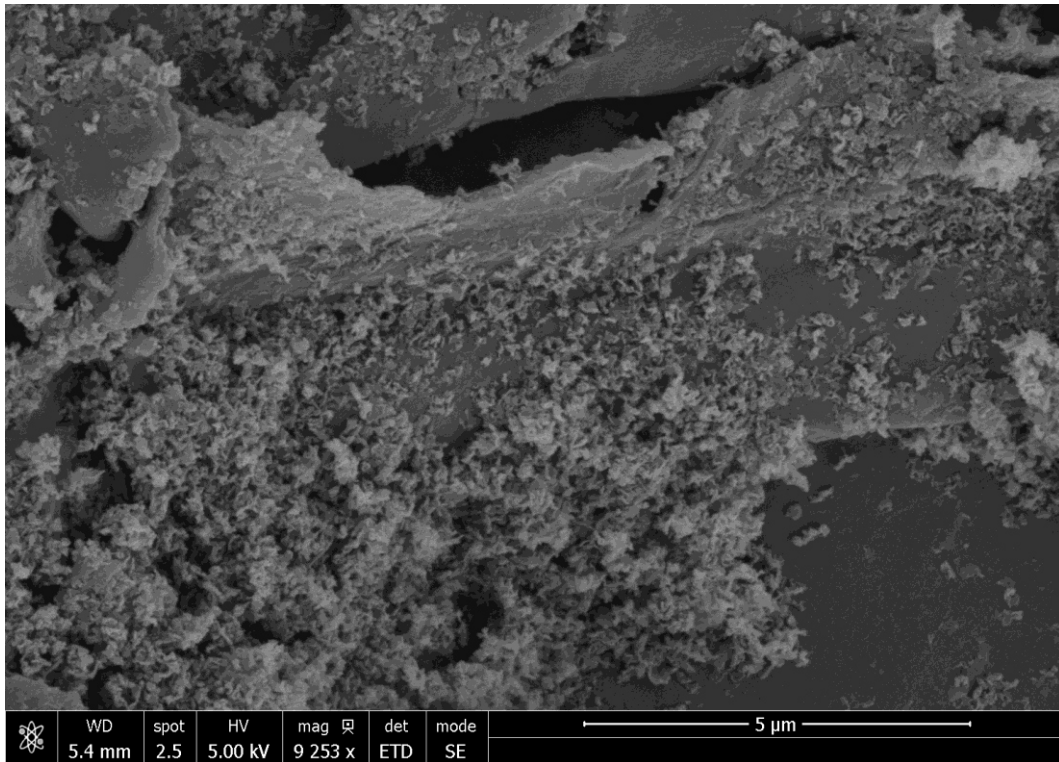


**Fig. S5** SEM image Gr/BW (size of image 20 μm x 20 μm).

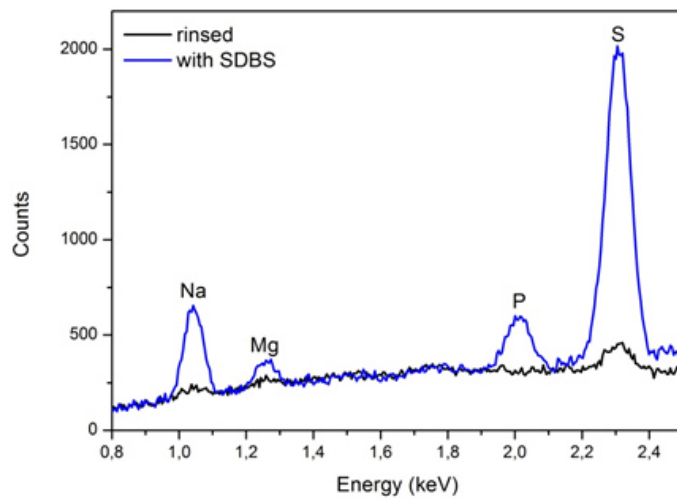


**Fig. S6** EDS spectra of CB/H2O/BW, before and after rinsing

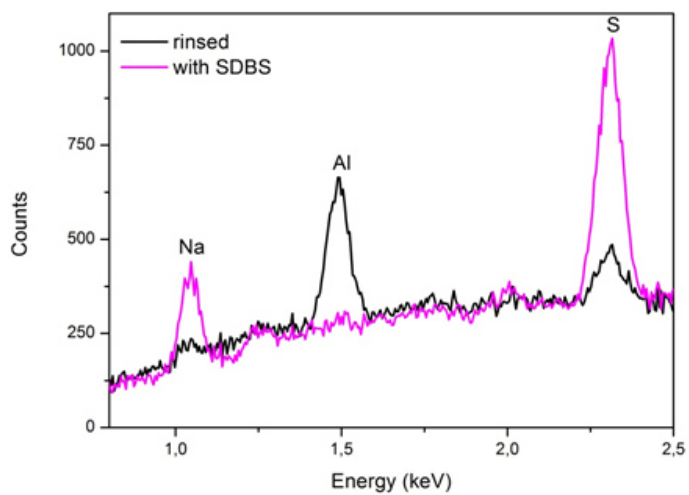


**Fig. S7** EDS spectra of CNT/H<sub>2</sub>O/BW, before and after rinsing.

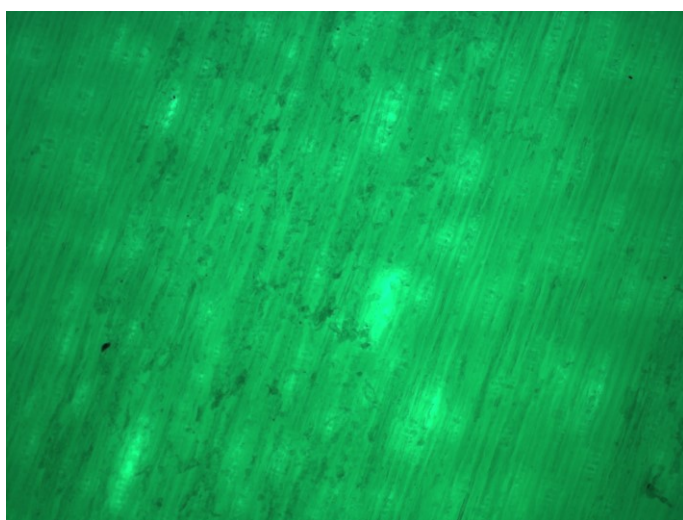


**Fig. S8** Fluorescence microscopy image of scots pine (size of image 2.78 mm x 2.09 mm)

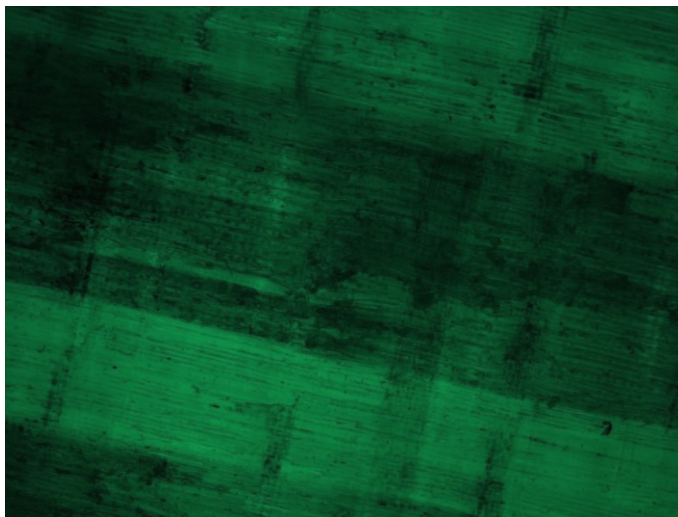


**Fig. S9** Florescence microscopy image of Gr/pine (size of image 2.78 mm x 2.09 mm).

.

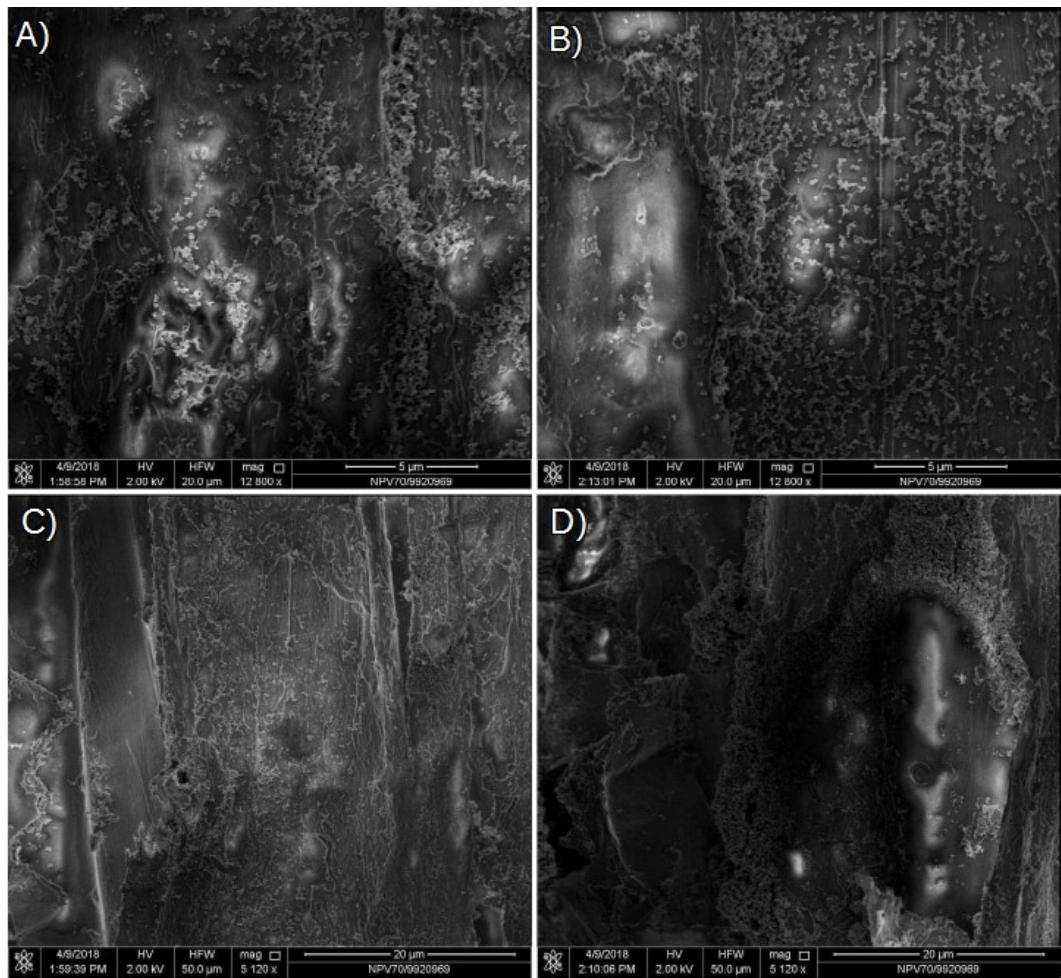


**Fig. S10** SEM images of CB/wood before (A and C) and after (B and D) sandpaper abrasion test.

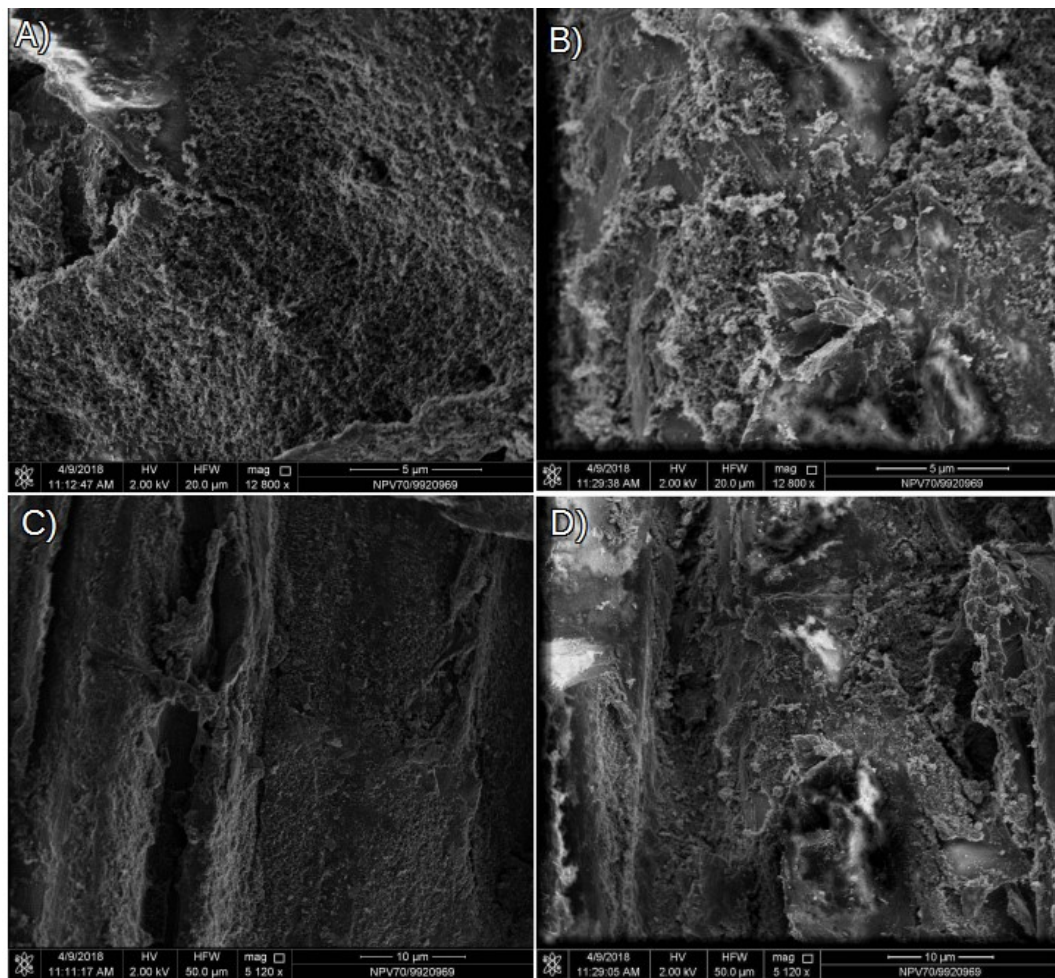


**Fig. S11** SEM images of Gr/wood before (A and C) and after (B and D) sandpaper abrasion test.

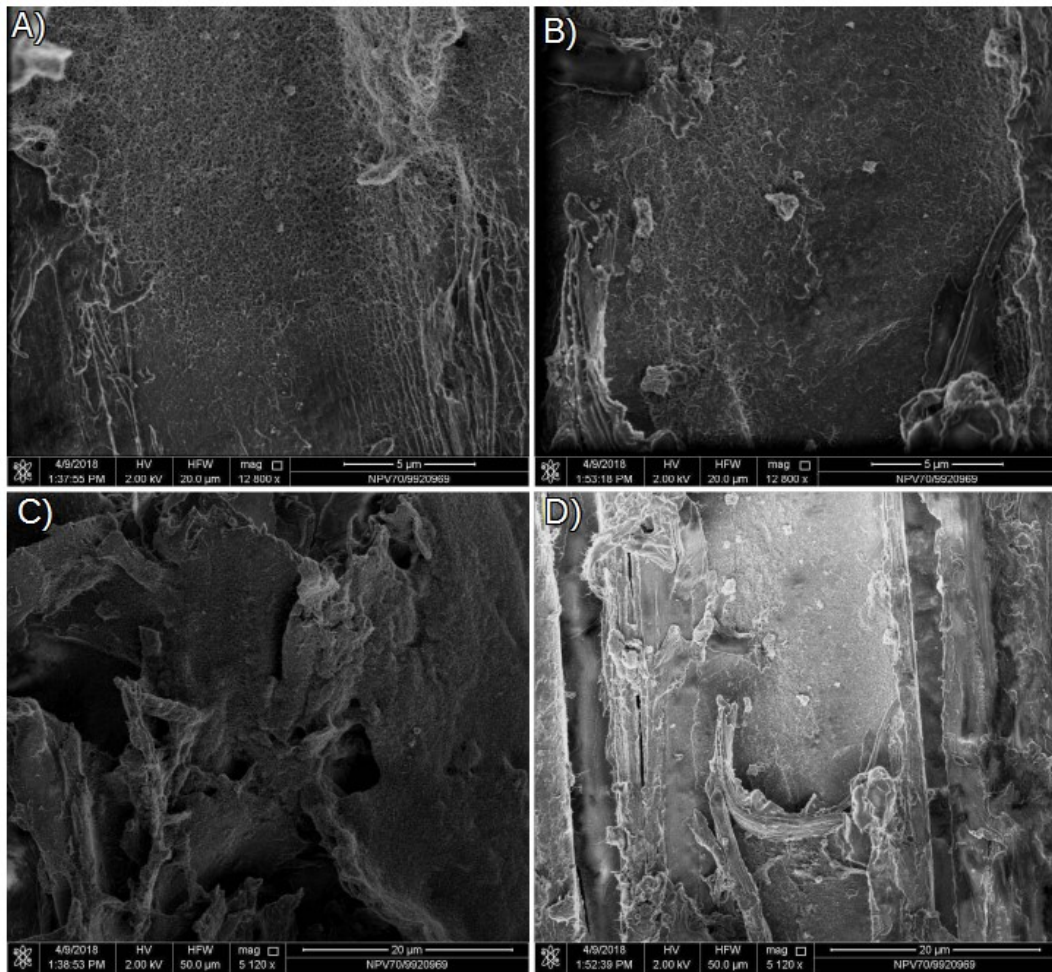


**Fig. 12** SEM images of CNT/wood before (A and C) and after (B and D) sandpaper abrasion test.

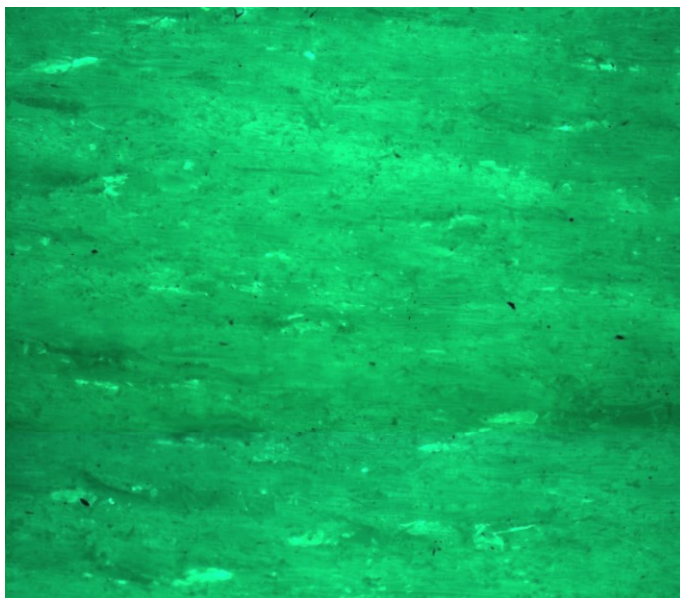


**Fig. S13** Fluorescence microscopy image of birch (size of image 2.78 mm x 2.09 mm).

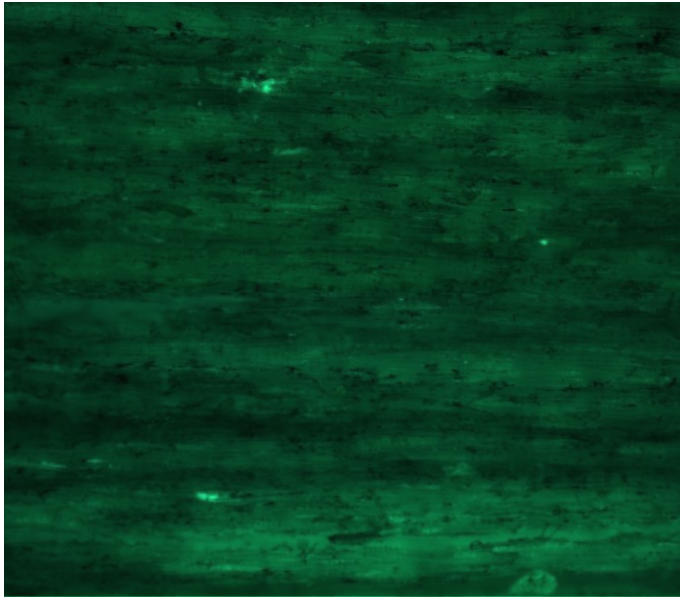


**Fig. S14** Florescence microscopy image of Gr/birch (size of image 2.78 mm x 2.09 mm).

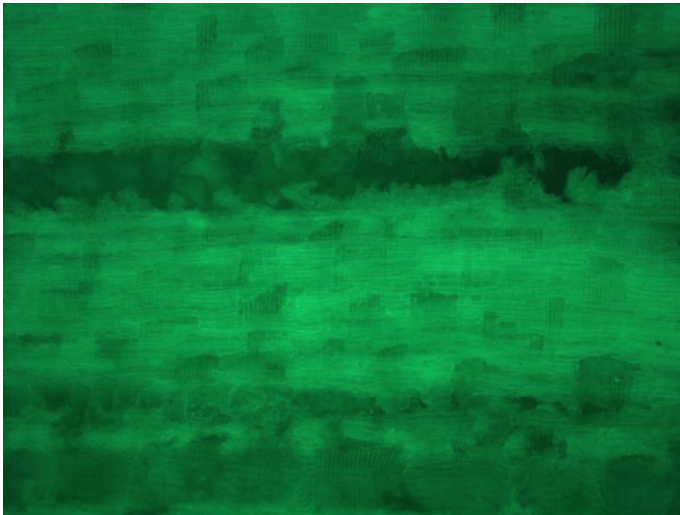


**Fig. S15** Florescence microscopy image of oak (size of image 2.78 mm x 2.09 mm).

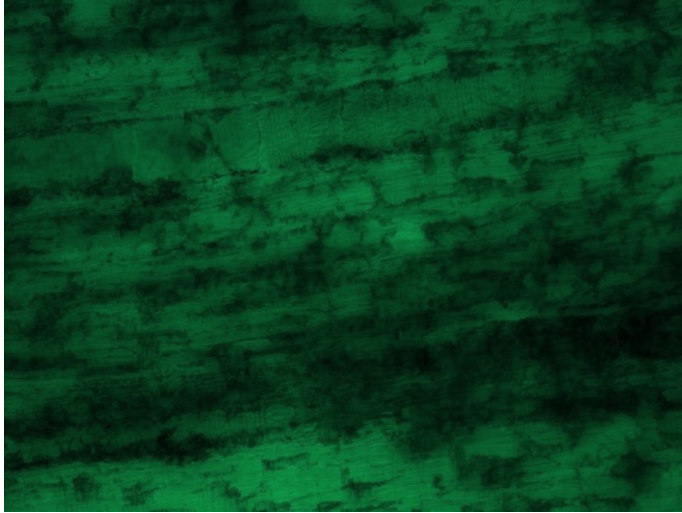


**Fig. S16** Florescence microscopy image of Gr/oak (size of image 2.78 mm x 2.09 mm).

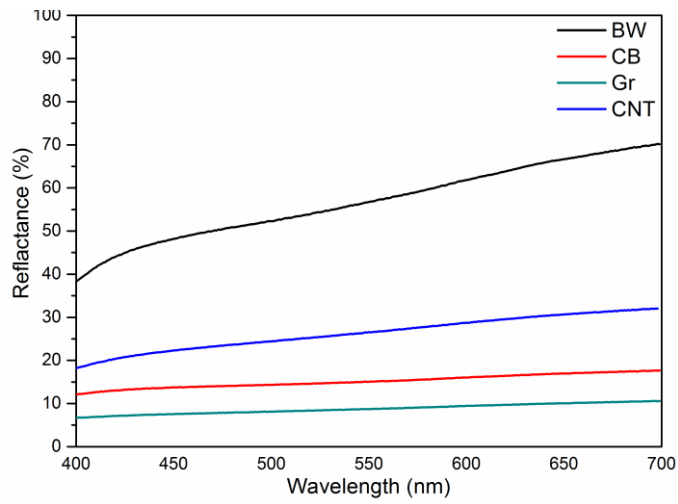


**Fig. S17** UV-VIS reflectance spectra of BW and CNM/BW performer by Carry 4000 spectrometer (using an integrating sphere).

**Przedruk opisu patentowego [Łukawski, UPRP 2017]**

D. Łukawski, A. Dudkowiak, A. Lekawa-Raus, *Sączek hydrofobowy selektywnie pochłaniający oleje i związki organiczne przeznaczony do oczyszczania wód oraz sposób wytworzenia sączka (P.423094/2017).*

RZECZPOSPOLITA  
POLSKA



Urząd Patentowy  
Rzeczypospolitej Polskiej

(12) **OPIS PATENTOWY** (19) **PL** (11) **233206**

(13) **B1**

(21) Numer zgłoszenia: **423094**

(22) Data zgłoszenia: **06.10.2017**

(51) Int.Cl.

**B01J 20/02 (2006.01)**

**B01J 20/20 (2006.01)**

**B01J 20/22 (2006.01)**

**C02F 1/28 (2006.01)**

**C09K 3/32 (2006.01)**

**B82Y 30/00 (2011.01)**

**C08L 97/02 (2006.01)**

(54) **Sączek hydrofobowy selektywnie pochłaniający oleje i związki organiczne przeznaczony do oczyszczania wód oraz sposób wytworzenia sączka**

(43) Zgłoszenie ogłoszono:  
**08.04.2019 BUP 08/19**

(45) O udzieleniu patentu ogłoszono:  
**30.09.2019 WUP 09/19**

(73) Uprawniony z patentu:

**POLITECHNIKA POZNAŃSKA, Poznań, PL**

(72) Twórca(y) wynalazku:

**DAMIAN ŁUKAWSKI, Konin, PL**

**ALINA DUDKOWIAK, Poznań, PL**

**AGNIESZKA ŁĘKAWA-RAUS, Warszawa, PL**

(74) Pełnomocnik:

**recz. pat. Marcin Walkowiak**

**PL 233206 B1**

## Opis wynalazku

Przedmiotem wynalazku jest sącdek hydrofobowy selektywnie pochłaniający oleje i związki organiczne przeznaczony do oczyszczania wód na bazie produktów drzewnych pokrytych nanomateriałami węglowymi oraz sposób jego wytworzenia. Sączki mogą znaleźć zastosowania głównie w oceanicznych wyciekach ropy naftowej, pochłaniając oleje i związki organiczne z tafli wody.

Wykorzystanie sączków na bazie włókien naturalnych jest jednym z możliwych sposobów usuwania oceanicznych rozlewów ropy naftowej. Najczęściej opisywane były włókna takie jak włókna kapokowe, bawełniane, trojeści i pałki [H. Choi i in., Environ. Sci. Technol. 1992, 26 (4), 772–776; Cao i in., J. Nat. Fibers 2017, 0 (0), 1–9].

Ponadto zaobserwowano, że czysta bawełna oraz włókno kapokowe wykazują właściwości hydrofobowe, obecne z powodu naturalnie obecnej cienkiej warstwy wosku jednocześnie absorbując oleje [Singh i in., Ind. Eng. Chem. Res. 2014, 53 (30), 11954–11961].

Także naturalne oraz syntetyczne polimery w postaci proszku, granulatu lub włókien, takie jak drewno, bawełna, trawa, słoma, celuloza z dodatkami związków metalu/amonowych wykazują selektywne pochłanianie olejów – opis patentowy US 4780518.

Nie tylko naturalne i polimerowe materiały są wykorzystywane jako selektywne sączki. Nanomateriały węglowe, takie jak grafen, tlenek grafenu, zredukowany tlenek grafenu, nanopłatki grafenu i nanorurki węglowe zostały uformowane w struktury gąbczaste lub aerożele o bardzo silnych właściwościach chłonnych (dla olejów i rozpuszczalników organicznych) oraz superhydrofobowości [Gupta i in., J. Mater. Chem. A 2016, 4 (5), 1550–1565].

Jednakże, pomimo bardzo dobrych właściwości selektywnego pochłaniania, nanomateriały węglowe w postaci gąbek i aerożeli nie są do tej pory powszechnie wykorzystywane z powodu wysokiej ceny. W związku z tym naturalne włókna zostały pokrywane w celu uzyskania selektywnego pochłaniania.

Bawełniane sączki były pokrywane z użyciem m. in. nanocząstek tlenku krzemu [Liu i in., Carbohydr. Polym. 2014, 103 (1), 480–487.], polimerów hydrofobizujących [Li i in., Phys. Chem. Chem. Phys. 2015, 17 (9), 6451–6457.; Lee i in. Lee, J. H.; Kim, D. H.; Kim, Y. D. J. Ind. Eng. Chem. 2016, 35, 140–145.] i nanomateriałów węglowych [Ge i in., Compos. Sci. Technol. 2014, 102, 100–105.; Hoai i in., Mater. Sci. Eng. B 2016, 216, 1–6.; Cortese i in., J. Mater. Chem. A 2014, 2(19), 6781.].

Ponadto, nanorurki węglowe, między innymi nanoszone na włókna naturalne, były także wykorzystywane do oczyszczania cieczy co ujawniają opisy patentowe EP1885647 oraz US2005263456.

Włókna naturalne pokryte nanorurkami węglowymi także mogą służyć jako rozdzielacz do płynów. Taki stan rzeczy jest znany z opisów patentowych US2010116751 oraz US 9126128.

Inne nanomateriały węglowe, w tym grafen, grafit i włókna węglowe zostały także opisane jako pokrycia do wytworzenia rozdzielaczy oleju od wody – opisy EP 2929925 oraz WO 2015141902. Dodatkowo, oleje mogą być usuwane lub filtrowane z powierzchni wody z użyciem wysięgnika, utrzymującego sącdek składający się z nanorurek węglowych naniesionych na włókna – opis US2015275452.

Nanorurki węglowe osadzone na włóknach takich jak włókno polietylenowe, bawełna inne włókna pochodzenia naturalnego mogą służyć do usuwania zanieczyszczeń z powierzchni ciał stałych. Do opisanych zanieczyszczeń należą zanieczyszczenia mikrobiologiczne, pyłki, ciecze i inne – opis US2009196909.

Rozwiązanie według wynalazku koncentruje się na zastosowaniu produktów będących pochodnymi przemysłu drzewnego, takimi jak mączka drzewna i inne, pokrytych nanomateriałami węglowymi, w celu wytworzenia selektywnego pochłaniacza oleju. Zastosowanie czystych materiałów drzewnych jako materiał sorpcyjny jest znane, jednak w związku z ich hydrofilowym charakterem i silnym pochłanianiem wody ich zastosowanie jest ograniczone. Ponadto, ich właściwości sorpcyjne oraz możliwość wielokrotnego użytku są nieznacznie gorsze niż w przypadku innych włókien jak kapok i bawełna. Jednakże, ich niska cena jest bardzo znacznym atutem w porównaniu do wszystkich innych materiałów sorpcyjnych. Pokrycie produktów drzewnych nanomateriałami węglowymi powoduje hydrofobizację i umożliwia zastosowanie wynalazku jako selektywnego pochłaniacza. Ponadto, użycie materiału siatkowego oplatającego użyty materiał drzewny uniemożliwia niekontrolowane rozsypanie lub rozplnięcie się materiału. Warto nadmienić, iż cena nanomateriałów węglowych w przeciągu ostatnich 20 lat spadła kilkaset razy i dopiero obecnie może ona być porównywalna z ceną materiału bazowego sączka. Ponadto w ostatnich kilku latach rozwinięto produkcję nanomateriałów węglowych umożliwiającą ich masową produkcję.

Istotą wynalazku jest sączonek hydrofobowy selektywnie pochłaniający oleje i związki organiczne przeznaczony do oczyszczania wód zawierający produkty drzewne, w którym produkty drzewne w postaci mączki drzewnej, wiórów drzewnych, miazgi drzewnej, ścinek drzewnych, włókien drzewnych, wełny drzewnej, pyłu drzewnego, trocin lub innych odpadów drzewnych, umieszczone (zamknięte) są luźno w materiale siatkowym z włókna naturalnego lub sztucznego pokrytym nanomateriałem węglowym. Materiał siatkowy z włókna naturalnego lub sztucznego posiada rozmiary otworów dobrane w taki sposób, aby ciecze mogły przedostawać się bez oporów, natomiast stosowane produkty drzewne powinny zostać w niej uwięzione.

W optymalnym wariantcie materiał siatkowy z włókna naturalnego stanowią hydrofobizowane włókna utkane z bawełny, lnu, wełny, bambusa, włókna kokosowego lub włókna bambusowego, a w przypadku włókna sztucznego: siatka polipropylenowa, polietylenowa, poliestrowa, poliuretanowa, poliwęglanowa, poliamidowa, poliolefinowa, włókno szklane lub włókno węglowe.

Korzystnym jest kiedy nanomateriał węglowy stanowią jednościenne i wielościenne nanorurki węglowe, śrubowate nanorurki węglowe (ang. helical carbon nanotubes), inne nanowłókna węglowe, nanopłatki grafenu, nanopłatki grafitu, zredukowany tlenek grafenu lub sadza.

Korzystnym jest kiedy wytworzony sączonek modyfikowany jest dodatkowo polimerem hydrofobizującym.

Istotą wynalazku jest również sposób wytwarzania sączoneka hydrofobowego przeznaczonego do oczyszczania wód, w którym w pierwszej kolejności sypkie produkty drzewne w postaci mączki drzewnej, wiórów drzewnych, miazgi drzewnej, ścinek drzewnych, włókien drzewnych, wełny drzewnej, pyłu drzewnego, trocin lub innych odpadów drzewnych, umieszcza się luźno w materiale siatkowym z włókna naturalnego lub sztucznego, po czym całość pokrywa się zawiesziną nanomateriału węglowego w związku organicznym, takim jak: chloroform, dichlorometan, dichloroetan, aceton, benzen, izopropanol, etanol, metanol, N-Metylopirolidon, toluen i podobne, lub mieszaninach tych związków lub ich mieszaninie z wodą, za pomocą metod zanurzeniowych lub natryskowych, a następnie odparowuje się związek organiczny. Dopuszcza się również zastąpienie zawiesziny nanomateriału węglowego w związku organicznym, lub mieszaninach tych związków lub ich mieszaninie z wodą – zawiesziną nanomateriału węglowego w roztworze wody z surfaktantem, takim jak dodecylosiarczan sodu, polisorbitat 80 i podobne lub polimerem stabilizującym, takim jak celuloza, skrobia, polialkohol winylowy i podobne, przy czym odpowiednio usuwa się surfaktant lub polimer stabilizujący odparowując uprzednio wodę.

Korzystnym jest kiedy zawieszinę nanomateriału węglowego w związku organicznym, lub mieszaninach tych związków lub ich mieszaninie z wodą uprzednio stabilizuje się poprzez dodatek polimeru stabilizującego, takiego jak: octan celulozy, metyloceluloza, polietylen, poli(tlenek etylenu) i podobne.

Korzystnym jest także kiedy jako materiał siatkowy z włókna naturalnego wykorzystuje się włókna utkane z bawełny, lnu, wełny, bambusa, włókna kokosowego lub włókna bambusowego, a z włókna sztucznego: siatka polipropylenowa, polietylenowa, poliestrowa, poliuretanowa, poliwęglanowa, poliamidowa, poliolefinowa, włókno szklane lub włókno węglowe.

W wariantcie sposobu według wynalazku przed umieszczeniem produktów drzewnych w materiale siatkowym, naturalny materiał siatkowy pokrywa się nanomateriałem węglowym w celu jego hydrofobizacji.

Korzystnym jest kiedy jako nanomateriały węglowe stosuje się jednościenne i wielościenne nanorurki węglowe, śrubowate nanorurki węglowe, inne nanowłókna węglowe, nanopłatki grafenu, nanopłatki grafitu, zredukowany tlenek grafenu lub sadzę.

Opcjonalnie nanomateriały węglowe mogą być modyfikowane polimerem hydrofobizującym.

W wariantcie realizacji sączoneki po wytworzeniu pokrywa się dodatkowo polimerem hydrofobizującym.

Zastosowanie nanomateriałów w rozwiązaniach według wynalazku ma na celu hydrofobizację powierzchni produktów drzewnych, przez co nie pochłaniają one wody. Jednocześnie ich zdolność do pochłaniania innych cieczy nie zostaje ograniczona. Zastosowanie produktów pochodzenia drzewnego, takich jak przykładowo mączka drzewna pokrytych nanomateriałami, jak nanorurki węglowe i nanopłatki grafenu, pozwoli na stworzenie taniego kompozytu do usuwania ropy naftowej z powierzchni wody. Wykorzystanie zaproponowanych sączoneków spowoduje wchłonięcie tylko rozlanej ropy naftowej, nie wchłaniając przy tym wody. Niski koszt wytworzenia sączoneka jest konieczny w przypadku aplikacji na oceanach wokół platformy wydobywczej.

Sączonek według wynalazku znajduje zastosowanie w dziedzinie oczyszczania wód i ochrony środowiska dla celów separacji olej-woda, selektywnego pochłaniania oleju z wody, pochłaniania substancji oleistych i ropy naftowej z powierzchni wody, jako bariera ochronna przed wyciekami oceanicznymi,

umożliwią też pochłanianie związków organicznych nierozpuszczalnych w wodzie z powierzchni lub objętości wody.

Wynalazek w przykładzie realizacji przedstawiono na rysunku, na którym fig. 1 przedstawia schemat ideowy sączka oraz cyklu jego wytworzenia. Na fig. 1 pod literą A) pokazano materiał drzewny 1 (rozdrobnione drewno) i materiał siatkowy 2 (hydrofobizowane włókno naturalne, w wariacie też naturalnie niepochlaniające wody włókno polimerowe lub węglowe). B) przedstawia naniesienie materiału 1 na materiał siatkowy 2 – siatkę z włókna, po czym zostaje nią owinięty. C) pokazuje materiał drzewny 1 owinięty materiałem siatkowym – włóknem 2.

Następnie nanomateriał węglowy zostaje naniesiony poprzez zanurzenie w zawieszynie nanomateriału węglowego w związku organicznym przykładowo chloroformie oraz wysuszenie próbki. Korzystnym jest powtarzanie procedury zanurzania kilkakrotnie w celu otrzymania jak najbardziej hydrofobowej warstwy.

Dla znawców oczywistym jest też, że procedurę można wykonać także w innej kolejności, to jest, nanieść odpowiednią ilość nanomateriału na sypką mączkę drzewną a następnie umieścić ją w siatce.

W przykładzie realizacji sączek wykonano używając grafenu jako nanomateriału węglowego, gazy bawełnianej jako materiału siatkowego 2 oraz mączki drzewnej jako materiał drzewny 1.

W sposobie I przykładu realizacji 1 g nanopłatków grafenu wrzucono do 1000 ml chloroformu. Zawiesina została poddana homogenizacji z wykorzystaniem homogenizatora ultradźwiękowego. Moc dostarczona przez homogenizator wynosiła 100 W. Czas procesu wynosił 20 min. Następnie 20 g rozwałkowanego drewna zostało umieszczone w naczyniu, a następnie zalane przez 200 ml wytworzonego roztworu. Nasączona mączka drzewna została suszona w temperaturze 70°C przez 2 godziny, do całkowitego odparowania chloroformu. Nasączenie i suszenie powtórzono 5-krotnie. Mączka drzewna pokryta nanopłatkami grafenu została następnie owinięta z użyciem siatki poliamidowej o wielkości oczka 1,2 mm.

W sposobie II przykładu realizacji 1 g nanopłatków grafenu został wrzuconych do 1000 ml dichlometanu. Zawiesina została poddana homogenizacji z wykorzystaniem homogenizatora ultradźwiękowego. Moc dostarczona przez homogenizator wynosiła 100 W. Czas procesu wynosił 20 min. Następnie 20 g mączki drzewnej zostało owinięte z użyciem siatki bawełnianej o wielkości oczka 2 mm. Owinięta siatką bawełnianą mączka drzewna została umieszczona w naczyniu, a następnie zalana przez 200 ml wytworzonego roztworu. Nasączona mączka drzewna została suszona w temperaturze 70°C przez 2 godziny, do całkowitego odparowania chloroformu. Nasączenie oraz suszenia powtórzono 5-krotnie. Następnie 2 ml polimeru hydrofobizującego, poli(dimetylosiloksan), zostało rozcieńczone w 200 ml chloroformu. Otrzymana owinięta siatką bawełnianą mączka drzewna została następnie zanurzona w rozcieńczonym roztworze poli(dimetylosiloksan). Nasączony sączek został suszony w temperaturze 70°C przez 2 godziny, do całkowitego odparowania chloroformu.

W wariacie realizacji wytworzony sączek może zostać dodatkowo zmodyfikowany polimerem hydrofobizującym. Opcjonalnie również same nanomateriały węglowe mogą być modyfikowane polimerem hydrofobizującym.

Skuteczność rozwiązania potwierdzając przeprowadzone próby. Zważoną próbkę zamocowano w wodzie i rozpuszczalniku organicznym (chloroformie), po każdym zanurzeniu ważąc ją ponownie i susząc. Obliczono selektywność pochłaniania i chłonność. Selektywność pochłaniania mierzona jako iloraz masy wchłoniętego związku organicznego do sumy mas wchłoniętej wody i związku organicznego wzrosła z 53% dla czystej mączki drzewnej do 97,8% dla mączki drzewnej pokrytej grafenem. Natomiast chłonność, mierzona jako masa wchłoniętej wody przypadająca na 1 g sączka spadła z 15.4 g/g do 0.4 g/g.

## Zastrzeżenia patentowe

1. Sączek hydrofobowy selektywnie pochłaniający oleje i związki organiczne przeznaczony do oczyszczania wód zawierający produkty drzewne **znamienny tym**, że stanowią go produkty drzewne (1) w postaci mączki drzewnej, wiórów drzewnych, miazgi drzewnej, ścinek drzewnych, włókna drzewnego, wełny drzewnej, pyłu drzewnego, trocin lub innych odpadów drzewnych pokryte nanomateriałem węglowym, korzystnie modyfikowanym polimerem hydrofobizującym, które umieszczone są luźno w materiale siatkowym (2) z włókna naturalnego lub sztucznego.

2. Sączek według zastrz. 1, **znamienny tym**, że materiał siatkowy (2) z włókna naturalnego stanowią hydrofobizowane włókna utkane z bawełny, lnu, wełny, bambusa, włókna kokosowego lub włókna bambusowego, a z włókna sztucznego: siatka polipropylenowa, polietylenowa, poliestrowa, poliuretanowa, poliwęglanowa, poliamidowa, poliolefinowa, włókno szklane lub włókno węglowe.
3. Sączek według zastrz. 1 lub 2 **znamienny tym**, że nanomateriał węglowy stanowią jednościenne i wielościenne nanorurki węglowe, śrubowate nanorurki węglowe, inne nanowłókna węglowe, nanopłatki grafenu, nanopłatki grafitu, zredukowany tlenek grafenu lub sadza.
4. Sączek według zastrz. od 1 do 3, **znamienny tym**, że pokryty jest dodatkowo polimerem hydrofobizującym.
5. Sposób wytwarzania sączka hydrofobowego selektywnie pochłaniającego oleje i związki organiczne przeznaczonego do oczyszczania wód **znamienny tym**, że sypkie produkty drzewne (1) w postaci mączki drzewnej, wiórów drzewnych, miazgi drzewnej, ściek drzewnych, włókna drzewnego, pyłu drzewnego, trocin lub innych odpadów drzewnych, umieszcza się luźno w materiale siatkowym (2) z włókna naturalnego lub sztucznego, po czym całość pokrywa się zawiesiną nanomateriału węglowego w związku organicznym, takim jak: chloroform, dichlorometan, dichloroetan, aceton, benzen, izopropanol, etanol, metanol, N-Metylopirolidon, toluen i podobne, lub mieszaninach tych związków lub ich mieszaninie z wodą, albo zawiesiną nanomateriału węglowego w roztworze wody z surfaktantem, takim jak dodecylosiarczan sodu, polisorbit 80 i podobne lub polimerem stabilizującym, takim jak celuloza, skrobia, polialkohol winylowy i podobne, za pomocą metod zanurzeniowych lub natryskowych, a następnie odparowuje się związek organiczny albo usuwa się surfaktant lub polimer stabilizujący odparowując uprzednio wodę.
6. Sposób wytwarzania sączków hydrofobowych według zastrz. 5, **znamienny tym**, że zawiesinę nanomateriału węglowego w związku organicznym, lub mieszaninach tych związków lub ich mieszaninie z wodą uprzednio stabilizuje się poprzez dodatek polimeru stabilizującego, takiego jak: octan celulozy, metyloceluloza, polietylen, poli(tlenek etylenu) i podobne.
7. Sposób wytwarzania sączków hydrofobowych według zastrz. 5 lub 6, **znamienny tym**, że jako materiał siatkowy (2) z włókna naturalnego wykorzystuje się hydrofobizowane włókna utkane z bawełny, lnu, wełny, bambusa, włókna kokosowego lub włókna bambusowego, a z włókna sztucznego: siatka polipropylenowa, polietylenowa, poliestrowa, poliuretanowa, poliwęglanowa, poliamidowa, poliolefinowa, włókno szklane lub włókno węglowe.
8. Sposób wytwarzania sączków hydrofobowych według zastrz. 5, 6 lub 7, **znamienny tym**, że przed umieszczeniem produktów drzewnych (1) w materiale siatkowym (2), naturalny materiał siatkowy (2) pokrywa się nanomateriałem węglowym.
9. Sposób wytwarzania sączków hydrofobowych według zastrz. 5, 6, 7 lub 8, **znamienny tym**, że jako nanomateriały węglowe stosuje się jednościenne i wielościenne nanorurki węglowe, śrubowate nanorurki węglowe, inne nanowłókna węglowe, nanopłatki grafenu, nanopłatki grafitu, zredukowany tlenek grafenu lub sadzę.
10. Sposób wytwarzania sączków hydrofobowych według dowolnego zastrz. od 5 do 9, **znamienny tym**, że nanomateriały węglowe mogą być modyfikowane polimerem hydrofobizującym.
11. Sposób wytwarzania sączków hydrofobowych według dowolnego zastrz. od 5 do 10, **znamienny tym**, że sączki po wytworzeniu pokrywa się dodatkowo polimerem hydrofobizującym.

## Rysunek

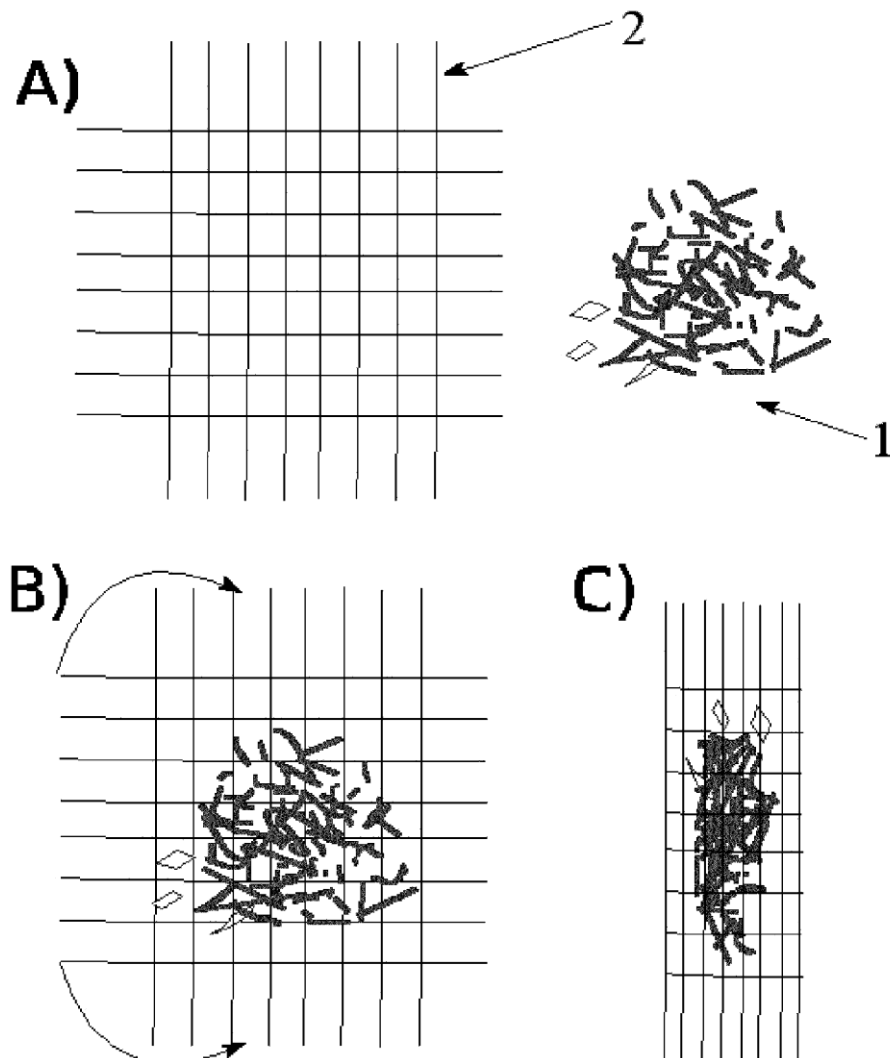


fig.1

**Przedruk publikacji [Łukawski, FiP 2018]**

D. Łukawski, F. Lisiecki, A. Dudkowiak, Coating cellulosic materials with graphene for selective absorption of oils and organic solvents from water, *Fibers and Polymers* 19 (2018) 524–530.

# Coating Cellulosic Materials with Graphene for Selective Absorption of Oils and Organic Solvents from Water

Damian Łukawski<sup>1</sup>, Filip Lisiecki<sup>2</sup>, and Alina Dudkowiak<sup>1\*</sup>

<sup>1</sup>Faculty of Technical Physics, Poznan University of Technology, Poznan 60-965, Poland

<sup>2</sup>Institute of Molecular Physics, Polish Academy of Sciences, Poznan 60-179, Poland

(Received October 13, 2017; Revised December 11, 2017; Accepted January 1, 2018)

**Abstract:** Development of efficient and eco-friendly sorbents used for selective oil removal after oil spill disasters is one of the main topics in environmental science. By using various cellulosic materials coated with graphene flakes, using simple, one-step dip-coating method, it was possible to manufacture environmentally friendly, selective oil sorbents. The cellulosic materials of different yarn size and distribution such as cotton roving, gauze, fabric, and cellulosic wipe and Whatman filter paper were chosen. The scanning electron microscopy showed that simple dip-coating of any cellulosic materials into graphene dispersion creates a uniformly distributed nanomaterial coating. The wetting tests confirmed that the coating endowed cellulosic materials with hydrophobic properties, regardless of their initial yarn distribution and purity. Moreover, the water repellent samples were simultaneously highly sorptive towards oils and organic solvents. Sorption tests performed for a representative group of organic solvents and oils have shown that depending on cellulosic material the oil sorption capacity varied from 4 g/g to 33 g/g for cotton fabric and roving, respectively. Moreover, the absorption selectivity of chloroform versus water exceeded 90 % for each sample and reached over 99 % for the graphene coated cotton roving and gauze. Finally, the recyclability tests have shown that graphene coated materials are less fragile for reuse than naturally hydrophobic sorbents.

**Keywords:** Graphene, Cellulose, Cotton, Hydrophobic properties, Oil sorbent

## Introduction

Oil spills are one of the major environmental threats caused by fuel industry. Only in the disaster in the Gulf of Mexico in 2010, approximately 4.9 million barrels of oil were spilled. These natural disasters have massive impact on the environment. Thus, development of methods of prevention and quick oil removal is necessary. One of the methods for oil removal and prevention of its further spreading is the use of oil sorbents. Much attention has been focused on selective sorbents, which are simultaneously superhydrophobic and superoleophilic. Those materials should soak up only spilled oil and do not absorb ocean water. Moreover, properly engineered selective sorbents should provide the possibility of oil retrieval, show high sorption capacity (*SC*), chemical stability, and environmental friendliness [1].

The materials that have found the largest interest in this field are carbon nanomaterials (CNMs), especially carbon nanotubes (CNTs) and graphene (Gr). CNMs are superhydrophobic due to their nanostructure and chemical composition [2]. Furthermore, the progress in CNM engineering has opened the possibility of their low cost production and deposition in many configurations.

In order to obtain selective membranes, CNTs were grown on metal meshes [3,4] used for oil filtration from water. The other approach was the development of CNM based sponges and aerogels. CNT [5] and Gr [6] sponges showed extremely high sorption capacity due to their low density and high

porosity. Even better results have been observed for Gr foams and aerogels [7,8]. Chemically modified Gr foam may also show switchable oil wettability via controlling pH [9]. However, engineering of CNM foams in the amounts sufficient for massive oil spills is highly difficult and alternative composite structures are also investigated. CNMs were used with polyvinylidene fluoride [10], vermiculite [11], cellulose acetate [12], and nanofibrillated cellulose [13] to create selectively absorbing sponges.

Although CNM based materials are highly efficient as selective sorbents, much research is also focused on applying natural materials such as kapok, milkweed, and cattail [14,15] for this purpose. However, cotton, especially naturally hydrophobic raw cotton was found to be the most popular material [16]. Despite worse *SC* and selectivity, its low cost is encouraging industrial use. The most significant obstacle in using cotton is low chemical stability caused by leaching hydrophobic waxes from cotton surface. Thus, more stable hydrophobic agent must be used. Therefore, coating natural fibers with hydrophobic polymers and nanoparticles has been proposed. Coating cotton with SiO<sub>2</sub> particles [17], SiO<sub>2</sub> functionalized with octadecyltrimethoxysilane [18], or polydimethylsiloxane [19] resulted in chemically stable cotton-based sorbents. Moreover, CNMs such as chemically [20] and thermally [21] reduced graphene oxide, diamond like carbon [22], and polydimethylsiloxane decorated graphene oxide [23] were found to be promising as coatings for cotton in selective sorbent applications.

Most of the studies are focused on fabrication of sorbents with the highest possible *SC*. However, for industrial

\*Corresponding author: alina.dudkowiak@put.poznan.pl

applications, more important factor is easiness of preparation and its low cost, whilst the *SC* exceeding 10 g/g may be sufficient. Thus, the aim of this research is to investigate whether coating various cellulose-based materials with Gr flakes may be used to manufacture selective sorbents. Cellulose materials are cheap and commonly accessible, whilst the cost of graphene production is becoming cheaper every year. Therefore, they may be soon applied in large-scale oil removal.

The recent studies of cotton-Gr sorbents were carried out on naturally hydrophobic cotton sponge, coated with graphene oxide decorated with hydrophobic polymer [23] or reduced graphene oxide [20,21]. Due to the preparation procedure, reduced graphene oxide may contain hydrophilic -O, -OH, and -COOH groups. Therefore, we wanted to check if the use of pristine Gr, produced by the method based on microwave plasma, without any additives, surfactants, catalyst, or metal impurities, will permit development of selective sorbents by a simple dip-coating method.

## Experimental

### Materials

The experiments were performed on five types of cellulosic materials such as raw cotton roving, cotton gauze, cotton fabric, cellulose filter paper (Whatman 2727 Chr, 1.4 mm thick), and cellulose wipe (Kimtech Science). Cotton roving is a natural bundle of raw cotton yarns, processed only by

industrial spinning. Raw cotton in over 90 % is composed of cellulose with addition of proteins, waxes, and other residues. It is light and fluffy with fibers of similar thickness, distributed randomly. Large spaces between yarns (Figure 1(b)) are responsible for large *SC*. Moreover, in contrast to the other investigated cellulosic materials it is naturally hydrophobic. Cotton gauze, mostly used for medical applications, is made of cleaned cotton fibers spun into yarns. It is highly absorptive material and shows regular structure of cotton fibers (Figure 1(c)). Cotton fabric is the most popular commercially available cotton-based material as the final product of textile industry. It is not used as sorbent due to low *SC*, although it may be used as potential filter. The advantage of fabric is regular internal structure of densely packed cotton fibers (Figure 1(d)). Cellulose wipe, in contrast to cottons, shows 100 % cellulose content. It is a popular, very hydrophilic, cellulose-based sorbent material. Due to fibers randomly mounted and freely packed, it is highly sorptive (Figure 1(e)). Cellulose filter paper was chosen, as a material of the best known sorption capabilities. It is a pure Whatman filter paper commonly used in chromatography, which is extremely hydrophilic and due to high density, it does not show high *SC*. It is made of irregular and short cellulose fibers (Figure 1(f)).

Gr flakes, with average diameter of 300 nm and thickness below 1 nm and specific surface area of 290 m<sup>2</sup>/g, were obtained from Cambridge Nanosystems Ltd. (Camgraph G1). Spectroscopic grade dichloromethane (DCM) and

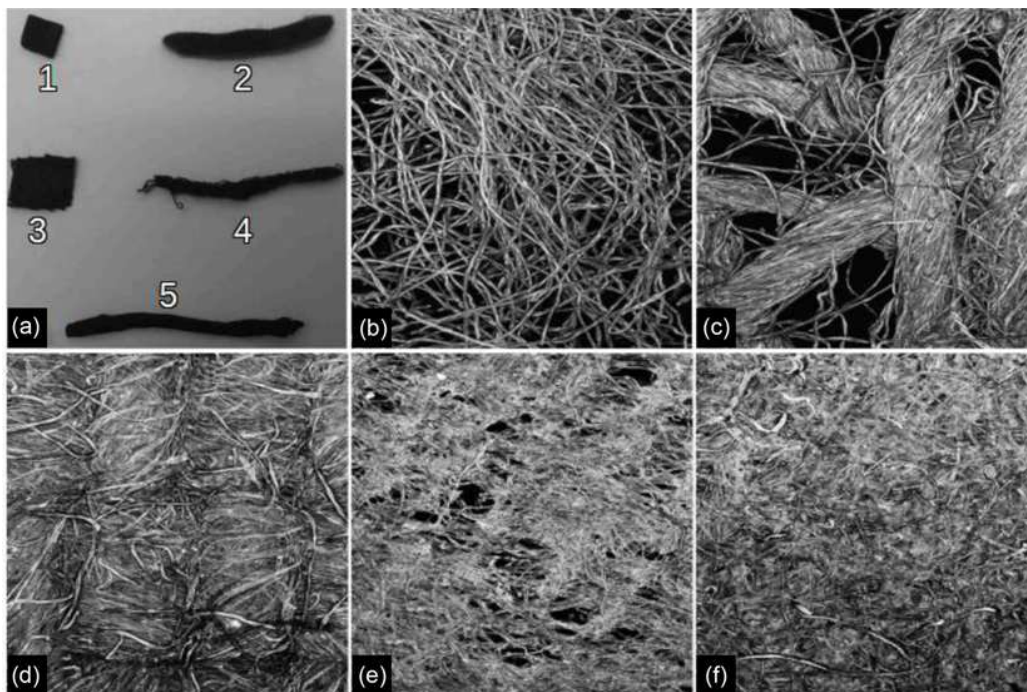


**Figure 1.** Camera photo of Gr coating samples (a) and fluorescence microscopy images (2.5 mm×2.5 mm) of pure cellulosic materials immersed in rhodamine (b-f): (b and 2) roving; (c and 4) gauze; (d and 3) fabric; (e and 5) wipe; (f and 1) paper.

hexane, fraction from pure petroleum were ordered from Avantor Performance Materials Poland SA. Toluene (99.5 % purity), chloroform (>99 % purity), and petroleum ether (boiling point 30–60 °C) were ordered from Sigma Aldrich. Natural motor oil (BDG Lux-10) and linseed oil (Bio, Look Food Ltd.) were purchased from the local store. Liquid paraffin was ordered from Chempur. Rhodamine B was purchased from Sigma Aldrich. Water was filtrated by Milli-Q® ultrapure water system.

### Preparation of Gr Cellulosic Sorbents

CNMs were dispersed using a Hielsher 400 St (400 W) ultrasonic horn. For most experiments, Gr was prepared in DCM in concentration of 1 mg/1 ml (for the microscope image of Gr suspension, please see supplementary materials, Figure S1). Cellulosic materials were cut to samples of 20±2 mg. In order to remove waxes and oily contaminations, they were washed in the following procedure: 20 min sonication in water, drying (at least 60 min in 90 °C), 20 min sonication in acetone, drying (at least 30 min in 90 °C). Then, the samples were immersed in Gr dispersion during 3 s for each dip coating and dried on a heat plate. The procedure was repeated six times in order to obtain uniform coating.

### Characterization

The SEM images were taken by an FEI Nova NanoSEM 650 and the EDS by a Bruker XFlash® 5010 detector. Due to excessive charging under SEM, all the samples were covered with approx. 10 nm layer of copper which enabled successful imaging of the surface.

The fluorescent microscopy images were taken by Zeiss LSM 510. In order to obtain high-resolution images, pure cellulosic samples were immersed in rhodamine B diluted in water. The fluorescence excitation was set at 548 nm laser beam.

Contact angle ( $\theta$ ) was measured with a CCD camera (Nikon D300s). Droplets of 13.0±0.5  $\mu$ l were deposited using a Hamilton micro-syringe (25  $\mu$ l). The droplet volume was increased with respect to its size in the standard contact angle measurements because of very high roughness of roving. The contact angles were measured on each surface three times with the aid of Dropsnake plugin to ImageJ software [24] and the results are presented as mean values with a standard deviation.

### Sorption Measurements

In order to investigate the water repellent properties, the samples were immersed for 3 s in pure water, organic solvents, or oils. Then, the excessive droplets deposited onto the surface were gently shaken off the sorbents. The saturation measurements were performed for five samples for each fluid. The result was calculated as the mean and the standard deviation was calculated as measurement uncertainty. In

order to obtain more repeatable results the gauze and wipe were rolled up (Figure 1(a)).

The *SC* was calculated according to

$$SC = \frac{m_f - m_0}{m_0} \quad (1)$$

where  $m_f$ : mass of sample after immersion in fluid,  $m_0$ : initial mass of sample.

In order to diminish the influence of absorbed fluids density, the volume sorption capacity (*VSC*) was calculated as follow:

$$VSC = \frac{m_f - m_0}{d \times m_0} = \frac{SC}{d} \quad (2)$$

where  $d$ : density of the absorbed fluid.

Selectivity was calculated as the ratio of the mass of selected absorbed fluid to the mass of absorbed water:

$$S = \frac{m_f - m_0}{(m_f - m_0) + (m_w - m_0)} \quad (3)$$

where  $m_w$ : mass of sample immersed in water.

Mass of the deposited Gr was calculated from average sorption of 1 mg/1 ml Gr in DCM, after six times repeated dip-coating.

To determine the recyclable properties of cellulosic sorbents, after conducting the sorption tests, the samples were immersed in petroleum ether and mechanically squeezed in order to recycle the absorbed fluid. The procedure was repeated 10 times and was followed by repeating absorption capacity measurement. Afterwards, the samples were immersed in motor oil and squeezed (5 times), using a similar procedure as described above.

## Results and Discussion

### Coating Cellulosic Materials with Graphene

The five cellulosic materials (cotton roving, gauze, fabric, and cellulosic wipe and Whatman filter paper) showing various yarn size, porosity, chemical composition, and *SC* towards water were selected in order to investigate their ability to absorb the oil or organic solvents. On the samples of this representative group of cellulosic materials, Gr was deposited (as described experimental section) to modify their wetting properties. The deposition process resulted in creating homogeneous Gr layer onto cellulosic fibers (Figure 2). Thanks to high affinity of Gr to cellulose [25] and relatively small size of Gr flakes (approximately 300 nm in diameter), after six Gr depositions it is hard to find any unprotected parts of yarn. It suggests that due to Gr hydrophobicity the coating may act as highly waterproofing barrier. After a few dip-coatings, Gr formed a multilayer on some parts of the fibers. Moreover, a similar quality of coverage was observed for the other Gr coated cellulosic samples (see supplementary materials, Figure S2). Despite

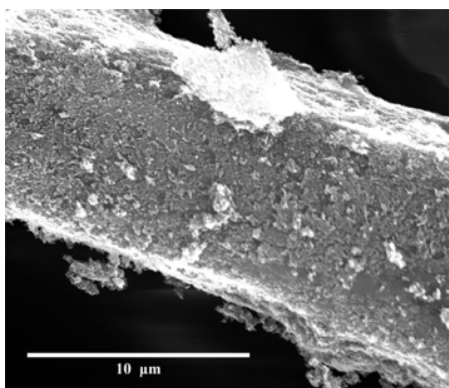


**Figure 2.** SEM image of Gr coated roving.

relatively low Gr content (see supplementary materials, Table S1) it creates a uniform coating, but free spaces between cellulosic fibers are not filled. The cross section of cellulose fibers, measured in 20 different places, showed that the coating thickness varies from 130 nm to 2.03  $\mu\text{m}$  (see supplementary materials, Figure S3). The SEM images show that Gr on the surface of fibers is highly folded which may cause an increase in roughness and in consequence can modify the hydrophobicity of the surface.

### Graphene Coated Cellulosic Materials as Selective Sorbents

The Gr coated cellulosic materials were tested for water repellent properties, which are important to create selective sorbents. As shown in Figure 3 (right side), the pure samples were initially highly hydrophilic (except cotton roving) and soaked up water immediately after droplet deposition. It is related to a high content (exceeding 90 %) of cellulose, having many -OH groups responsible for high affinity to water. But in general, all the cellulosic materials became highly hydrophobic after Gr deposition (Figure 3, left side), as Gr created a water repellent layer. Moreover, according to Wenzel prediction [26], the rough Gr coated surface may become even superhydrophobic.

Gr coated gauze (Gr-gauze), fabric (Gr-fabric), and paper (Gr-paper) (Figure 3(b),(c),(e)) showed stable hydrophobic properties and water droplets deposited onto their surface did not soak inside the sample, even after a few minutes. On the other hand, Gr coated wipe (Gr-wipe) (Figure 3(d)) was found to be hydrophobic, but the contact angle measured for Gr-wipe was smaller than for the other samples, which may be caused by the presence of some unprotected with Gr areas. Any unprotected area causes soaking water into fiber, followed by its distribution in its volume driven by capillary forces. In contrast to other described materials, roving was hydrophobic even before Gr deposition (Figure 3(a)), due to the presence of hydrophobic wax onto the surface of fibers [16]. Thus, to determine whether deposition of Gr onto roving increased its hydrophobicity, contact angle measurements

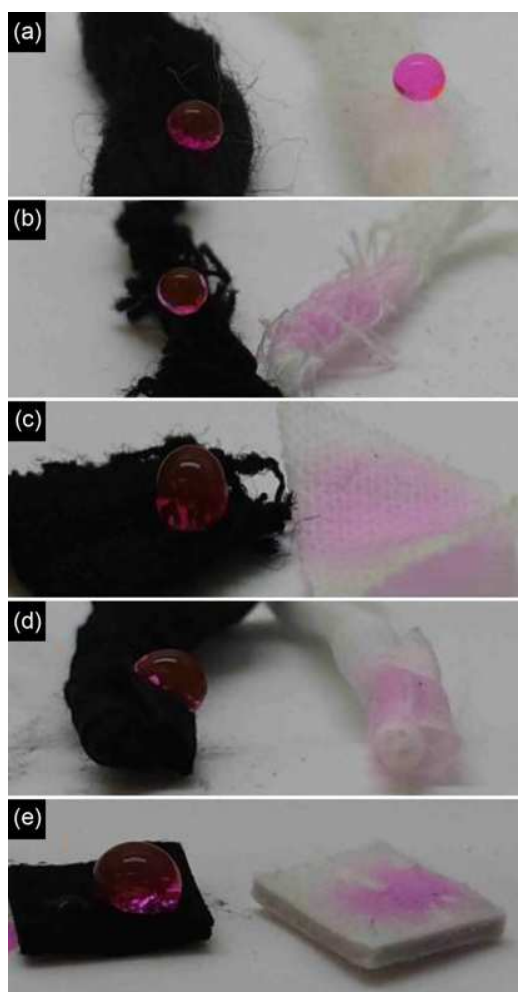


**Figure 3.** Camera photos of water droplets (dyed with rhodamine B) onto Gr coated (left) and pure (right) cellulosic sorbents; (a) roving, (b) gauze, (c) fabric, (d) wipe, and (e) paper.

were performed. The obtained  $\theta$  values were equal to  $139^{\circ}\pm 2^{\circ}$  and  $148^{\circ}\pm 2^{\circ}$ , before and after Gr coating, respectively (see supplementary materials, Figure S4). Thus, to some extent, hydrophobicity increased for Gr coated roving (Gr-roving). There are two possible mechanisms to explain this observation. Either, more hydrophobic Gr substitutes wax or they act synergistically and create a more hydrophobic layer.

In order to determine the volume sorptive properties, pure cellulosic materials were investigated for water soaking. For comparison, Gr coated samples, created via single Gr deposition or by six times repeated Gr deposition, were tested (Figure 4(a)). It is easily noticeable that pure fabric and paper did not soak up large amount of water in comparison to cotton gauze and wipe, which is caused by their microstructure (free spaces between yarns and size of macropores). In addition, roving shows low *SC* (equation (1)), due to its natural water repellent properties.

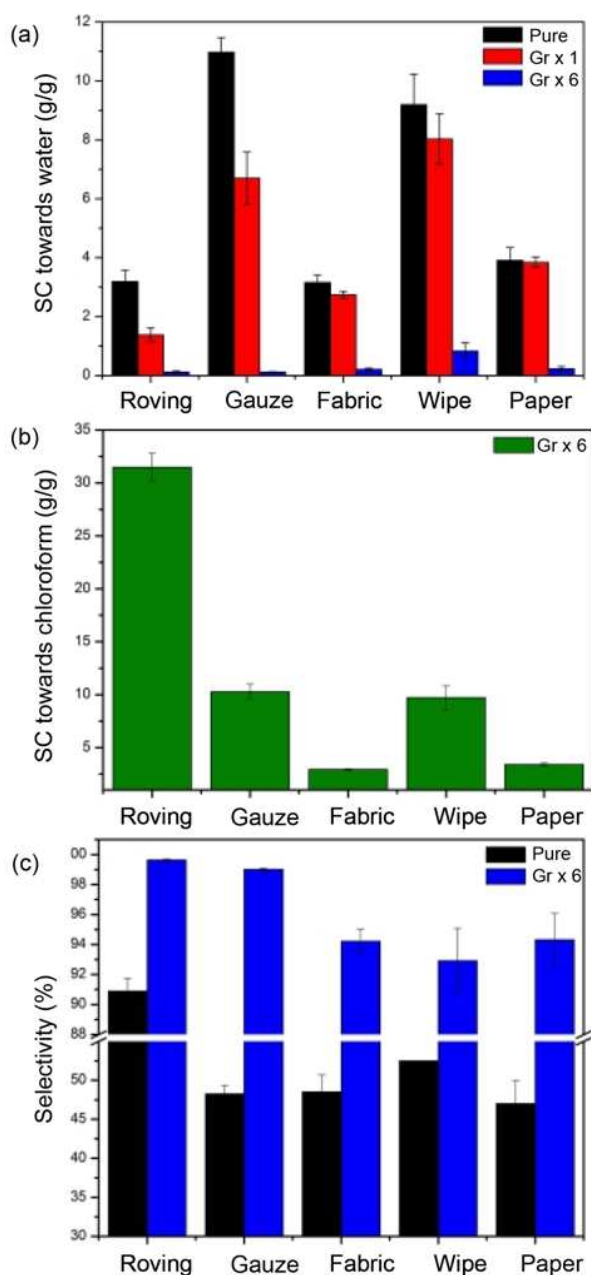


**Figure 4.** Results of sorption capacity (*SC*) towards water (a) and chloroform (b) and selectivity of chloroform versus water (c), of cellulosic sorbents (pure), cellulosic sorbents with single ( $\text{Gr}\times 1$ ) and six times ( $\text{Gr}\times 6$ ) deposited Gr.

The single Gr coverage caused some decrease in *SC* towards water in almost every tested sample (except paper). In the best case *SC* of roving decreased from  $3.19\pm 0.38$  g/g to  $1.38\pm 0.24$  g/g, which was about 57 % reduction after single Gr-coating. It is also noticeable that a single Gr coating caused a relatively high change in sorptivity for gauze (a 39 % decrease in *SC*). In comparison to other samples,

gauze and roving showed also high *SC* towards DCM (see supplementary materials, Table S1), which was the solvent used for Gr dispersion. Thus, dip-coating of roving and gauze showed higher uptake of Gr onto the fibers (see supplementary materials, Table S1). In general, it was found that single deposition of Gr does not induce satisfying water repellent properties and the excellent hydrophobic surfaces of all samples were obtained only after six dip-coating cycles. Almost all  $\text{Gr}\times 6$  coated samples showed *SC* towards water below 0.5 g/g, the one exception was wipe with *SC* equal  $0.8\pm 0.3$  g/g (Figure 4(a)). These results are in good agreement with those presented in Figure 3 and the observations described earlier.

*SC* towards water is the key factor describing sorptive properties of materials. Nevertheless, the *SC* towards water may be significantly different from the *SC* towards other liquids and the comparison of these results is crucial to determine the quality of selective sorbents. Therefore, it is necessary to carry out measurements using the organic solvents and oils. Chloroform was chosen as a representative organic solvent, due to its high surface pressure. The values of *SC* towards chloroform measured for the majority of Gr coated samples (Figure 4(b)) are proportional to the values of *SC* towards water obtained for pure filters (Figure 4(a)). The exception is roving, which shows very high *SC* towards chloroform in comparison to the other cellulosic materials. It could be explained by large distances between fibers, causing large internal volume and by initial hydrophobic properties of roving.

However, the measurements for roving performed on pure and Gr coated samples have shown very similar *SC* towards chloroform and oils (see supplementary materials, Figure S5). Thus, the presence of Gr does not significantly influence the *SC* towards organic solvents or oils, because both Gr and cellulose show high affinity to them.

Another highly important parameter which determines the fluid absorption is the selectivity (equation (3)). The selectivity of the pure cellulosic materials (except roving) was equal approx. 50 % which means that water and chloroform are absorbed almost equally (Figure 4(c)). However, after Gr coating, the same materials became highly selective, with the selectivity of gauze even exceeding 98 %. The improvement of selectivity is also observed for the initially hydrophobic roving and Gr coated roving, which increased from 90 % to 99 %, respectively. Thus, all the Gr coated sorbents absorb at least 10 times more chloroform than water (Figure 4(c)).

Although *SC* towards chloroform and selectivity of Gr coated sorbents were very promising, the measurements on other organic fluids must have been performed. Representatives of high viscosity liquids were motor oil, liquid paraffin, and linseed oil (see supplementary materials, Table S2). Toluene, chloroform, hexane, and petroleum ether were investigated as various low viscosity organic solvents. It is important to notice that hexane, petroleum ether, liquid paraffin, and

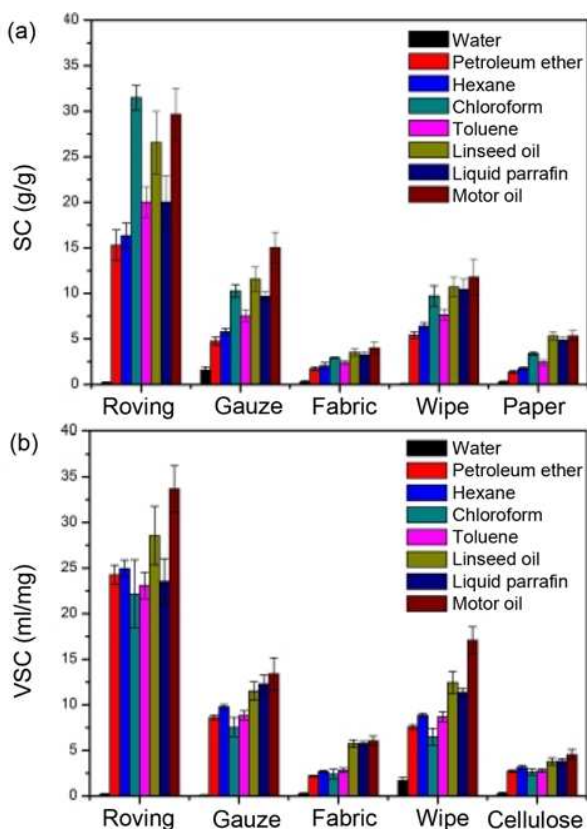


**Figure 5.** Sorption capacity ( $SC$ ) (a) and volume  $SC$  ( $VSC$ ) (b) of Gr coated cellulosic materials towards various fluids.

motor oil are the representative group of organic compounds of oil spills, whilst linseed oil is a natural oil with many different fractions.

In comparison to other fluids,  $SC$  towards water is almost negligible for all samples. In general, the sorption capacities of the samples studied towards the organic solvents are proportional to those towards chloroform (Figure 5(a)). Gr-roving showed the best sorptive properties in comparison to other materials, and also Gr-wipe and Gr-gauze show high sorptivity. Most samples revealed the highest  $SC$  towards chloroform of all organic solvents studied. However, analysis of  $VSC$  (equation (2)) has shown that high  $SC$  towards chloroform is related to its high density (see supplementary materials, Table S2) and in terms of volume absorption, chloroform is absorbed at a level similar to the other low viscosity organic solvents.

Analysis of  $SC$  (Figure 5(a)) and  $VSC$  (Figure 5(b)) results has also pointed out that the sorption properties of used Gr coated materials are well correlated with the viscosity of fluids to be adsorbed. The differences in sorption of low viscous (toluene, chloroform, hexane, ether) and highly viscous (paraffin and oils) fluids are especially visible for Gr-fabric. Because of high density of fibers, it does not

**Table 1.** Sorption capacity ( $SC$ ) towards water, before and after multiple soaking in petroleum ether and motor oil

Material	$SC$ towards water (g/g)		
	Initial	After ether treatment	After oil treatment
Untreated roving	$0.83 \pm 0.21$	$1.66 \pm 0.47$	$2.83 \pm 0.23$
Gr-roving	$0.12 \pm 0.04$	$0.04 \pm 0.04$	$1.10 \pm 0.23$
Gr-gauze	$0.07 \pm 0.04$	$0.05 \pm 0.02$	$0.48 \pm 0.02$
Gr-fabric	$0.08 \pm 0.04$	$0.08 \pm 0.04$	$0.24 \pm 0.07$
Gr-wipe	$0.13 \pm 0.09$	$0.03 \pm 0.06$	$0.42 \pm 0.09$

absorb large amounts of low viscous solvents in contrast to high viscous oils which are probably sticking to the sorbent surface.

### Recyclability of Graphene Coated Cellulosic Sorbents

In industrial applications, selective filters must show high selectivity,  $SC$  or  $VSC$ , but also recyclability. Once used filter should not change its initial parameters significantly, therefore the wear tests were conducted for the purpose of this research. The initial experiments showed that fluids, soaked into Gr coated paper, were not possible to recycle, for this reason these samples were not investigated any further. Thus, the tests on initially hydrophobic untreated roving and on the other Gr coated sorbents were performed using selected fluids (water, petroleum ether, and motor oil).

Multiple soaking in petroleum ether increased the  $SC$  towards water from  $0.83 \pm 0.21$  g/g to  $1.66 \pm 0.47$  g/g, because hydrophobic wax layer was partly dissolved. The petroleum ether treatment did not influence water absorption (Table 1) by Gr coated samples. However, the treatment with motor oil reduced hydrophobic properties of each sample. The highest increase in  $SC$  towards water was observed for pure and Gr coated roving (Table 1). It is caused by flushing out the protective layers, wax and/or Gr, respectively. A significant increase was observed for Gr-wipe and Gr-gauze, whilst the least influenced was Gr-fabric. It may be concluded that oils diminish selective absorption properties much more significantly than organic solvents. The following explanation could be proposed. In ether, due to its low viscosity, viscous force between fluid and surface are not strong. For this reason, Gr layer which interacts with cellulose fibers only via relatively weak physical force is not destroyed during recycling. On the other hand, very viscous motor oil wipes off Gr layers and causes the appearance of unprotected, hydrophilic spots on the fiber surface. Thus, the obtained results prove that Gr-roving which is the most absorptive, is also the most fragile for recycling treatment, whilst the least sorptive Gr-fabric is almost invulnerable for fatigue. Additionally, even the most fragile to wear Gr coated samples were less vulnerable than wax coated raw cotton. Finally, it was found out that for each investigated sample the  $SC$  towards ether and  $SC$  towards oil

did not change significantly after multiple soaking (see supplementary materials, Table S3) and its selectivity was dependent mostly on the changes in *SC* towards water.

### Conclusion

The low cost and mass production of graphene flakes, developed in recent years, makes it a reasonable coating material for industrial applications. We have shown that by coating popular cellulosic materials (such as cotton roving, gauze, fabric and cellulose wipe and paper) with Gr, via simple, one-step, dip-coating from organic solvent Gr dispersion, they are endowed with water repellent properties. Moreover, it was found out that similarly to reduced graphene oxide [20,21], pristine Gr, manufactured using microwave plasma, was responsible for a dramatic decrease in *SC* towards water of cellulosic materials, but it did not influence *SC* towards organic solvents and oils. From among the investigated samples, it seems that Gr coated roving and gauze may be used as selective oil sorbents. The *SC* towards oil was equal 30.6 g/g and 12.8 g/g, for Gr-roving and Gr-gauze, respectively. As their selectivity exceeded 99 % and *SC* towards motor oil was greater than 10 g/g, we believe that both materials may find applications in organic solvent and oil removal from water.

Furthermore, Gr coated fabric may act as a proper selective oil filter, due to its very high selectivity towards organic fluids versus water and low susceptibility to wear. The recyclability tests exhibited that Gr coated samples were less fragile to reuse than raw cotton. Additionally, we found that absorption of high viscosity fluids diminished the hydrophobic properties to greater extent than the absorption of low viscosity ones. It was surprising that the use of highly absorptive cotton roving might be less interesting for some specific applications than that of the less absorptive materials (e.g. fabric), as the susceptibility to wear of the sorbent seems to be correlated to *SC*.

### Acknowledgements

Presented work has been financed by the Ministry of Science & Higher Education in Poland in 2017 year under Project No 06/62DSMK/6201 to D.Ł. and Project No 06/62/DSPB/2171 to A.D.

**Electronic Supplementary Material (ESM)** The online version of this article (doi:10.1007/s12221-018-7879-7) contains supplementary material, which is available to authorized users.

### References

1. S. Gupta and N.-H. Tai, *J. Mater. Chem. A*, **4**, 1550 (2016).

2. M. J. Nine, M. A. Cole, D. N. H. Tran, and D. Losic, *J. Mater. Chem. A*, **3**, 12580 (2015).
3. C. Lee and S. Baik, *Carbon*, **48**, 2192 (2010).
4. C. H. Lee, N. Johnson, J. Drelich, and Y. K. Yap, *Carbon*, **49**, 669 (2011).
5. X. Gui, J. Wei, K. Wang, A. Cao, H. Zhu, Y. Jia, Q. Shu, and D. Wu, *Adv. Mater.*, **22**, 617 (2010).
6. D. D. Nguyen, N.-H. Tai, S.-B. Lee, and W.-S. Kuo, *Energy Environ. Sci.*, **5**, 7908 (2012).
7. H. Ha, K. Shanmuganathan, and C. J. Ellison, *ACS Appl. Mater. Interfaces*, **7**, 6220 (2015).
8. X. Dong, J. Chen, Y. Ma, J. Wang, M. B. Chan-Park, X. Liu, L. Wang, W. Huang, and P. Chen, *Chem. Commun.*, **48**, 10660 (2012).
9. H. Zhu, D. Chen, N. Li, Q. Xu, H. Li, J. He, and J. Lu, *Adv. Funct. Mater.*, **25**, 597 (2015).
10. Y. Yu, H. Chen, Y. Liu, V. S. J. Craig, L. H. Li, Y. Chen, and A. Tricoli, *Polymer*, **55**, 5616 (2014).
11. M. Q. Zhao, J. Q. Huang, Q. Zhang, W. L. Luo, and F. Wei, *Appl. Clay Sci.*, **53**, 1 (2011).
12. Y. Shang, Y. Si, A. Raza, L. Yang, X. Mao, B. Ding, and J. Yu, *Nanoscale*, **4**, 7847 (2012).
13. X. L. Yao, W. J. Yu, X. Xu, F. Chen, and Q. Fu, *Nanoscale*, **7**, 3959 (2015).
14. H. M. Choi and R. M. Cloud, *Environ. Sci. Technol.*, **26**, 772 (1992).
15. S. Cao, T. Dong, G. Xu, and F. Wang, *J. Nat. Fibers*, **5**, 727 (2017).
16. V. Singh, S. Jinka, K. Hake, S. Parameswaran, R. J. Kendall, and S. Ramkumar, *Ind. Eng. Chem. Res.*, **53**, 11954 (2014).
17. F. Liu, M. Ma, D. Zang, Z. Gao, and C. Wang, *Carbohydr. Polym.*, **103**, 480 (2014).
18. J. Li, L. Yan, Y. Zhao, F. Zha, Q. Wang, and Z. Lei, *Phys. Chem. Chem. Phys.*, **17**, 6451 (2015).
19. J. H. Lee, D. H. Kim, and Y. D. Kim, *J. Ind. Eng. Chem.*, **35**, 140 (2016).
20. B. Ge, Z. Zhang, X. Zhu, X. Men, X. Zhou, and Q. Xue, *Compos. Sci. Technol.*, **102**, 100 (2014).
21. N. T. Hoai, N. N. Sang, and T. D. Hoang, *Mater. Sci. Eng. B*, **216**, 1 (2016).
22. B. Cortese, D. Caschera, F. Federici, G. M. Ingo, and G. Gigli, *J. Mater. Chem. A*, **2**, 6781 (2014).
23. H. X. Sun, Z. Q. Zhu, W. D. Liang, B. P. Yang, X. J. Qin, X. H. Zhao, C. J. Pei, P. Q. La, and A. Li, *RSC Adv.*, **4**, 30587 (2014).
24. A. F. Stalder, G. Kulik, D. Sage, L. Barbieri, and P. Hoffmann, *Colloids Surf. A*, **286**, 92 (2006).
25. R. Alqus, S. J. Eichhorn, and R. A. Bryce, *Biomacromolecules*, **16**, 1771 (2015).
26. R. N. Wenzel, *J. Psychosom. Res.*, **53**, 1466 (1949).

Supporting information for:

**Coating cellulosic materials with graphene for selective absorption of oils and organic solvents from water**

*Damian Łukawski<sup>a</sup>, Filip Lisiecki<sup>b</sup>, Alina Dudkowiak<sup>a\*</sup>*

*<sup>a</sup>Faculty of Technical Physics, Poznan University of Technology, Poland*

*<sup>b</sup>Institute of Molecular Physics, Polish Academy of Sciences, Poland*

*\*tel: +48 665 31 81, fax: +48 61 665 3201, email: [alina.dudkowiak@put.poznan.pl](mailto:alina.dudkowiak@put.poznan.pl)*

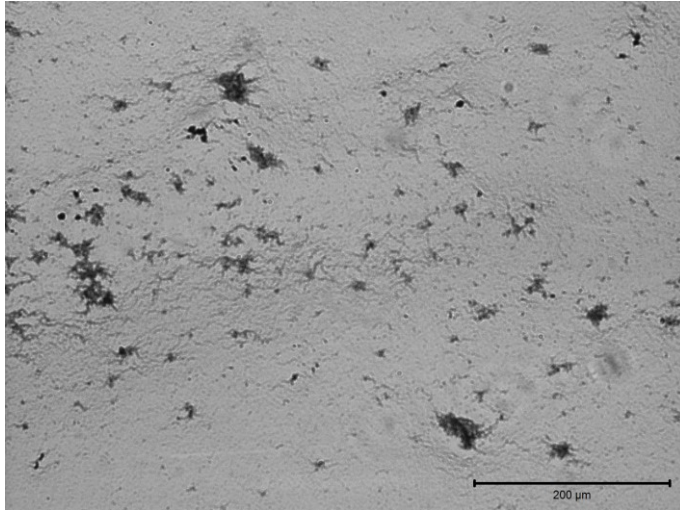


Fig. S1 Optical microscope image of Gr suspension onto microscope slide.

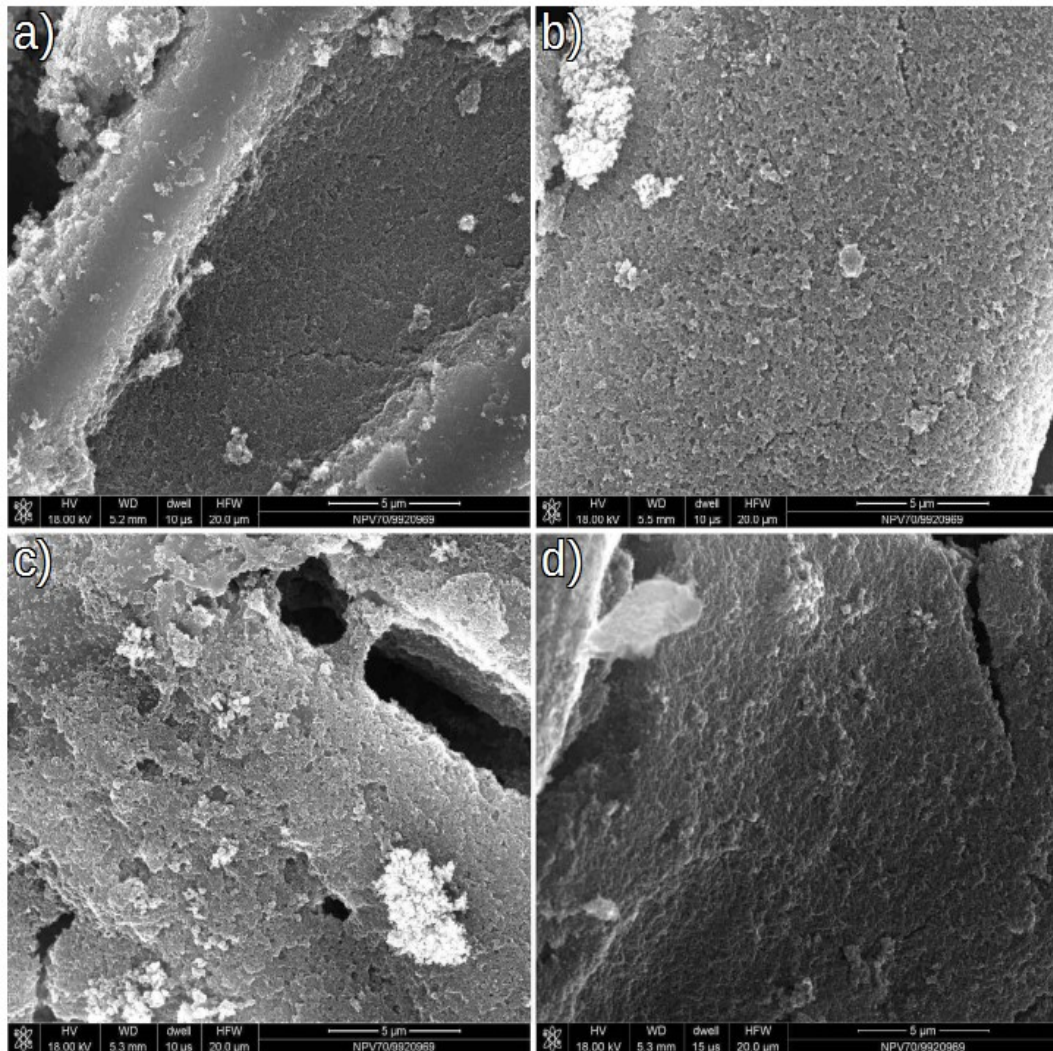


Fig. S2 SEM image of Gr-gauze (a), Gr-fabric (b), Gr-wipe (c) and Gr-paper (d).

Table S1 Mass of the deposited Gr on cellulosic materials.

Sample	SC towards DCM (g/g)	Amount of deposited Gr	
		(mg/sample)	(wt%)
Gr-roving	32.2±3.9	<2.30	<11.9
Gr-gauze	9.5±1.0	<0.85	<4.3
Gr-fabric	2.7±0.2	<0.25	<1.2
Gr-wipe	9.0±1.7	<0.80	<4.1
Gr-paper	3.0±0.2	<0.26	<1.3

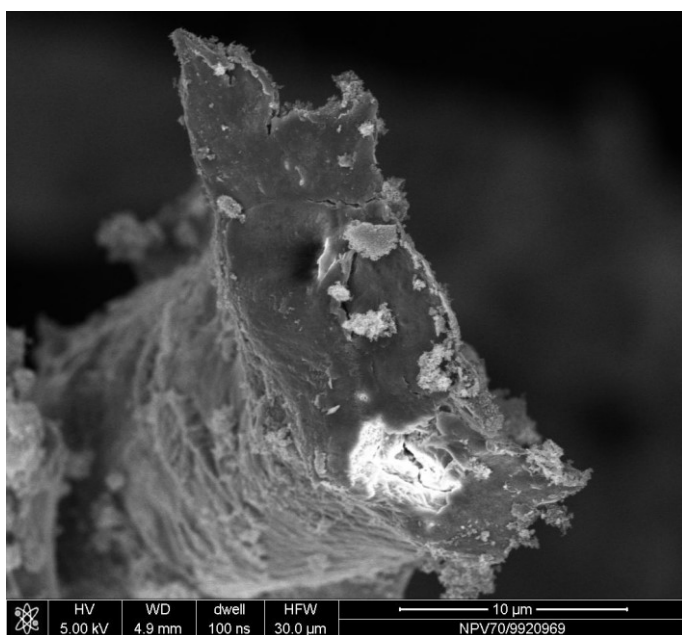


Fig. S3 The representative cross section of Gr-roving

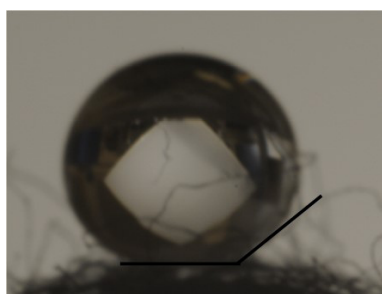


Fig. S4 A droplet onto the surface of Gr-roving.

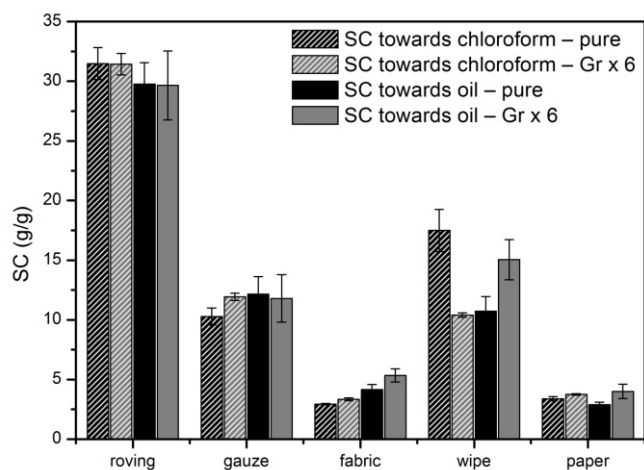


Fig. S5 Sorption capacity (SC) towards oil and chloroform for cellulosic materials (pure) and six times coated with Gr (Gr x 6).

Table S2 Viscosity and density of fluids used for SC measurements.

Fluids	Dynamic viscosity (mPa*s)	Density (g/cm <sup>3</sup> )
motor oil	200-400	0.88
liquid paraffin	110-230	0.85
linseed oil	33	0.93
toluene	0.55	0.867
chloroform	0.53	1.49
hexane	0.3	0.655
petroleum ether	0.22	0.63

Table S3 Sorption capacity (SC) and selectivity of Gr-cellulose sorbents after wear tests.

Sample	SC towards ether (g/g)		Selectivity (ether versus water) (%)		SC towards oil (g/g)		Selectivity (oil versus water) (%)	
	Initial	After ether treatment	Initial	After ether treatment	Initial	After oil treatment	Initial	After oil treatment
pure roving	16.5±1.4	11.8±1.1	93.5±3.3	87.8±3.8	32.6±2.4	28.7±2.2	95.0±1.9	91.1±1.2
Gr-roving	10.8±0.6	10.0±0.9	98.9±0.4	99.6±0.4	27.6±2.0	25.3±1.6	99.8±0.2	95.8±1.0
Gr-gauze	5.3±0.3	4.7±0.4	98.5±0.4	99.0±0.5	14.9±1.1	16.3±2.0	99.7±0.2	97.1±0.6
Gr-fabric	1.5±0.1	1.3±0.2	94.9±2.1	94.2±2.5	6.3±0.7	6.0±0.3	98.8±0.6	96.1±1.1
Gr-wipe	5.0±0.4	4.9±0.4	97.5±1.1	99.4±1.1	14.0±0.9	13.2±1.1	99.8±0.4	97.0±0.8

**Przedruk publikacji [Łukawski, Drewno 2019]**

D. Łukawski, W. Grześkowiak, D. Dukarska, B. Mazela, A. Lekawa-Raus, A. Dudkowiak, The influence of surface modification of wood particles with carbon nanotubes on properties of particleboard glued with phenol-formaldehyde resin, *Drewno* 203 (2019) 93–105.

**Damian ŁUKAWSKI, Wojciech GRZEŚKOWIAK, Dorota DUKARSKA,  
Bartłomiej MAZELA, Agnieszka LEKAWA-RAUS, Alina DUDKOWIAK**

## **THE INFLUENCE OF SURFACE MODIFICATION OF WOOD PARTICLES WITH CARBON NANOTUBES ON PROPERTIES OF PARTICLEBOARD GLUED WITH PHENOL-FORMALDEHYDE RESIN**

*Research was carried out on a newly manufactured particleboard (PB) containing carbon nanotubes (CNTs) to determine the effect of the CNTs on physical, mechanical and combustion properties of the board. The experiment consisted of two stages. In the first, wood particles were treated with an aqueous suspension of CNTs (0.2% w/w) and sodium dodecylbenzenesulfonate (0.2% w/w) as a dispersant. After drying to constant weight, a modified form of the ASTM E69 method was used to determine the effectiveness of fire protection provided by CNT-modified wood chips. The rate of wood decomposition decreased significantly, and the time to complete combustion increased from 18 to 22.5 min for the reference and CNT-modified wood particles respectively. In the second stage of the experiment a particleboard bonded with phenyl-formaldehyde resin was produced, in which the particles were modified with CNTs using the method described in the first stage. Selected physical and mechanical properties of the final board were determined. Samples of the board were tested using a mass loss calorimeter in accordance with the ISO 13927 standard, and mechanical tests were performed by applicable standard methods. However, no significant improvement in the properties of the PB were observed.*

**Keywords:** carbon nanotubes, wood chips, particleboard, flammability, mechanical properties

### **Introduction**

Nanotechnology is applied nowadays in many fields, including energy storage, nanoelectronics and biotechnology, as well as materials science. Recent studies

---

Damian ŁUKAWSKI✉ ([damian.m.lukawski@doctorate.put.poznan.pl](mailto:damian.m.lukawski@doctorate.put.poznan.pl)), Alina DUDKOWIAK ([alina.dudkowiak@put.poznan.pl](mailto:alina.dudkowiak@put.poznan.pl)), Faculty of Technical Physics, Poznan University of Technology, Poznan, Poland; Wojciech GRZEŚKOWIAK ([wojblack@up.poznan.pl](mailto:wojblack@up.poznan.pl)), Dorota DUKARSKA ([d dukar@up.poznan.pl](mailto:d dukar@up.poznan.pl)), Bartłomiej MAZELA ([bartsimp@up.poznan.pl](mailto:bartsimp@up.poznan.pl)), Faculty of Wood Technology, Poznań University of Life Sciences, Poznan, Poland; Agnieszka LEKAWA-RAUS ([alekawa@mchtr.pw.edu.pl](mailto:alekawa@mchtr.pw.edu.pl)), Faculty of Mechatronics, Warsaw University of Technology, Warsaw, Poland

have resulted in applications of nanomaterial composites, including wood-based panels.

Studies to date have shown that the inclusion of small quantities of various types of nanomaterials, such as nano-SiO<sub>2</sub>, nano-ZnO, nano-Al<sub>2</sub>O<sub>3</sub>, nano-CuO, nano-TiO<sub>2</sub>, nano-Ag, nanoclay, nanocellulose, etc., can significantly change the properties of both adhesive resins and joints bonded with those resins. The addition of nanoparticles helps to control the viscosity of resin solutions, increases the strength and thermal and water resistance of adhesive-bonded joints, and improves their barrier properties [Romueli et al. 2012; Dukarska and Bartkowiak 2016; Dukarska and Czarnecki 2016]. Reinforcement of adhesive-bonded joints by the addition of nanoparticles results in improved strength parameters, water resistance and hygienic properties of wood-based materials [Zhang and Smith 2010; Taghiyari et al. 2011; Veigel et al. 2012; Salari et al. 2013; Taghiyari and Farajpour Bibalan 2013; Liu and Zhu 2014; Candan and Akbulut 2015; Dukarska and Czarnecki 2016]. The use of nanomaterials also enables the production of wood-based boards with required physical and mechanical properties from alternative raw materials, most often of inferior quality, such as date or paulownia wood or annual plant waste [Salari et al. 2013; Rangavar and Fard 2015]. As regards technological processes, the use of nanoparticles enables optimization of the manufacture of particleboards (PBs). The introduction of such particles into the adhesive resin solution increases the thermal conductivity of the pressed mat and enhances heat transfer from the external layers to the core layer. This in turn improves the conditions of condensation of the adhesive resin. As a consequence, the pressing time of the boards may be shortened without impairing their physical or mechanical properties [Lei et al. 2008; Zhang and Smith 2010; Taghiyari et al. 2011, 2013; Kumar et al. 2013]. Promising results have also been obtained for the biological resistance of materials modified with nanoparticles, as they have been found to be more resistant to various types of molds and termites [Taghiyari and Farajpour Bibalan 2013; Gao and Du 2015; Marzbani et al. 2015; Dukarska et al. 2017].

When PBs are used in construction, great importance attaches not only to their mechanical properties, but also to their fire resistance, in view of the flammability of boards of this type. To reduce the fire risk, a wide range of flame retardants is used to improve the properties of flammable materials [Boruszewski et al. 2011]. It has already been proposed that recent progress in nanotechnology may be of use in producing fire retardant coatings or additives. The most promising nanomaterials include carbon nanotubes (CNTs). Their unique chemical [Lin et al. 2003; Tasis et al. 2006], thermal [Berber et al. 2000; Kim et al. 2001] and mechanical properties [Treacy et al. 1996] have been widely researched in recent years. The development of chemical vapor deposition enabled the manufacture of cheap mass-produced CNTs [Cassell et al. 1999; Chhowalla et al. 2001], which may be used *inter alia* in polymer

composites and coatings. Currently, CNTs are a popular additive to polymer composites to improve their mechanical properties and to act as a flame retardant.

CNTs dispersed in polystyrene and poly(methyl methacrylate) (PMMA) matrices may serve as a flame retardant, reducing the two key parameters of mass loss rate (MLR) and peak heat release rate (PHRR) [Kashiwagi et al. 2005; Cipiriano et al. 2007]. Not only CNTs dispersed in the polymer matrix, but also CNT-based coatings, reduced the flammability of composites. PETI330/T650 covered by thin CNT film exhibited decreases PHRR and total mass loss, and increased time to ignition (TTI) [Fu et al. 2010]. Anderson et al. [2010] made a multifunctional cellulose/CNT composite paper, which demonstrated greatly reduced flammability [Anderson et al. 2010]. Thermogravimetric measurements on a phenol-formaldehyde/cellulose composite showed that thermal stability increased slightly on the addition of 1.0 wt% of multiwall (MW) CNTs [Park and Kadla 2012]. Cotton fabrics cross-linked with polyvinylphosphonic acid presented delayed ignition and a decreased burning rate after the incorporation of MWCNTs [Gashti and Almasian 2013]. Although research on cellulose/CNT composites is not a novel area, there are few studies describing composites containing bulk wood or wood-based materials, not only cellulose, mixed with carbon nanotubes. Some current studies on the use of carbon nanomaterials and wood-related products are focused on wood-plastic composites (WPC) made of wood flour and polymer. It has been reported that the addition of CNTs to the composite lowers flammability and increases mechanical strength. Polypropylene/wood flour with 2 wt% of CNTs showed a 25% fall in PHRR and total heat released (THR) and a significant decrease in CO yield [Farsheh et al. 2011].

Unfortunately, all nanomaterials tend to aggregate in such applications. The aggregates not only diminish the positive effect, but may also clog the nozzles used for spraying resin during PB production. Therefore, we propose using CNTs as coating materials for wood particles instead of incorporating them into resins. The main aim of this research is to investigate the flammability of wood particles coated with MWCNTs. Moreover, CNT-modified wood particles were used to manufacture a CNT-modified particleboard, and the flammability, water resistance and mechanical properties of that board were then investigated.

## Materials and methods

### Materials

Industrial-grade NC7000 CNTs were obtained from Nanocyl SA. The dispersant used to prepare the aqueous dispersion of CNTs was sodium dodecylbenzenesulfonate (SDBS) supplied by Sigma Aldrich. The wood particles used were industrial Scots pine (*Pinus sylvestris* L.) chips with average dimensions of  $15.91 \times 1.81 \times 0.91$  mm and a moisture content of 4%. The binder

used to manufacture the PB was phenol-formaldehyde resin (PF) with viscosity 679 mPas (at 25°C), density 1.215 g/cm<sup>3</sup>, solids content 48.5%, pH 8.45 and gel time 271 s (at 130°C).

### Sample preparation

In the first stage of the study, wood particles were coated with CNTs. An aqueous dispersion of CNTs (0.2% w/w) and SDBS (0.2% w/w) was sonicated using a Hielsher UP400 ultrasonic homogenizer for 20 min. CNTs were deposited onto wood particles in a simple dip-coating process. A CNT suspension (4 l) was used to obtain 2 kg of CNT-modified wood particles, so that the final ratio of CNTs to wood was approximately 0.4% (w/w). Afterwards, the wood particles were dried at 105°C to obtain the humidity of the reference chips (4%).

Single-layer PBs were produced in laboratory conditions with the following parameters: thickness 12 mm, resination 8%, and density 650 kg/m<sup>3</sup>. The pressing process was carried out at 200°C, with a unit pressure of 2.5 N/mm<sup>2</sup> and for a time of 23 s per mm of board thickness. The PBs were prepared according to the same procedure: the first contained pure wood particles, and the second contained wood particles modified with CNTs.

### Flammability

The study was conducted in several stages. In the first stage, a modified form of the ASTM E69 method was used to determine the effectiveness of the protection of pine wood particles with an aqueous CNT suspension. The next step was to produce particleboard from protected chips and to test it for flammability using a mass loss calorimeter (MLC), and to carry out strength tests based on current standards.

The test of the flaming properties of wood particles was performed according to a modified form of the ASTM E69 method, by burning protected and control (unprotected) samples in a tubular furnace. The modification consisted in the making of a special basket of approximately one-liter volume, made of 2 × 2 mm steel mesh, with diameter 5 cm and length 50 cm. The empty basket was weighed before the test. The test pieces were poured into portions of the basket, being successively whipped using a wooden plunger. When the basket was filled, the whole was weighed to calculate the bulk density. Then the filled basket was suspended in the tube. A burner was placed under the suspended sample, with a flame height of approximately 25 cm. The flame acted on the sample for 3 minutes. The percentage mass loss and the exhaust gas temperature at the outlet of the pipe were recorded every 0.5 minutes. Further observations and recordings were made from the moment the burner was extinguished until three weight loss measurements returned the same value. At

the same time measurements of the flue gas temperature at the outlet of the tube were made using a thermocouple.

The following types of board were investigated: pure PB (control) and PB modified with CNTs. Flammability tests were carried out on three samples for each type. MLC is a benchmark that enables the measurement of mass loss rate and HRR (heat release rate) for any heat flux used for full-scale cone calorimetry (ISO 5660). The tests were carried out in accordance with ISO 13927, with a radiant heat of 35 kW/m<sup>2</sup>. The applied radiant intensity corresponds to fire protection targets, especially for polymers, and corresponds to the intensity of heat flux in a small-scale fire [Schartel and Hull 2007]. In the tests we used 100 × 100 mm particleboard samples with a thickness of 12 mm. Using the standard calorimeter software, the following combustion properties of the examined materials were determined: heat release rate (HRR), mass loss rate (MLR), THR, effective heat of combustion (HOC), final sample weight (FSW) and TTI. Average results are reported here for HRR, max. PHRR, mass loss [%] and TTI [s].

### Particleboard properties

Before testing, all samples of the manufactured boards were subjected to conditioning to achieve a constant mass at 20°C and relative humidity 65%. The moisture content of the samples was about 8%. The mechanical properties of the experimental boards and their water resistance were tested according to relevant standards. We determined the modulus of rupture (MOR) and modulus of elasticity (MOE) according to EN 310 and the internal bond (IB) according to EN 319. The water resistance of the boards was investigated by measuring the internal bond after a boil test (V-100) according to EN 1087-1, and the thickness swelling (TS) after 2 and 24 h of soaking in water according to EN 317. As well as thickness swelling the water absorption (WA) was also calculated, using equation (1):

$$WA = \frac{m_2 - m_1}{m_1} \cdot 100 \quad (1)$$

where  $WA$  is the water absorption (%), and  $m_1$  and  $m_2$  are the sample mass before and after soaking (g).

Each test was performed in 15 replicates. The results obtained for the physical and mechanical properties of the experimental boards were statistically analyzed using Statistica software (version 13.1). To compare the average values of the physical and mechanical properties of the tested boards, we carried out a single-factor analysis of variance and Tukey's post hoc test, on the basis of which uniform average values were determined for each of the investigated properties, with the boundary significance level equal to 0.05.

## Results and discussion

### Fire retardant properties of CNT-modified wood particles

The burning of wood is a very complex physicochemical process. Flammable gases such as ethane, methane, and hydrogen are the main causes of flammability. As the temperature rises, the intensity of evolution of the gases increases. In the wood, as a result of low heat permeability, it is mostly the top layer that is burned. Incineration is slow, and a layer of charred wood effectively slows down the process, thanks to the very low thermal conductivity of char [Kozłowski and Władyska-Przybylak 2001; Hankalin et al. 2009]. The thermal conductivity of char is several times smaller than that of wood. After the formation of this layer and removal of the heat source, the process is suppressed, and self-extinguishing can even occur.

The highest temperatures during this part of the experiment were  $177 \pm 23^\circ\text{C}$  and  $191 \pm 10^\circ\text{C}$  respectively for the reference and CNT-modified wood particles. Despite the slightly higher temperature of the exhaust gases, the mass loss following exposure to the flame for 3 minutes was lower for the CNT-modified wood particles ( $12 \pm 1\%$ ) than for the reference samples ( $16 \pm 3\%$ ).

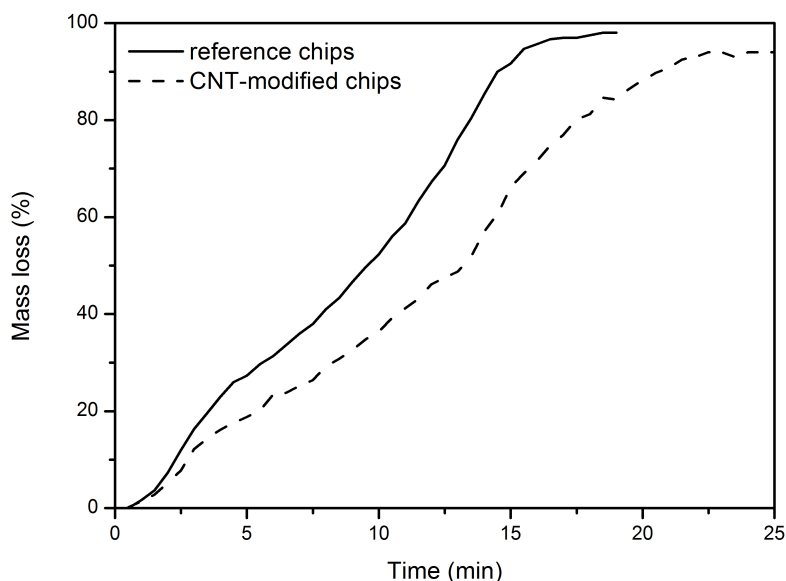


**Fig. 1.** Mass loss of reference and CNT-modified wood chips

Removal of the flame caused a rapid decrease in temperature followed by smoldering of the samples. After 10 minutes, the average mass loss was  $52 \pm 4\%$  and  $36 \pm 2\%$  for the reference and CNT-modified samples respectively. Therefore, the presence of CNTs caused a significant reduction in the rate of decomposition. Afterwards, from the beginning of the experiment, the process of combustion of the reference wood particles was accelerated and the temperature increased to  $347 \pm 52^\circ\text{C}$  in  $14.0 \pm 1.0$  minutes. Similar behavior was observed for

the CNT-modified wood particles, for which the temperature reached  $323 \pm 47^\circ\text{C}$  after  $17.0 \pm 1.5$  minutes. Such temperatures are the result of the re-emergence of flames in the higher layers of chips placed in the basket. These results suggest that the CNT coating produces a clear retardation of wood particle combustion. The whole process lasted for  $18.0 \pm 1.0$  minutes and  $22.5 \pm 1.5$  minutes, and the mass loss was  $98.0 \pm 0.5\%$  and  $94.5 \pm 1.5\%$ , for the reference and CNT-modified samples respectively. The results suggest that covering wood particles with CNTs produces a fire retardant effect. The retardation of combustion is clearly visible on the dynamic mass loss graph (fig. 1), which shows that the combustion process was much slower after modification with CNTs. However, the observed smoke temperatures were not significantly changed, which may be explained by the lack of an active mechanism of flame suppression.

Several possible mechanisms have been proposed to explain the flame retardant properties of composites containing CNTs in the polymer matrix. The thermal conductivity of polymers increases after the incorporation of CNTs, particularly above  $160^\circ\text{C}$  [Kashiwagi et al. 2004]. The presence of CNTs in the matrix may also help to create a thermally insulating char layer [Kashiwagi et al. 2005]. Moreover, the change in the viscoelastic properties of polymers when CNTs are added may lead to an anti-dripping effect when the polymers burn [Capiriani et al. 2007].

In the case of the CNT-modified wood particles, CNTs were located only on the surface of the samples. Therefore, the CNTs did not change any physical properties of the wood, and only surface action could be observed. Among the proposed mechanisms, the most probable is the influence of CNTs on char formation. Char may either be formed more rapidly or be mechanically enhanced to become more durable. As no significant differences were recorded in the first minutes of combustion between the reference and CNT-modified particles (fig. 2), the faster formation of char is unlikely. Therefore, reinforcement of the char layer is a more probable cause. The other mechanism which may be responsible for the fire retardant action is faster heat dissipation during slow burning, caused by the high surface area of CNTs and their high conductivity.

### **Fire retardant properties of CNT-modified particleboards**

Although the mechanism of fire retardation in CNT-modified wood particles may be of interest, it is important to investigate the flammability of complete particleboards. Therefore, a CNT-modified PB was prepared (as described in the Sample Preparation section) and tested by MLC. The average TTI was 4 s shorter for the CNT-modified PB, which may be due to the stronger infrared absorption of black CNTs. The kinetics of HRR after ignition were similar for the reference and the modified PB. The first peak value of HRR was  $102 \text{ kW/m}^2$ ; then, after a slight decrease in HRR, its value rapidly increased. The PHRR was recorded 25 s earlier for CNT-modified PB. As in the case of TTI, the

explanation of the earlier PHRR may be the stronger infrared absorption. The values of time to PHRR and THR were slightly lower for the CNT-modified PB than for the reference, but the difference lies within the limits of measurement uncertainty. Also, no significant change was observed for total mass loss.

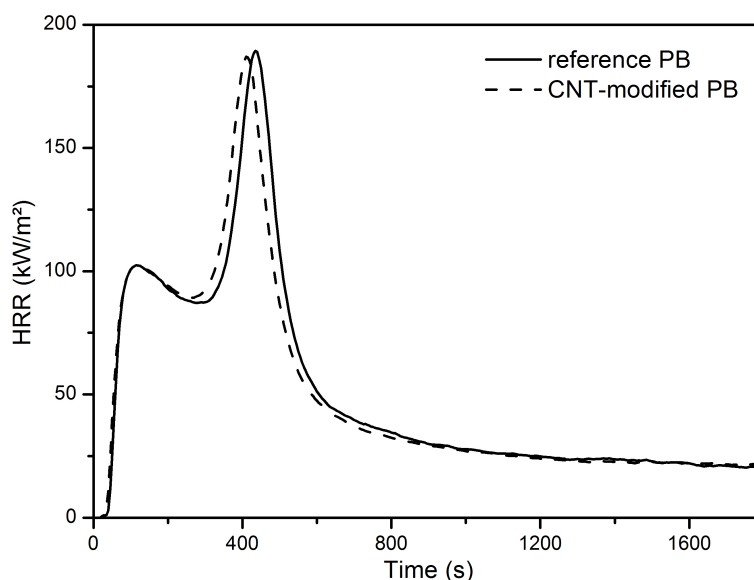


**Fig. 2. Heat release rate measured by MLC during combustion of reference and CNT-modified PBs**

Ineffective fire protection may be explained by the fact that the protective charred layer loses its properties during radiant heat flux. The rapid thermal decomposition causes the formation of large amounts of volatile components which, when mixed with air, ignite and influence the rate of fire spread and the rate of combustion [Grześkowiak and Wiśniewski 2010; Mačiulaitis and Praniauskas 2010]. As explained in the previous section, CNTs may either dissipate heat or enhance the char layer. Neither mechanism involves active flame suppression. The slightly decreased time to PHRR for CNT-modified PB is probably caused by stronger IR absorption and faster heating due to the optical properties of CNTs. In general, it may be claimed that although CNTs retard burning at the initial stage of combustion, there are no active flame suppressive mechanisms which might decrease HRR as observed in high-energy cone calorimetry.

### **Strength properties and water resistance of CNT-modified PB**

Because the CNTs were located only on the surface of wood particles, they should not be expected to influence the physical properties of a single wood particle. However, the interaction between phenol-formaldehyde resin and wood particles might significantly change after CNT deposition. Another important

**Table 1. Combustion properties, investigated by MLC, of reference and CNT-modified PB**

	TTI (s)	THR (MJ/m <sup>2</sup> )	PHRR (kW/m <sup>2</sup> )	Time to PHRR (s)	Total mass loss (%)
Reference PB	38.5 (3.0)*	88 (4)	191 (5)	437 (6)	87.3 (0.7)
CNT-modified PB	34.7 (3.2)	86 (2)	197 (13)	412 (15)	88.3 (2.0)

\*Standard deviations in parentheses.

factor was the presence of SDBS, used as a stabilizing agent for CNT dispersion. The properties of the reference and CNT-modified PBs are presented in table 1. A comparison of mean values obtained for each tested parameter shows that both the strength and swelling of boards made from CNT surface-modified wood chips were slightly higher than those of the reference boards. However, on consideration of the standard deviations associated with the mean values, and above all the results of post hoc analysis used for the determination of homogeneous groups, the differences between the CNT-modified and reference boards were found to be insignificant. Tukey's homogeneous group tests performed for the majority of the investigated properties identified the same homogeneous group, for which the statistical significance level  $p$  took values above the assumed value of 0.05. Only in the case of bending strength and swelling after two hours of water soaking did one-way analysis of variance enable the identification of two different homogeneous groups (a, b), indicating a statistically significant effect of CNT-modified wood chips on these two parameters. Modification of wood chips with carbon nanotubes resulted in a slight increase in board bending strength by ca. 15% (intergroup MS = 2.3665,  $df = 18.000$ ,  $p < 0.05$ ) and slightly increased swelling after short-term water treatment (by ca. 13%, intergroup MS = 4.0367,  $df = 18.000$ ,  $p < 0.05$ ). However, the lower water resistance of the CNT board after short-term water exposure was of little importance, as its swelling after 24 hours of soaking in water was similar to that of the reference boards. A general conclusion is that the modification of wood chips by the method of CNT dispersion investigated in this study does not significantly affect the strength and water resistance of the resulting PBs. This is probably due to the relatively low CNT concentration and the presence of hydrophilic SDBS. This assumption has been confirmed by other researchers studying the effects of surface modification of wood with various types of nanoparticles, who have reported significant changes in strength, hydrophobicity, color durability, fire resistance and bioresistance only at higher concentrations of nanoparticle suspensions [Nowaczyk-Organista 2009; Dong et al. 2015; Soltani et al. 2016; Taghiyari et al. 2016]. Nevertheless, preliminary results, particularly those concerning fire resistance, are promising and encourage further research in this area.

**Table 2. Strength properties and water resistance of the experimental boards**

Property	Reference PB	CNT-modified PB
MOR [N/mm <sup>2</sup> ]	12.9 <sup>a</sup> (1.8)*	14.8 <sup>b</sup> (1.0)
MOE [N/mm <sup>2</sup> ]	2250 <sup>a</sup> (260)	2400 <sup>a</sup> (180)
IB [N/mm <sup>2</sup> ]	0.69 <sup>a</sup> (0.11)	0.64 <sup>a</sup> (0.06)
V-100 [N/mm <sup>2</sup> ]	0.37 <sup>a</sup> (0.04)	0.40 <sup>a</sup> (0.047)
TS – 2 h [%]	22.3 <sup>a</sup> (1.4)	25.1 <sup>b</sup> (2.7)
TS – 24 h [%]	25.9 <sup>a</sup> (2.4)	27.5 <sup>a</sup> (2.5)
WA – 2 h [%]	72.1 <sup>a</sup> (2.6)	72.8 <sup>a</sup> (3.1)
WA – 24 h [%]	85.8 <sup>a</sup> (3.2)	87.2 <sup>a</sup> (2.7)

\*Standard deviations in parentheses, a, b – homogeneous groups, CNT – carbon nanotubes, MOR – modulus of rigidity, MOE – modulus of elasticity, TS – thickness swelling, WA – water absorption.

## Conclusions

In this study, wood particles were coated with a 0.2% (w/w) aqueous dispersion of carbon nanotubes, stabilized with SDBS. The prepared CNT-modified particles were tested using a modified form of the ASTM E69 method. The modification of wood particles with CNTs significantly influenced their combustion properties, and thermal decomposition significantly decreased. We have proposed two models describing the fire retardancy. First, due to their high surface area and thermal conductivity, the CNTs might increase heat dissipation; and second, the CNTs may mechanically enhance the char layer, which thermally insulates the wood from fire. However, although fire retardant properties were observed for CNT-modified wood particles, no significant decrease in the flammability of particleboards was observed after the addition of CNTs. A possible explanation is that during cone calorimetry the combustion was too rapid, and the fire suppressive properties of CNTs are significant only during low-energy thermal degradation. Moreover, tests of strength and water resistance in boards manufactured from both unmodified and CNT-modified wood chips did not show any significant changes in these properties, apart from a slight increase in bending strength. This may be because of the relatively low quantity of CNTs, the presence of SDBS, or the method of modification. However, the preliminary research results presented in this paper may provide a basis for further investigation into the potential of carbon nanotubes in the production of wood-based products.

## References

- Anderson R.E., Guan J., Ricard M., Dubey G., Su J., Lopinski G., Dorris G., Bourne O., Simard B.** [2010]: Multifunctional single-walled carbon nanotube-cellulose composite paper. *Journal of Materials Chemistry* 20: 2400-2407
- Berber S., Kwon Y.-K., Tománek D.** [2000]: Unusually high thermal conductivity of carbon nanotubes. *Physical Review Letters* 84: 4613-4616
- Boruszewski P., Borysiuk P., Jaskółowski W., Świącki A., Mamiński M., Jencyk-Tołoczko I.** [2011]: Influence of flakes impregnation with salt flame retardants on selected physical and mechanical properties of OSB. *Annals of Warsaw University of Life Sciences – SGGW, Forestry and Wood Technology* [73]: 147-152
- Candan Z., Akbulut T.** [2015]: Physical and mechanical properties of nanoreinforced particleboard composites. *Maderas. Ciencia y Tecnología* 17 [2]: 319-334
- Cassell M., Raymakers J., Kong J., Dai H.** [1999]: Large scale CVD synthesis of single-walled carbon nanotubes. *The Journal of Physical Chemistry B* 103: 6484-6492
- Cipiriano B.H., Kashiwagi T., Raghavan S.R., Yang Y., Grulke E., Yamamoto K., Shields J.R., Douglas J.F.** [2007]: Effects of aspect ratio of MWNT on the flammability properties of polymer nanocomposites. *Polymer* 48: 6086-6096
- Chhowalla M., Teo K., Ducati C., Rupesinghe N.L., Amaratunga G., Ferrari A.C., Roy D., Robertson J., Milne W.I.** [2001]: Growth process conditions of vertically aligned carbon nanotubes using plasma enhanced chemical vapor deposition. *Journal of Applied Physics* 90 [10]: 5308-5317
- Dong Y.M., Yan Y.T., Zhang S.F., Li J.Z., Wang J.J.** [2015]: Flammability and physical-mechanical properties assessment of wood treated with furfuryl alcohol and nano-SiO<sub>2</sub>. *European Journal of Wood and Wood Products* 73 [4]: 457-464
- Dukarska D., Bartkowiak M.** [2016]: The effect of organofunctional nanosilica on the cross-linking process and thermal resistance of UF resin. *Journal of Polymer Research* 23 [8]: 1-8
- Dukarska D., Czarnecki R.** [2016]: Fumed silica as filler for MUPF resin in the process of manufacturing water-resistance plywood. *European Journal of Wood and Wood Products* 74 [1]: 5-14
- Dukarska D., Cofta G., Krzykowska J.** [2017]: Resistance of selected wood-based materials glued with nano-SiO<sub>2</sub>/UF resin to *A. niger* infestation. *Annals of Warsaw University of Life Science – SGGW, Forest and Wood Technology* 97: 114-117
- Farsheh A.T., Talaeipour M., Hemmasi A.H., Khademislam H., Ghasemi I.** [2011]: Investigation on the mechanical and morphological properties of foamed nanocomposites based on wood flour/PVC/multi-walled carbon nanotube. *BioResources* 6: 841-852
- Fu X., Zhang C., Liu T., Liang R., Wang B.** [2010]: Carbon nanotube buckypaper to improve fire retardancy of high-temperature/high-performance polymer composites. *Nanotechnology* 21: 235701-235708
- Gao W., Du G.B.** [2015]: Physico-mechanical properties of plywood bonded by nano cupric oxide (CuO) modified PF resins against subterranean termites. *Maderas. Ciencia y Tecnología* 17 [1]: 129-138
- Gashti M., Almasian A.** [2013]: UV radiation induced flame retardant cellulose fiber by using polyvinylphosphonic acid/carbon nanotube composite coating. *Composites Part B: Engineering* 45: 282-289
- Grześkowiak W.L., Wiśniewski T.** [2010]: Fire safety of fireplaces – wood based products: speed of charring. *Annals of Warsaw University of Life Sciences – SGGW, Forestry and Wood Technology* [71]: 229-234

- Hankalin V., Ahonen T., Raiko R.** [2009]: On thermal properties of a pyrolysing wood particle. In Finnish-Swedish Flame Days 2009, January 28-29, 2009, Naantali, Finland. 2009. p. 16
- Kashiwagi T., Grukle E., Hilding J., Groth K., Harris R., Butler K., Shields J., Kharaechenki S., Douglas J.** [2004]: Thermal and flammability properties of polypropylene/carbon nanotube nanocomposites. *Polymer* 45: 4227-4239
- Kashiwagi T., Du F., Winey K.I., Groth K.M., Shields J.R., Bellayer S.P., Kim H., Douglas J.F.** [2005]: Flammability properties of polymer nanocomposites with single-walled carbon nanotubes: Effects of nanotube dispersion and concentration. *Polymer* 46 [2]: 471-481
- Kim P., Shi L., Majumdar A., McEuen P.L.** [2001]: Thermal transport measurements of individual multiwalled nanotubes. *Physical Review Letters* 87: 215502
- Kozłowski R., Władyka-Przybylak M.** [2001]: Natural polymers, wood and lignocellulosic materials in Fire Retardant Materials. Edited by: A.R. Horrocks and D. Price ISBN: 978-1-85573-419-7: 293-317
- Kumar A., Gupta A., Sharma K.V., Nasir M.** [2013]: Use of aluminum oxide nanoparticles in wood composites to enhance the heat transfer during hot-pressing. *European Journal of Wood and Wood Products* 71 [2]: 193-198
- Lei L.H., Du G., Pizzi A., Celzard A.** [2008]: Influence of nanoclay on urea-formaldehyde adhesives for wood adhesives and its model. *Journal of Applied Polymer Science* 109: 2442-2451
- Lin T., Bajpai V., Ji T., Dai L.** [2003]: Chemistry of carbon nanotubes. *Australian Journal of Chemistry* 56: 635-651
- Liu Y., Zhu X.** [2014]: Measurement of formaldehyde and VOCs emissions from wood-based panels with nanomaterial-added melamine-impregnated paper. *Construction and Building Materials* 66: 132-137
- Mačiulaitis R., Praniauskas V.** [2010]: Fire tests on wood products subjected to different heat fluxes. *Journal of Civil Engineering and Management* 16: 484-490
- Marzbani P., Afrouzi Y.M., Omidvar A.** [2015]: The effect of nano-zinc oxide on particleboard decay resistance. *Maderas. Ciencia y Tecnología* 17 [1]: 63-68
- Nowaczyk-Organista M.** [2009]: Protection of birch and walnut wood colour from the effect of exposure to light using ultra-fine zinc white. *Drewno* 52 [181]: 19-41
- Park B.-D., Kadla J.F.** [2012]: Thermal degradation kinetics of resole phenol-formaldehyde resin/multi-walled carbon nanotubes/cellulose nanocomposite. *Thermochimica Acta* 540: 107-115
- Roumeli E., Papadopoulou E., Pavlidou E., Vourlias G., Bikiaris D., Paraskevopoulos K.M., Chrissafis K.** [2012]: Synthesis, characterization and thermal analysis of urea-formaldehyde/nanoSiO<sub>2</sub> resin. *Thermochimica Acta* 527: 33-39
- Rangavar H., Fard H.M.S.** [2015]: The effect of nanocopper additions in a urea-formaldehyde adhesive on the physical and mechanical properties of particleboard manufactured from date palm waste. *Mechanics of Composite Materials* 51 [1]: 119-126
- Salari A., Tabarsa T., Khazaeian A., Saraeian A.** [2013]: Improving some of applied properties of oriented strand board (OSB) made from underutilized low quality paulownia (*Paulownia fortunei*) wood employing nano-SiO<sub>2</sub>. *Industrial Crops and Products* 42: 1-9
- Schartel B., Hull T.R.** [2007]: Development of fire-retarded materials – Interpretation of cone calorimeter data. *Fire and Materials* 31: 327-354
- Soltani A., Hosseinpourpia R., Adamopoulos S., Taghiyari H.R., Ghaffari E.** [2016]: Effects of heat-treatment and nano-wollastonite impregnation on fire properties of solid wood. *BioResources* 11 [4]: 8953-8967

- Taghiyari H.R., Rassam G., Ahmadi-Davazdah Emam K.** [2016]: Effects of densification on untreated and nano-aluminum-oxide impregnated poplar wood. *Journal of Forestry Research* 28 [2]: 403-410
- Taghiyari H.R., Rangavar H., Farajpour Bibalan O.** [2011]: Effect of nano-silver on reduction of hot-pressing time and improvement in physical and mechanical properties of particleboard. *Bioresources* 6: 4067-4075
- Taghiyari H.R., Farajpour Bibalan O.** [2013]: Effect of copper nanoparticles on permeability, physical and mechanical properties of particleboard. *European Journal of Wood and Wood Products* 71 [1]: 69-77
- Taghiyari H.R., Mobini K., Sarvari Samadi Y., Doosti Z., Karimi F., Asghari M., Jahangiri A., Nouri P.** [2013]: Effects of nano-wollastonite on thermal conductivity coefficient of medium-density fiberboard. *Journal of Nanomaterials and Molecular Nanotechnology* 2: 1-5
- Tasis D., Tagmatarchis N., Bianco A., Prato M.** [2006]: Chemistry of carbon nanotubes. *Chemical Reviews* 106: 1105-1136
- Treacy M., Ebbesen T.W., Gibson J.M.** [1996]: Exceptionally high Young's modulus observed for individual carbon nanotubes. *Nature* 381: 678-680
- Zhang C., Smith G.D.** [2010]: Effect of nanoclay addition to phenol – formaldehyde resin on the permeability of oriented strand lumber. *Wood Fiber Science* 42 [4]: 1-3
- Veigel S., Rathke J., Weigl M., Gindl-Altmutter W.** [2012]: Particle board and oriented strand board prepared with nanocellulose-reinforced adhesive. *Journal Nanomaterials* 158503: 1-8

### List of standards

- ASTM E69** Standard test method for combustible properties of treated wood by the fire-tube apparatus
- EN 310:1993** Wood based panels. Determination of modulus of elasticity in bending and of bending strength. European Committee for Standardization, Brussels
- EN 317:1993** Particleboards and fiberboards. Determination of swelling in thickness after immersion in water. European Committee for Standardization, Brussels
- EN 319:1993** Determination of tensile strength perpendicular to the plane of the board. European Committee for Standardization, Brussels
- EN 1087-1:1995** Particleboards – Determination of moisture resistance – Boil test
- ISO 13927:2015** Plastics – Simple heat release test using a conical radiant heater and a thermopile detector
- ISO 5660** Cone calorimeter, heat release and smoke production

### Acknowledgements

The research was financed by grants from the National Science Centre, Poland (project no. 2015/19/N/ST8/02184) (to DŁ), and from the Ministry of Science & Higher Education in Poland (project no. 06/62/DSPB/2171) (to AD).

*Submission date: 21.12.2017*

*Online publication date: 8.10.2018*

**Przedruk publikacji [Łukawski, Composites A 2019]**

D. Łukawski, A. Dudkowiak, D. Janczak, A. Lekawa-Raus, Preparation and applications of electrically conductive wood layered composites, *Composites Part A: Applied Science and Manufacturing* 127 (2019) 105656: 1–10.



# Preparation and applications of electrically conductive wood layered composites



Damian Łukawski<sup>a</sup>, Alina Dudkowiak<sup>a</sup>, Daniel Janczak<sup>b</sup>, Agnieszka Lekawa-Raus<sup>b,\*</sup>

<sup>a</sup> Poznan University of Technology, Faculty of Technical Physics, 60-965 Poznan, Poland

<sup>b</sup> Warsaw University of Technology, Faculty of Mechatronics, 02-525 Warsaw, Poland

## ARTICLE INFO

### Keywords:

- A. Carbon nanotubes and nanofibers
- A. Multifunctional composites carbon nanotubes
- A. Wood fibres
- B. Electrical properties

## ABSTRACT

This paper presents simple, inexpensive and industrially-viable methods of creating electronically-active carbon nanotube and graphene-based coatings for wood, capable of bringing a wide range of new functionalities to traditionally passive wood-based construction elements, including furniture and flooring. The coating methods are tested against the surface properties of wood/wood-based materials and specific application requirements. Furthermore, a set of examples of wood-based electronic applications potentially useful in a wood industry context is demonstrated/tested. These include liquid, pressure and temperature sensors for such applications as flood, occupancy or fire detection, as well as nano/microthin heaters for residential heating or drying of moist construction wood.

## 1. Introduction

Although used for thousands of years, wood is still one of the most popular materials deployed in engineering. Its applications are nowadays primarily, but not exclusively, construction, decoration, flooring and furniture. However, due to such issues as global warming and an overproduction of non-recyclable waste, wood has recently gained even broader attention as a natural, biodegradable, recyclable, widely available and inexpensive material. Therefore, it is quite expected that in the current era of rapid development of materials engineering, interest in the design of completely new wood-derived materials, composites and applications is also growing quickly [1–5].

Believing in the potential of wood, we have recently proposed to hybridize it with carbon nanomaterials (CNMs), such as carbon nanotubes (CNTs) or graphene. Graphene is a two-dimensional one-atom thick sheet of carbon atoms arranged in a hexagonal lattice and CNTs are one-dimensional tubules with the walls made of graphene. CNMs may be mass produced from greenhouse gases such as methane [6–8], and can be easily and safely recycled, biodegraded, or combusted producing only gases appearing in the natural wood thermal decomposition process [9–11]. Therefore, CNMs seem much more compatible with natural wood than commonly used synthetic polymers or metals. Simultaneously, being inexpensive they are of great interest from both the scientific and applications perspective.

Our previous work has shown that CNMs are attracted to natural

cellulose structures present in wood, and hence may be successfully deposited on its surface in the pure form using inexpensive industrial techniques, forming a strongly integrated, irremovable surface layer [12]. The paper has shown that due to intrinsic properties of CNTs such coatings may turn wood superhydrophobic. However, individual CNMs have much more to offer. They are also highly conductive electrically and thermally, mechanically strong, chemically resistant, extremely light-weight, absorptive for UV radiation, and many more.

Out of the above, electrical conductivity is a particularly interesting property. To this point, it has enabled the manufacture of many new types of electrical/electronic elements, including sensors [13–15], heaters [16–18] or simply antistatic coatings or shielding [19]. However, to the best of our knowledge, it has not been considered in the context of wood.

Therefore, in the following paper we propose that the purpose designed CNM coatings on wood can serve as various sensors, heaters or antistatic coatings, introducing new functionalities into traditionally passive wood elements and changing the way the wood materials are perceived and used.

First, the paper identifies possible methods allowing the manufacture of inexpensive, industrially-viable electronically-functional coatings/layers with the desired conductivity, layout and properties, on wood and wood-based products. Next, examples of applications which could become highly useful in the wood industry are carried out and tested (Fig. 1). These include: antistatic surfaces, floor heaters, furniture

\* Corresponding author.

E-mail address: [alekawa@mchtr.pw.edu.pl](mailto:alekawa@mchtr.pw.edu.pl) (A. Lekawa-Raus).

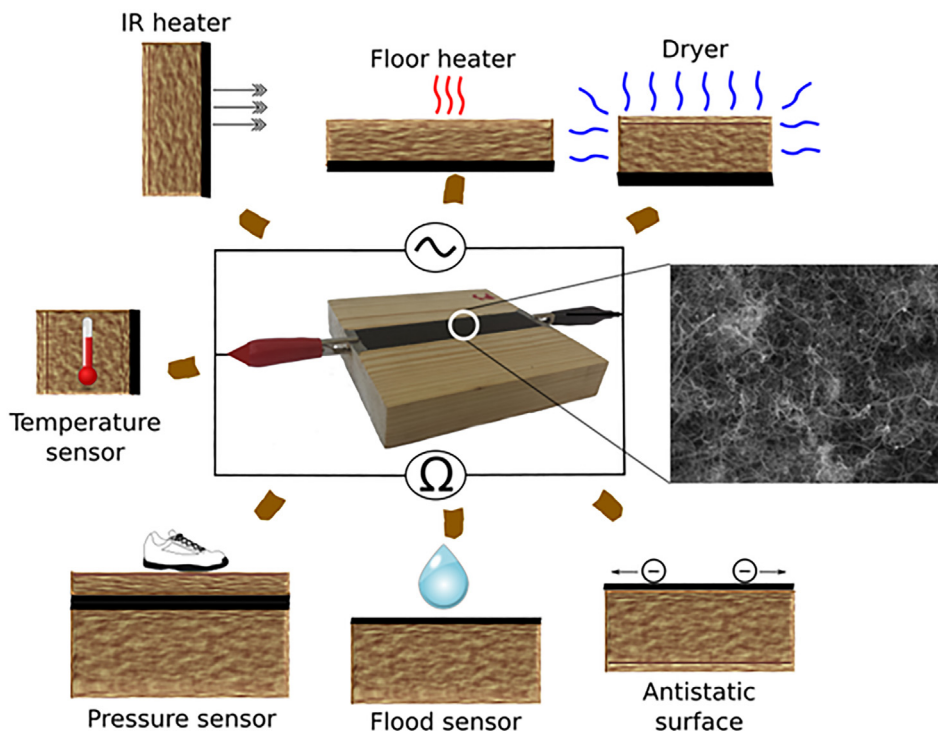


Fig. 1. Scheme of the concept of functional wood/CNT composite. (For interpretation of the references to colour in this figure legend, the reader is referred to the web version of this article.)

IR heaters and self-drying wood blocks, as well as sensors for temperature monitoring, flood alarming and motion or crack detection. This list of possible applications is definitely not exhaustive, yet it shows a set of representative ideas which would not be possible or practical to perform with the use of silicone or metallic materials, due to environmental incompatibility, integration difficulties, size or weight.

## 2. Experimental Section

### 2.1. Materials

Wood and wood based materials (Scots pine, balsa, plywood, fiberboard, chipboard, beaverboard, OSB) were obtained from local suppliers. Industrial grade CNTs of 1.5  $\mu\text{m}$  length and 8 nm diameter and 90% carbon purity were purchased from Nanocyl SA (NC7000). Diethylene glycol butyl ether acetate, PMMA ( $M_w = 350,000$ ) and sodium dodecylbenzene sulfonate (technical grade) were ordered from Sigma Aldrich. Acetone was obtained from Lineal Chemicals. Hexane used for the liquid sensor was ordered from Avantor Performance Materials Poland S.A.. To avoid the influence of water conductivity, water was filtered by the Milli-Q ultrapure water system. To investigate the possibility of using the other CNMs for electrically active layer, two types of MWCNTs of 8–15 nm diameter and lengths of 2  $\mu\text{m}$  and 50  $\mu\text{m}$ , ordered from Carbon Nanotubes Plus and graphene nanoplatelets (GNPs) with 25  $\mu\text{m}$  average diameter and graphene flakes with 400 nm average diameter purchased from Cheap Tubes Inc. and Cambridge Nanosystems Ltd., respectively, were also used in some experiments. The wood based materials (WBM) used in the experiments included medium and high density fiberboards (MDF/HDF), oriented-strand board (OSB), chipboard, beaverboard, pure Scots pine and balsa wood (for camera and scanning electron microscopy images, see SI, Figs. S1 and S2).

### 2.2. Ink and paste preparation

Raw CNT ink was prepared by ultrasonic homogenization (horn sonifier Hielsher UP400S, power 50 W/40 ml beaker, 20 min, ice bath cooling) of 0.2 wt% of CNTs in acetone. CNT/SDBS were prepared by ultrasonic homogenization of an aqueous solution consisting of 0.1 wt% and 0.5 wt% CNTs and 0.3 wt% and 1.5 wt% SDBS, respectively. To obtain the CNT/PMMA paste, 8 wt% PMMA was dissolved in DB acetate and mixed for 3 days in a magnetic stirrer at 45  $^{\circ}\text{C}$  [20]. The 3 wt% CNTs were subsequently added to the PMMA dispersion. The paste was first homogenized by mortar and pestle and then calendered twice in a three roll mill with a roll distance of 5  $\mu\text{m}$ . Four dispersions prepared as alternative to NC7000 MWCNTs were prepared in SDBS (0.3 wt%) aqueous solution with addition of MWCNT (2  $\mu\text{m}$ ), MWCNT(50  $\mu\text{m}$ ) and GNPs (400 nm) and GNPs (25  $\mu\text{m}$ ), respectively.

### 2.3. Deposition

First type of samples was coated with raw CNTs. These samples were prepared by spray coating of raw CNT ink using an Adler AD776B aerograph, with a pressure of 0.5 MPa. Initially, a 5 cm  $\times$  1 cm (L  $\times$  W) tape-based mask was used. Then, to prepare highly-conductive raw CNT heaters, the procedure was repeated several times (using a 10 cm  $\times$  2 cm mask) until the sheet resistance dropped below 200  $\Omega/\text{sq}$ .

Second type of samples was prepared using CNT/SBDS coatings. These were spray coated using an IWATA LPH-80 spray gun under 0.2 MPa. 5 cm  $\times$  1 cm (W  $\times$  L), and later 2 cm  $\times$  10 cm conducting patterns were created by using tape-based masks for all spray-coated samples. The amount of CNTs deposited by spray coating was calculated according to Eq. (1)

$$m_{\text{CNT}} = \frac{V \times c}{A} \quad (1)$$

where  $A$  is the spray gun coating area,  $V$  is the volume of CNT/SDBS dispersion and  $c$  is the CNT concentration. Finally, the third type of samples was prepared using CNT/PMMA. The CNT/PMMA composite

was deposited by screen printing, using a 10  $\mu\text{m}$  thick, no mesh mask. Silver paint was used at the ends of the CNT-based elements in order to improve electrical contact between external equipment and the CNTs. Afterwards all samples were briefly preheated to approx. 80  $^{\circ}\text{C}$  by applying current increasing at a rate of 1 mA/s. Each of the proposed coatings (Raw CNT, CNT/SDBS and CNT/PMMA) were deposited on wooden boards (Scots Pine and Balsa) for initial tests and sensing applications. Additionally raw CNT and CNT/PMMA coatings were deposited on other types of WBMs (please see Section 2.1.) for electrothermal measurements. Wood/CNT composite was created by coating bulk wood elements with either raw CNT, CNT/SDBS or CNT/PMMA layers and with a decorative element (0.5 mm balsa wood). The bulk wood samples covered with CNTs were joined with a decorative element using 0.8 g/10  $\text{cm}^2$  of Vicol adhesive, consisting of methylchlorisothiazolinone and methylisothiazolinone.

#### 2.4. Testing

The roughness of wood was measured using a Zeiss LSM 510. The measurement and calculations were performed according to Bezak et al. [21]. In brief, a topography map was obtained using the LSM, with an argon laser (458 nm) and EC Epiplan-Nefluar 20  $\times$  lens. The roughness was then calculated by ZEN2011 software, as the arithmetic mean of total surface height values  $R_{\text{sa}}$ , according to DIN EN ISO 428. Reflectance was measured by a Carry 400 spectrometer, using an integrating sphere and uncovered balsa wood as a reference sample. Liquid sensing was conducted by dropping 0.1 ml of water/hexane and acetone onto the CNT element. Drying (removing residual liquid) was performed using a 50 W halogen lamp. Electrical resistance was measured by Keithley 2000 (two point probe). The pressure/flood/temperature sensor performance was investigated using a BioLogic SP-200. Pressure sensing was investigated by loading samples with 0.1 kg, 1 kg, 5 kg and 65 kg weights, equivalent to approx. 0.6 kPa, 6 kPa, 30 kPa, 0.4 MPa. Temperature sensing measurements were performed by gradual heating and cooling of the samples in a laboratory oven with an average heating rate of 1  $^{\circ}\text{C}/\text{min}$ . The reference temperature was measured using a PT100 sensor. Thermal camera images were taken using an FLIR ETS320. Electrothermal testing was conducted using a TTi QL564P DC power supply together with a Therm Metis MY84 pyrometer.

### 3. Results and discussion

#### 3.1. Preparation of wood integrated with CNMs

The CNT deposition methods included spray coating and screen printing. Due to the high roughness of wood and WBMs (see SI, Figs S3, Table S1) and the strong affinity between CNTs and the basic constituents of wood (cellulose, hemicelluloses and lignin [22,23]) originating from  $\pi$ -interactions and van der Waals forces [24–26], CNTs attach strongly to wood surfaces without any additional binder. Therefore, the application onto wood of pure CNTs dispersed in organic solvents of high vapour pressure or water-based solutions of CNTs with surfactants via spray coating method enables the formation of pure CNM coatings (if needed, surfactants left after the water has evaporated may be removed by rinsing, according to the procedure presented in our previous report) [12]. Such an approach enables the formation of semi-transparent or nontransparent coatings, depending on the amount of CNTs deposited. The formation of pure coatings may be important for both heaters and sensors as the presence of polymers or resins [27] (often unavoidable in the production of coatings on other materials) is likely to degrade the sensing properties and decrease conductivity of the layer.

Fig. 2A presents the sheet resistance changes for coatings on balsa wood prepared using high vapour pressure solvents. As the measurements were performed for an increasing number of coatings (1–5) we

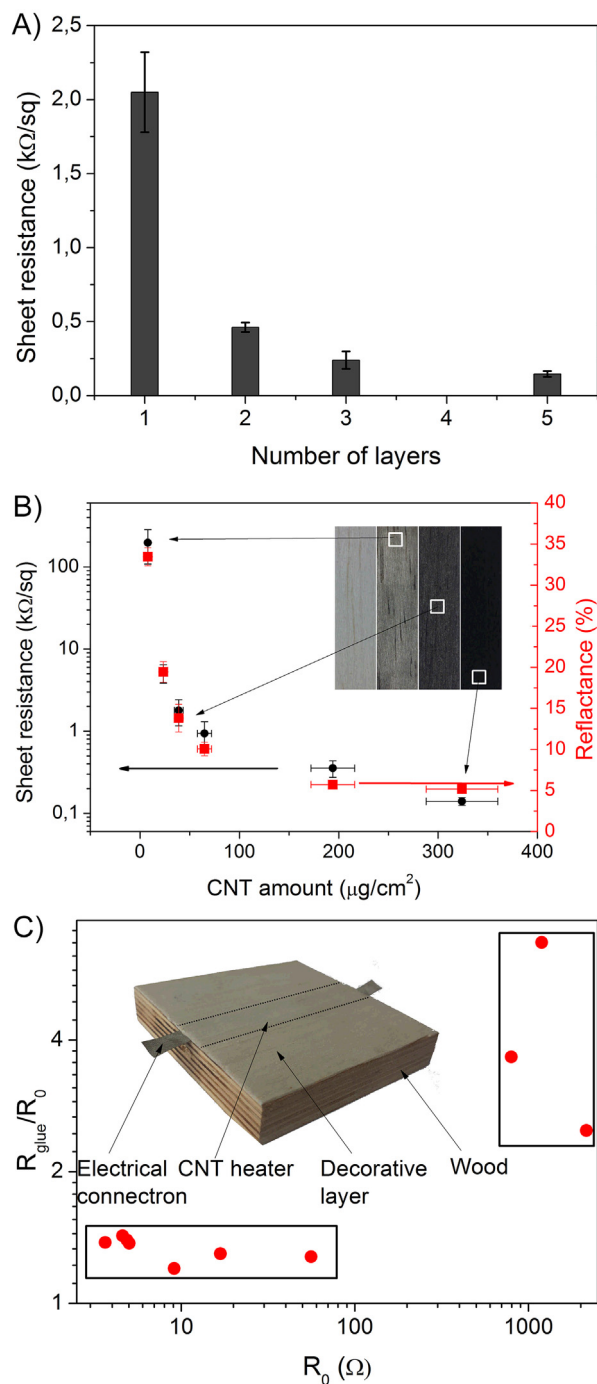


Fig. 2. (A) Sheet resistance of raw CNT coatings on balsa wood after deposition of 1, 2, 3 and 5 layers; (B) the relationship between sheet resistance, coating reflectance and amount of deposited material for CNT/SDBS spray coated samples; inset - camera image of balsa wood (left) and balsa wood coated with varying amounts of CNTs; (C) relative resistance change between initial resistance ( $R_0$ ) of CNT/SDBS and the resistance after using adhesive ( $R_{\text{glue}}$ ). (For interpretation of the references to colour in this figure legend, the reader is referred to the web version of this article.)

would expect the thickness of the coating to increase. For theoretical uniform coatings of the constant resistivity and the same thickness, this would mean  $R_s$  should decrease as the inverse of the number of layers (in the same way as the decrease of equivalent resistance of a set of parallel resistors), as  $R_s = \Omega/\text{sq}$ , where  $\Omega$  is a volumetric resistivity while  $t$  is the thickness of a layer. However, the decrease between the first and second layer presented in Fig. 2A is larger than expected. This

may be explained by two major factors, the first being the very high roughness of the wood-based surfaces and the second being the tendency of CNTs to agglomerate, which may hinder percolation (especially for the first coating) and result in a dependency of volumetric resistivity on the number of layers, as well as produce local changes in resistivity and thickness of the coating. As visible in Fig. 2A, the larger number of coatings mitigates this effect, with further layers following the expected dependence. However, the agglomeration also makes it difficult to estimate precisely the quantity of CNTs deposited on the wood and to determine reliably the transparency of the layer. For this reason, subsequent experiments were performed using aqueous CNT dispersion stabilized with a SDBS (CNT/SDBS) and spray coated in a similar way to raw CNTs. Fine control over the concentration and the amount of spray-coated dispersion enabled precise determination of the amount of CNTs deposited on the surface and control over electrical resistance and transparency of CNT layers (Fig. 2B). Depositing  $7.8 \pm 0.9 \mu\text{g}/\text{cm}^2$  of CNT/SDBS onto balsa wood formed an antistatic layer of sheet resistance of  $200 \pm 90 \Omega/\text{sq}$ . Smaller amounts of CNT/SDBS were below the percolation threshold for the CNTs used in this study and did not make the wood electroconductive. The antistatic CNT coating is semi-transparent to the naked eye and in UV-VIS spectroscopy reflects 33% light compared to uncoated wood (CNTs are efficient absorbers of light [28]). Increasing the amount of CNTs by a factor of 3 caused a decrease in measured reflectance to 19%, with a two orders of magnitude drop in resistance to  $5.2 \pm 1.3 \Omega/\text{sq}$ . This is caused by the formation of a well-connected CNT network on the surface of the rough wood. As may be expected, a further increase in the CNT amount causes a decrease in both reflectance and sheet resistance, but the relative changes are smaller. After deposition of further CNT layers the reflectance decreases asymptotically to approx. 5%, creating an almost completely black sample, whilst sheet resistance constantly decreases. Additionally, it was observed that all of the CNT/SDBS samples were superhydrophilic, independent of their electrical resistance.

The other inexpensive and industrially viable deposition method for the preparation of conductive coatings is screen printing. Due to the presence of the binder, the coatings are durable even when very thick, although they cannot be transparent. In contrast to superhydrophobic raw CNTs and superhydrophilic CNT/SDBS coatings, all of the CNT/PMMA surfaces showed low wetting angles towards water, yet the barrier formed was fully impermeable. Finally, for all coating types the sheet resistances of the samples showed no clear WBM type dependency, although significant differences are observed upon heating, as will be described in Section 2.3.1.

Freshly prepared raw CNTs and CNT/PMMA samples prepared on various surfaces were also internally heated by 1 min long pulses of DC electric current and thus heated to  $80^\circ\text{C}$ . The short heating pulses did not cause any significant resistance change for the raw CNT sample, while for the CNT/PMMA sample, a 5% decrease was observed, probably related to evaporation of residual DB acetate trapped in the PMMA matrix.

To investigate the stability of electrical properties, both spray-coated (raw CNT i.e. from organic solvent dispersion) and screen printed coatings were prepared on a range of WBMs (see SI, Table S2). It was observed that 3 months' exposure to ambient conditions (temperature of approx.  $22^\circ\text{C}$ , relative humidity of approx. 40%) had no influence on CNT/PMMA samples while the raw CNT samples increased in resistance by  $11 \pm 3\%$ , probably due to atmospheric adsorbents such as  $\text{H}_2\text{O}$ ,  $\text{N}_2$  or aromatic hydrocarbons [29,30]. Next, a 10 min long heating caused a further 4% drop in resistance, but after the subsequent 20 min long cycle, the resistance did not decrease further (see SI, Table S2). This suggests that a short pretreatment of CNT/PMMA samples may be necessary before use.

In order to obtain most conductive CNT layers on wood, the coating should be black and nontransparent. Yet, as wood often plays a decorative role, it would be desirable to investigate the possibility of placing CNT functional layers beneath the decorative element. For this

purpose, raw CNTs, CNT/SDBS and CNT/PMMA coated WBMs were prepared, and a decorative wood element was glued on the top of them, using a standard wood-specific adhesive. As mentioned earlier, the entry of insulating molecules into the CNT network may decrease its resistance, and therefore the resistance of the coating was recorded before the gluing process and after the glue had set.

The relative increase in resistance was measured as  $(9 \pm 3)\%$ ,  $(27 \pm 5)\%$  and  $(3 \pm 4)\%$ , for all fully black coatings of type raw CNT, CNT/SDBS and CNT/PMMA coatings, respectively. Those results show that CNT/PMMA is practically insensitive to the presence of adhesive, which is potentially related to the much higher thickness and presence of binder in the screen printed coating. It may mean that the penetration of insulating glue is smaller, and that the percolating current may be easily redirected into the other parts of the coating. A greater decrease in resistance of  $(9 \pm 3)\%$  for the raw CNT thin coatings could support these conclusions. The interestingly much larger drop in resistance for CNT/SDBS coatings is probably attributed to the strongly hydrophilic character of this coating and better infiltration of the adhesive. To explore the issue further, more transparent samples were also investigated. So as to avoid the issue of agglomeration, CNT/SDBS coatings were chosen for these experiments.

In total, nine samples with resistivity in the range of  $300 \Omega - 3 \text{ M}\Omega$  were studied. As shown in Fig. 2C, all the samples with resistance below  $100 \text{ k}\Omega$  showed a relative resistance change in the range of 19–43%, while the antistatic surfaces showed a much higher increase (150–570%). This expected result may be explained by fewer network connections in the more visually transparent coating. The cutoff of existing current pathways due to the presence of insulating glue causes a drastic decrease in the number of routes available for the current percolation. For highly conductive samples, the number of electrical connections is so large that the current may be easily redirected from the insulated areas.

Spray coated raw CNTs and CNT/SDBS coatings can be semi-transparent and form much thinner coatings than screen printed ones (below  $1 \mu\text{m}$ ). They may be superhydrophobic or superhydrophilic depending on the use of the dispersant. The presence of SDBS makes the effect of glue on the resistance more pronounced, and therefore the surfactant may need rinsing in some cases.

On the other hand, screen-printed CNT/PMMA paste forms layers of approximately  $10 \mu\text{m}$  after drying and thus requires fewer application steps to obtain a low surface resistance, although the resistivity (i.e. resistance multiplied by cross-sectional area and divided by length) of the pathways may be higher due to the presence of polymer binders in the nanotube network. The presence of polymer binder also potentially decreases the sensitivity to ambient conditions, although the thickness of the surface may be the reason for the presence of residual dispersant which can be removed by short thermal pre-treatment. On the other hand, the thickness of the layer and the presence of binder also makes the screen-printed surfaces the most insensitive to gluing in terms of resistivity. Finally, it is worth mentioning that by using masks, both spray coating and screen printing enable the formation of any desired pattern (see SI, Fig. S4, S5). Spray coating also offers the possibility of forming conductive coatings on non-flat surfaces.

To understand the pros and cons of each coating technique and characteristics of the formed coatings, the conductive layers were further tested in practical applications, which could find immediate application in the wood industry (see SI, Table S3, for comparison of raw CNT, CNT/SDBS and CNT/PMMA features).

### 3.2. Sensors

The first opportunity offered by CNT based coatings is their use as sensors. The live-monitoring of the physicochemical state of wood may significantly increase the number of potential applications of wood as a construction or furniture material.

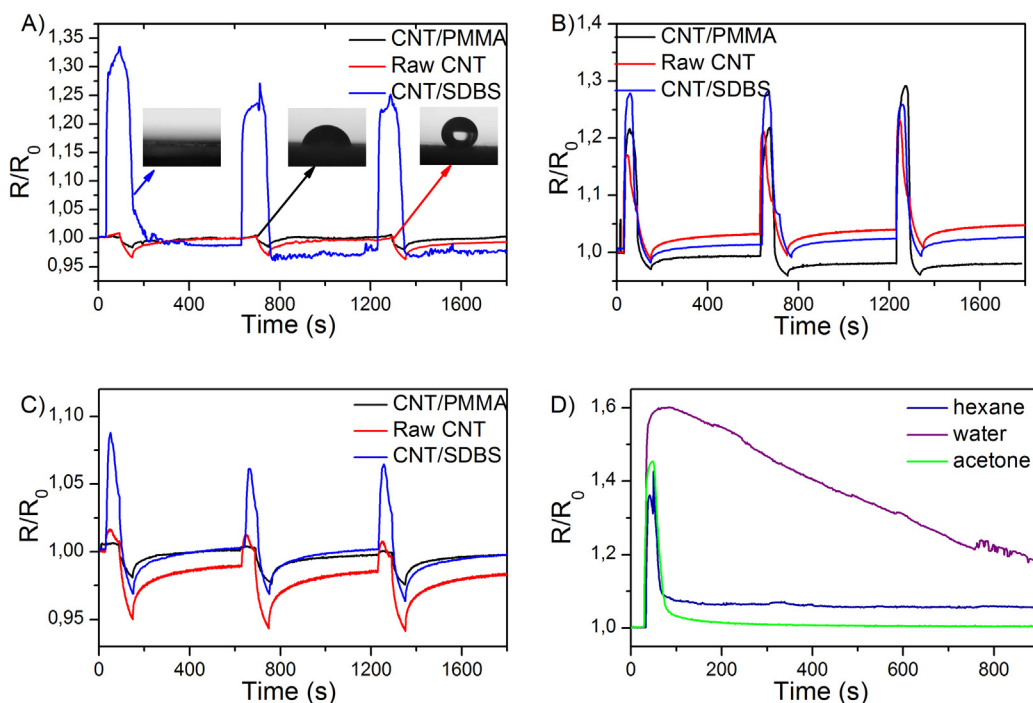


**Fig. 3.** Response in resistance of CNT/PMMA, raw CNT and CNT/SDBS ( $2 \times 10$  cm) after liquid deposition: (A) water, (B) acetone, (C) hexane; (D) electrical signal of CNT/SDBS sensor ( $4 \times 1$  cm) after depositing water, acetone and hexane. (For interpretation of the references to colour in this figure legend, the reader is referred to the web version of this article.)

### 3.2.1. Liquids sensors

Raw CNT, CNT/PMMA and CNT/SDBS deposited onto Scots pine samples ( $2 \times 10$  cm - WxL) were investigated as potential liquid sensors (Fig. 3). Such sensors could be used for example as flood sensors in flooring applications. The experiment was conducted as follows: 0.1 ml of liquid was dripped onto the sensor. After 60 s water was gently removed using a cellulose wipe and the sample was heated by a halogen lamp for the next 60 s to remove residual water. After 8 min the procedure was repeated. Due to the superhydrophobic properties of raw CNT film, water does not wet the surface of the sensor and often rolls off onto the wood (Fig. 3A). Therefore, its electrical response to water deposition is very limited (the pronounced drops in resistance are related to halogen lamp heating). CNT/PMMA is wetted more significantly, but the polymer creates a protective layer and water also does not influence electrical resistance. Finally, due to the presence of SDBS the surface of CNT/SDBS is completely wetted. The electrical response is also very significant and rapid, and the resistance ( $R/R_0-1$ ) increases by up to 35% after first deposition of only 0.1 ml of water onto a  $20 \text{ cm}^2$  sensor. Although further responses are slightly smaller the multiple repetition of the experiment (data presented in SI, Fig. S6) shows that the response stabilizes after sixth cycle, at 27% which is still a very pronounced result. The decrease is probably related to the removal of residual water in the CNT/SDBS coating and relocation of SDBS, which stops after several first cycles. It is also worth noting that the use of a smaller sensing area would enhance the signal further (see SI, Fig. S7).

For the wetting experiment we used not only water, but also representative polar and nonpolar organic solvents: acetone and hexane. The tests were performed in a similar way to the one described for water.

Each sample: raw CNT, CNT/PMMA and CNT/SDBS showed a visible electric signal after deposition of acetone. For each sample ( $R/R_0-1$ ) exceeded 15% and reached even 50% for the CNT/SDBS sample (Fig. 3B). On the contrary, despite very strong wetting, hexane does not influence the resistance of either raw CNT or CNT/PMMA films. Only in the case of CNT/SDBS did ( $R/R_0-1$ ) vary from 5% to 15% after hexane deposition (Fig. 3C). Because CNT/SDBS showed a significant temperature change for all tested liquids, the single signal-response without halogen lamp heating was collected (Fig. 3D). In order to enhance the

signal, a smaller sensor ( $1 \text{ cm} \times 4 \text{ cm}$ ) was used. Depositing a 0.1 ml water droplet shows the highest ( $R/R_0-1$ ) of 60%. Due to the low vapour pressure of water (2.3 kPa at  $20^\circ \text{C}$ ) the resistance ( $R/R_0-1$ ) decreases to its initial value very slowly, dropping to 20% after 15 min. Signals from acetone and hexane are significantly different. Both signals show maximum resistance after approx. 25 s. Subsequently, a rapid drop is observed due to fast evaporation of acetone (vapour pressure: 25 kPa at  $20^\circ \text{C}$ ) and hexane (vapour pressure: 16 kPa at  $20^\circ \text{C}$ ). It is easily noticeable that despite high vapour pressure, hexane adsorb onto CNT/SDBS and resistance does not drop to the initial value (Fig. 3D). However, the molecules are easily desorbed after heating to approx.  $70^\circ \text{C}$  using a halogen lamp or pulse Joule heating.

### 3.2.2. Pressure sensors

Another type of highly useful application in wood technology would be pressure sensing. Pressure sensors could act as on/off switches or occupancy detection systems.

To create a pressure sensor, all three types of CNT-based films were investigated (raw CNT, CNT/PMMA and CNT/SDBS). However, none of these films showed any electrical response after applying pressure (see SI, Fig. S8), which ensures good selectivity with regard to the liquid sensing presented in Section 3.2.1. Consequently, a different approach was proposed. The stress sensor was made of two parts of CNT-coated WBMs (Fig. 4). The base part is raw CNT or CNT/PMMA electrical film ( $2 \times 10$  cm). The second part is CNT/SDBS film ( $4 \times 4$  cm).

The measurement was performed by loading the sensor with various weights. The weight was kept on the sensor for 10 s, followed by a 10 s release. Two types of wood-based materials were tested for pressure sensors – highly-rough Scots pine panels and fiberboard of low roughness, so as to check the influence of the WBM roughness on the sensor performance. The CNT/PMMA + CNT/SDBS sensor showed significant electrical response after applying external pressure for both Scots pines and fiberboards. The Scots pine sensor showed relatively small resistance change ( $1-R/R_0$ ) after applying 0.6 kPa (0.1 g), with the response significantly increased to 16% for 6 kPa (1 kg). At 0.4 MPa (65 kg), the sensor showed a 26% drop in resistance.

The fibreboard-based sensors also showed significant but less repeatable changes. In the case of Scots pine, CNT/SDBS creates a thin, conducting film without changing the naturally high surface roughness,

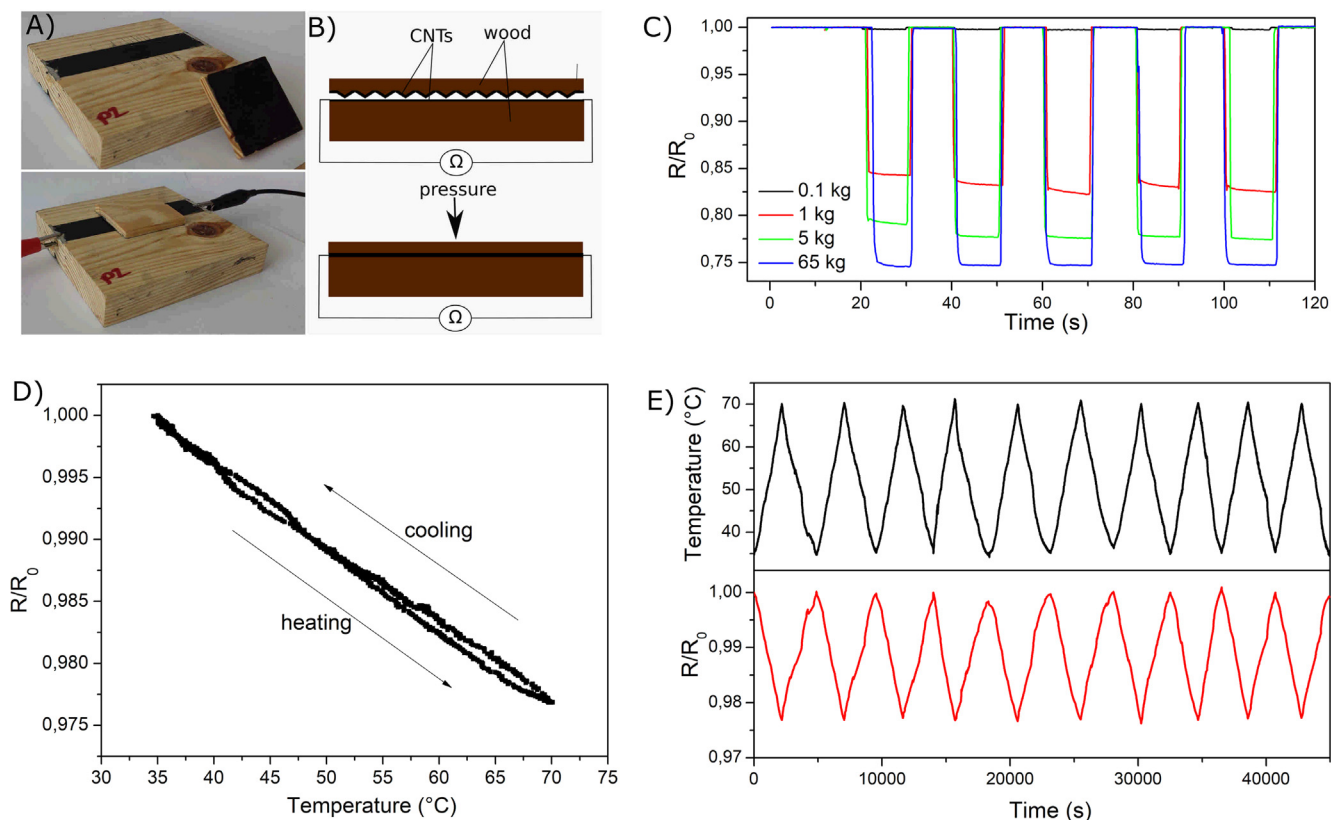


**Fig. 4.** (A) Two-element stress sensor based on CNT electronics integrated with wood; (B) schematic principle of stress sensor operation; (C) operation of CNT/PMMA stress sensor on Scots pine; (D) operation of raw CNT temperature sensor, (E) multi-cycle operation of raw CNT temperature sensor. (For interpretation of the references to colour in this figure legend, the reader is referred to the web version of this article.)

while the CNT/PMMA film, due to the presence of a polymer matrix and screen printing method, creates less rough film. Therefore, before applying pressure, the contact area between CNT/PMMA and CNT/SDBS is relatively low, and gradually increases after applying pressure. In contrast to Scots pine, fiberboards show low roughness. Therefore both the CNT/PMMA and CNT/SDBS films are relatively flat, creating a higher contact surface area even without external pressure. In contrast to the CNT/PMMA + CNT/SDBS sensor system, the use of raw CNT + CNT/SDBS as a pressure sensor is limited due to two main factors. Firstly, high roughness (and consequently surface area) of both raw CNT and CNT/SDBS films causes high contact between films even without external pressure. Secondly, strong Van der Waals interaction between CNTs causes sticking of both CNT films, which then causes deterioration of films and low repeatability of sensors signal (see SI, Fig. S9).

### 3.2.3. Temperature sensor

Another example of a highly useful application would be temperature sensing, which could be useful in e.g. fire detection, heating control or simple monitoring. The classical Pt100 or thermocouples cannot be easily and fully integrated with wood based materials. To obtain a temperature sensor on wood, two water insensitive films: raw CNT and CNT/PMMA were investigated. Gradual heating of the samples in a laboratory oven showed that CNT/PMMA has a nonlinear temperature dependence even in the 30–70 °C temperature range. On the contrary, as presented in Fig. 4D, raw CNT coatings show linear  $R(t)$  characteristics in the temperature range investigated. As expected for mixed CNT coatings with randomly aligned misaligned nanotubes, it shows a clear decrease of resistance upon heating, indicating the semiconducting character of the coatings [31,32]. A little hysteresis present between the heating and cooling cycle is potentially related to the intrinsic heat capacity of the CNT/wood material. The measurement performed in 10

cycles (Fig. 4E) proved very good repeatability of electrical signal for many heating/cooling procedures.

The above section presents several representative examples of sensors possible by the use of nano-micro thin CNT based coatings deposited directly on WBMs. The examples chosen for this study (liquid, pressure and temperature sensors) seem the most universal and likely to find application in the widest range of wood products. Yet knowing the potential of CNTs and graphene, it may be expected that based on the manufacture approaches proposed here, a whole family of other sensors may be derived, including but not limited to fire, humidity, formaldehyde, mould, crack, stress and strain sensors. In order to do so, many previous approaches to manufacture of CNT-based sensors may be applied [14,15,33–37].

### 3.3. Heaters

The extension of wood functionality by the introduction of carbon based sensors may result in a dramatic change in the applications of this material. However, no less important may be the use of CNT coatings as heaters. These heating elements powered with “green” electrical energy could for example replace environmentally unfriendly furnaces or be used as fast on-site dryers of wet wood elements

#### 3.3.1. Joule heating on wood versus WBMs surface roughness

Four types of WBMs – fiberboard (MDF), chipboard, Scots pine board and OSB – were coated by raw CNT and CNT/PMMA. After brief preheating to approximately 70 °C, the initial characterisation of heaters was performed with the use of a thermal camera. First, the power was set at 1 W (Fig. 5) and 4 W and thermal camera images were taken after 10 mins.

1 W heating of a 2 cm × 10 cm sample caused heating of both CNT/PMMA and raw CNT to an average temperature ranging between 40 °C

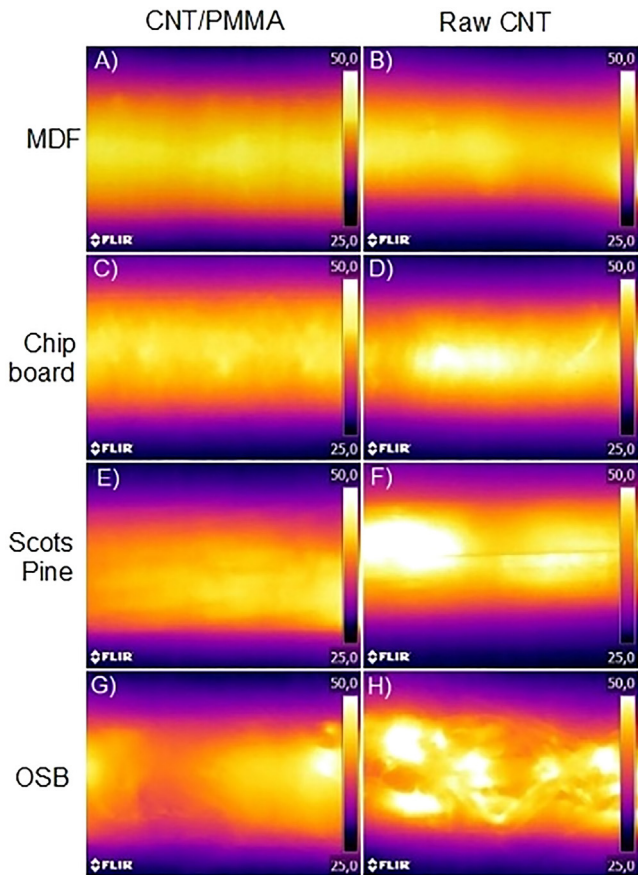


Fig. 5. Thermal camera images of CNT heaters after 10 min heating with 1 W for CNT/PMMA: (A) fiberboard, (C) chip board, (E) Scots pine, (F) OSB and raw CNT heaters: (B) fiberboard, (D) chipboard, (F) Scots Pine, (H) OSB. (For interpretation of the references to colour in this figure legend, the reader is referred to the web version of this article.)

and 50 °C (1 W was the initial power setting, although during heating with constant current, the power may have decreased to 0.95 W), which is within the desirable temperature for floor heating applications. It is also noticeable that CNT/PMMA heaters are characterized by more uniform heat distribution. The most uniform heat distribution was found for WBMs with the lowest roughness (arithmetical mean deviation of the assessed surface  $R_{sa}$  (see SI, Table S1)). Analysis of the longitudinal profile (see SI, Fig. S10) shows that temperature ranged from 42.1 °C to 43.4 °C and 41.7 °C to 42.3 °C for fiberboard ( $R_{sa} = 4.87 \mu\text{m}$ ) and chipboard ( $R_{sa} = 6.87 \mu\text{m}$ ), respectively. Also,

Scots pine showed uniform temperature distribution. A significantly worse result is observed for very rough OSB ( $R_{sa} = 33.4 \mu\text{m}$ ) where hot spots are also easily observed on thermal camera images. Heating CNT/PMMA with higher power (4 W) cause the increase of overall temperature to approx. 90 °C, but the temperature distribution for MDF, chipboard and Scots pine was still uniform (see SI, Fig. S11). On the contrary, the raw CNT heater is very much affected by surface roughness. For smooth MDF, the heat distribution is uniform and temperatures in the longitudinal profile range from 43.8 °C to 46.5 °C. However, with increasing roughness the temperature deviation increases and reaches the highest value for OSB. Here, the raw CNT heater temperature ranged from 41.8 °C to 50.8 °C. Also, despite relatively low roughness, some hot spots are observed for raw CNT heaters on Scots pine, which is caused by microstructure or chemical heterogeneity in some parts of the bare wood. Similarly, for CNT/PMMA heaters, after increasing the power to 4 W, the temperature increased to approx. 90 °C and the distribution was analogous to the results of 1 W heating. Taking into account the dangers caused by the presence of hot spots, in the next part of the study, only CNT/PMMA heaters were studied, and due to the lowest surface roughness, MDF was chosen for further investigation.

### 3.3.2. Electrothermal characterization of CNT heaters

DC electric currents of set values ranging from 40 mA to 210 mA were passed through CNT/PMMA heaters (Fig. 6). Temperatures higher than 90 °C were not recorded due to the risk of PMMA, wood or adhesive deterioration. The power needed for 20 cm<sup>2</sup> heater to work at 30 °C and 70 °C is between 0.5 W and 4 W and the required temperature may be easily controlled by the current setting. Afterwards, the heat capacity of the heater was calculated as the reverse slope of the linear part of T(Q) curve (see SI, Figure S12), where Q is the total Joule heat applied to the system. The T(Q) curve was obtained by heating the sample with constant current and high average Joule power of 9 W per 20 cm<sup>2</sup> sample, so as to reduce the effect of convective and conductive heat losses. The calculated heat capacity of the CNT/PMMA heater was 2.8 J/K.

CNT/PMMA heaters on fiberboard were also tested for longer, 20 min heating, using a current setting of 120 mA and average power 3.7 W (see SI, Fig. S13). 70% of the final temperature increase (obtained after 20 min) was achieved after 180 s, whilst 90% was achieved by 500 s. After 10 mins the temperature growth became much slower, but the temperature was still increasing slightly.

For heating applications, it is important not only to see the heating curve, but also how the temperature changes in a repeated heating-cooling cycles. Therefore, the thermoelectric response during 5-min heating followed by 5-min cooling cycles was recorded (Fig. 5B). The maximum temperatures were 73.2 °C, 75.0 °C and 75.6 °C for the first, second and third heating cycles, respectively, whilst the minimum

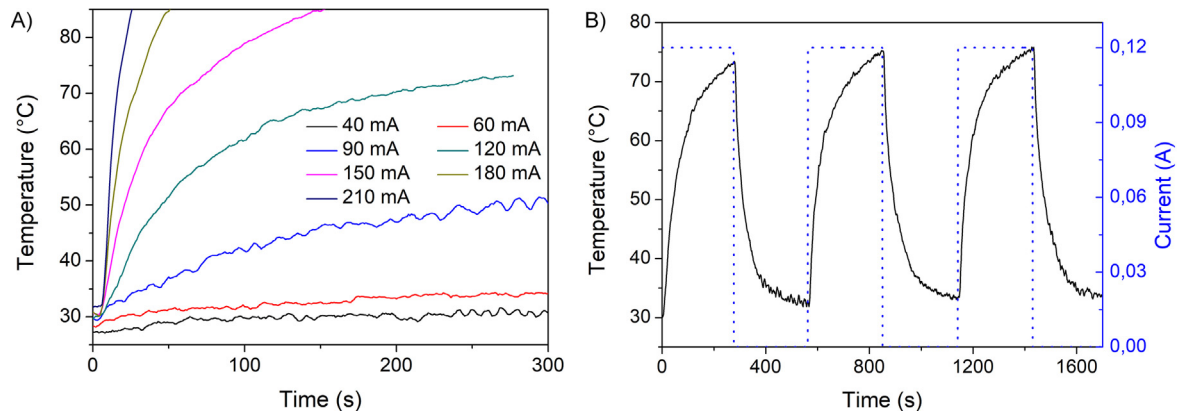
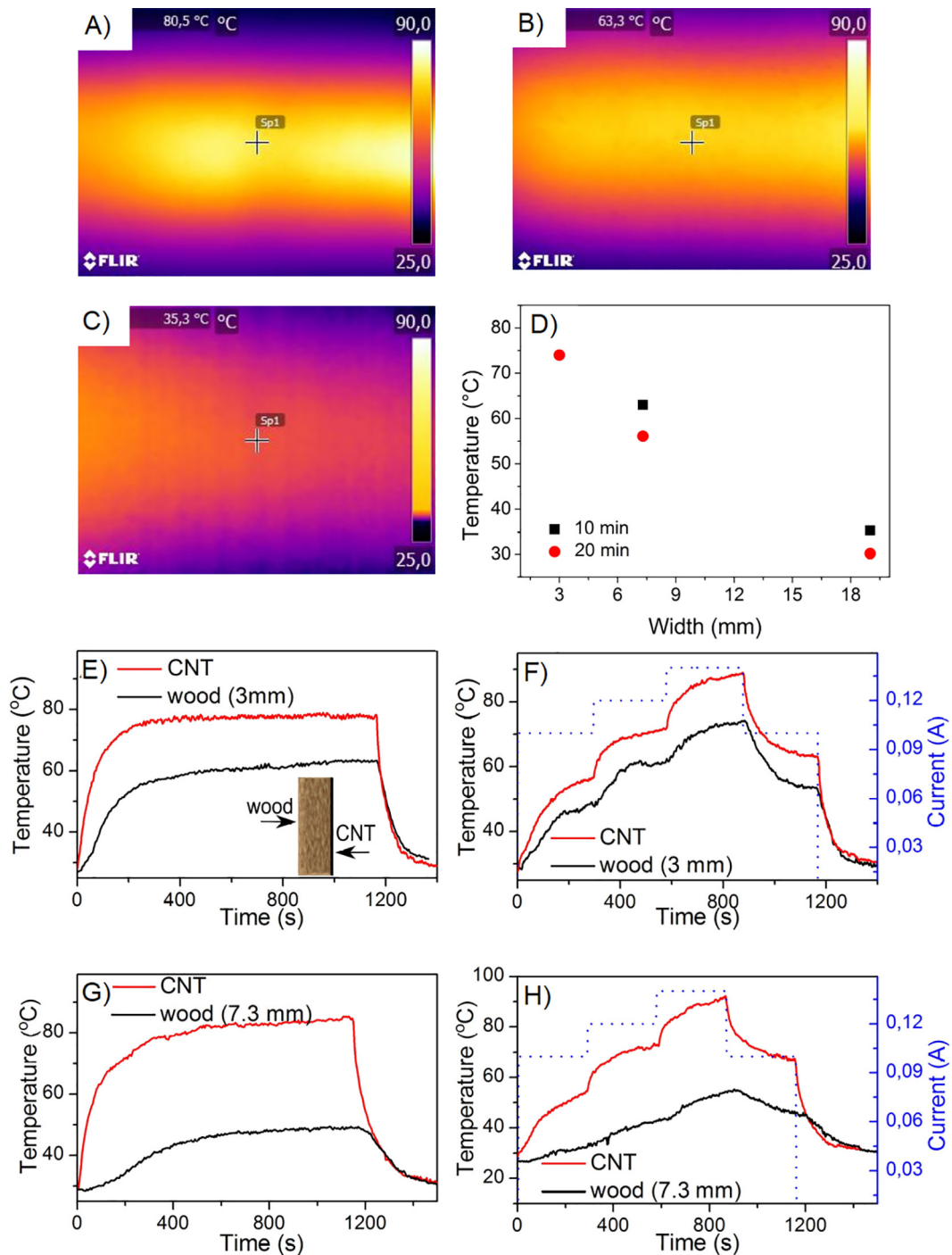


Fig. 6. Thermoelectric response of CNT/PMMA heater on fiberboard ( $R = 268 \Omega$ ) (A) to various current sets and (B) upon several on/off current modes. (For interpretation of the references to colour in this figure legend, the reader is referred to the web version of this article.)



**Fig. 7.** Thermal response measured by thermal camera on the opposite (to the CNT/PMMA heater) side of the boards of various thickness (A) 3 mm, (B) 7.3 mm, (C) 19 mm; (D) averaged temperature of 1 cm<sup>2</sup> of fiberboard after 10 mins and 20 mins for 3, 7.3 and 19 mm thick boards; (E–H) electrothermal response of CNT/PMMA heater and temperature across wood board measured by pyrometer: (E) and (G) 3 mm; (F) and (H) 7.3 mm thick fiberboard. (For interpretation of the references to colour in this figure legend, the reader is referred to the web version of this article.)

temperature were 32.4 °C, 33.4 °C, 33.8 °C after first, second and third cooling cycles, respectively. The insignificant differences are caused by heat gathered in the wood during each cycle due to its high heat capacity. However, each time by simple current switching the temperature rapidly decreases and increases, which makes the CNT/PMMA heater easily controllable.

### 3.3.3. CNT/PMMA as heaters

In some applications, such as flooring, WBMs are not only a constructing material, but also a decorative element. In those applications

CNT/PMMA heaters should be placed on the other side of the board and energy will be transferred first by conduction and radiation to the wooden board and then by convection to the air.

The temperature on the other side of the board is dependent on thickness and type of WBMs. To test this behavior, a heating test of a CNT/PMMA coating on fiberboard was performed using a power of 4 W, which corresponded to a mean heater temperature of approx. 90 °C. The heating of the opposite side of fiberboard of different thicknesses (3 mm, 7.3 mm and 19 mm) was simultaneously recorded by a thermal camera (Fig. 7A–C). The average temperature of the

opposite sides of all heated fiberboards after 10 and 20 min is presented in Fig. 7D. The thinnest sample (3 mm) heated to 78 °C, whilst the thickest (16 mm) to 35.3 °C after 20 min of 4 W Joule heating.

The average temperature and its distribution on the fiberboard surface is the most important parameter for WBM heating, but the heating time is also very important, as a quick electrothermal response and low thermal inertia are among the major advantages over water-based heating systems. Due to high specific heat of fiberboards, ranging from 1200 to 1400 J kg<sup>-1</sup>K<sup>-1</sup> [38,39] the thermal response may be long, especially for thick fiberboards. In order to determine the time characteristics of thermal response of 3 mm and 7.3 mm fiberboards, CNT/PMMA heaters were heated for 20 min with constant current (120 mA) and average power equaling 4.2 W.

First, the tests were performed on 3 mm fiberboard (Fig. 7E). The temperature of the CNT/PMMA heater reached 75 °C after first 5 min and increased to only 78 °C after the next 15 min. Temperatures on the reverse side of 3 mm thick fiberboard were lower and reached 56 °C and 63 °C after 5 and 20 min, respectively. Therefore, although the temperature was lower the thermal response is only slightly slower on the opposite side of heater. On the other hand, the temperature on the opposite side of 7.3 mm fibreboard is significantly lower, at 40 °C and 49 °C after 5 and 20 min, respectively (Fig. 7F). Thus, for 7.3 mm fiberboard the heat transfer inertia is non-negligible. Despite differences in heating curves, during cooling both 3 mm and 7.3 mm fiberboards cooled to 31 °C after approx. 5 min.

Taking into account the results from Fig. 7 E and F the electrothermal response for a varying DC current was also tested. The current was first set to 100 mA and after 5 min increased to 120 mA. After the next 5 min it was increased to 140 mA, decreased to the initial value of 100 mA and finally dropped to 0 mA. The data shows a very good correlation between temperature of CNT/PMMA heater and the surface of 3 mm fiberboard (Fig. 7G). The temperature of the fiberboard increases and decreases immediately after changes in current. A 5-minute interval between changes in applied power is sufficient to reach the plateau in temperature.

Due to its greater thickness, the 7.3 mm fiberboard shows higher temperature inertia. The temperature rises after an increase of current, but the rise is slow and the temperature does not reach a plateau (Fig. 7H). However, if the time intervals are increased, the 7.3 mm fiberboard may also be precisely controlled by changing power input (see SI, Fig. S14).

### 3.3.4. Dryers

The other important problem, which may be solved by the use of the nanocarbon heaters, is moisture uptake of some WBMs, which causes the growth of mould and fungi and the deterioration of mechanical properties. Hence, drying WBMs with CNT heaters was also investigated. For this purpose, a CNT/PMMA heater was produced on highly hygroscopic beaverboard. The samples were left in a chamber at over 90% relative humidity (RH) for 1 week to increase moisture content and mass of the sample by 8.5%. Two samples were left in ambient conditions ( $T = 21$  °C,  $RH = 20\%$ ) and two were heated using the CNT/PMMA heater described in previous sections with 4 W power. The mass of beaverboard decreased to 102% of initial mass after 100 min of heating, whilst the reference samples only dropped to 106% (Fig. 8).

The heaters presented above could find applications as floor heaters, replacing water pipes or electric mats as currently used, which apart from having larger volume have also poorer contact with the wood surface, reducing heat transfer. Existing heaters also have to be placed beneath the flooring, causing larger heat losses due to poor thermal conductivity of wood, while the solutions proposed here could be sandwiched into engineered wood boards just beneath the decorative layer. The heaters are thin and light-weight, and could therefore easily be used on or within the structure of furniture. Applications could also include wood dryers e.g. built into the construction of housing to dry wood directly, or even to thermally eliminate the mould and prevent its

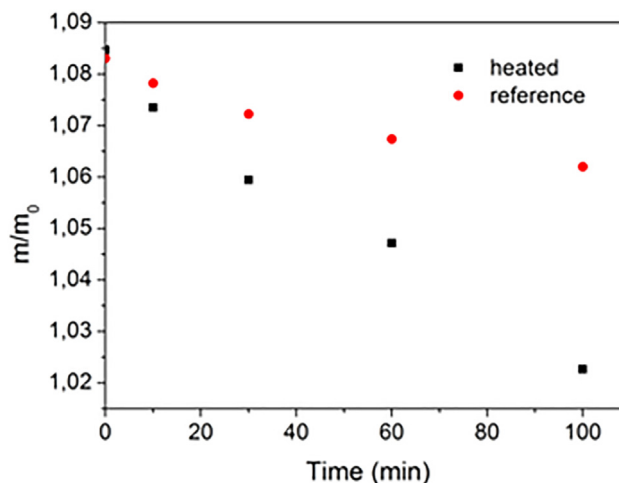


Fig. 8. Drying moist beaverboard by CNT/PMMA heater with 4 W power. (For interpretation of the references to colour in this figure legend, the reader is referred to the web version of this article.)

further growth.

### 3.4. Practical aspects of application

#### 3.4.1. Using other carbon nanomaterials

In the above work a series of studies showing possible methods of production of CNT-based electronics on wood was presented. It has been shown that the use of specific binders, application techniques or WBMs of chosen roughness may influence the potential applications. The majority of research was performed on industrial grade multiwall CNTs Nanocyl (NC7000) with average diameter ( $d$ ) and length ( $l$ ) of approx. 9 nm and 1.5  $\mu$ m, respectively, yet the findings of this paper should also be generally true for other CNMs, with the only difference being that the ratios of the CNMs may need to be adjusted. For comparison, deposition of approx. 40  $\mu$ g of CNT/SDBS (NC7000) by spray coating caused the formation of a half-transparent electroconductive layer with sheet resistance of 1.8 k $\Omega$ /sq. The same amount of CNTs from Carbon Nanotubes Plus with different parameters (2  $\mu$ m and 50  $\mu$ m long) gave a resistance of  $42 \pm 3$  k $\Omega$ /sq and  $520 \pm 110$  k $\Omega$ /sq, for 2  $\mu$ m and 50  $\mu$ m long CNTs, respectively. This is probably due to the fact that that they are generally less conductive (particularly the 50  $\mu$ m long CNTs) owing to e.g. defects or the presence of a larger amount of impurities, requiring more CNTs to be applied to obtain the desired conductivity.

Tests were also performed on graphene flakes (Gr) (400 nm diameter). The deposition of 40  $\mu$ g of the above Gr flakes, dispersed in SDBS, resulted in  $570 \pm 410$  k $\Omega$ /sq sheet resistance, which is as expected, since small curled flakes do not support a low percolation threshold.

The latter material was also used for production of PMMA-based screen printing pastes. The optimal amount of 18% Gr in 8% PMMA base gave approximately  $5 \pm 0.2$  k $\Omega$ /sq for  $10 \pm 2$   $\mu$ m thickness. For comparison the Nanocyl CNT paste presented in this study gave  $76 \pm 10$   $\Omega$ /sq for the same thickness. The better result may be again attributed to easier percolation of relatively long CNTs. Similar results were obtained when the paste was produced out of graphene nanoplatelets (GNPs), large stiff platelets of 25  $\mu$ m diameter, which make them similar to graphite (the printed layers appear grey rather than black). The 8% PMMA paste with an optimal amount of 10% GNPs gave approx. 100  $\Omega$ /sq. This result may be attributed to the high quality of these GNPs and their large diameters (see SI, Fig. S15).

As may be concluded from the above, the results obtained here are definitely not limited to Nanocyl industrial grade CNTs tested in the paper. However, the use of other CNMs may need some revision in

terms of concentrations and number of layers applied depending on the type and quality of CNM material used.

### 3.4.2. Cost of manufacture

Another important aspect to be considered here is the cost of production of wood integrated with carbon electronics. Although pure wood may be a costly material, WBMs and engineered wood products are expected to be common and inexpensive materials. Calculating both the cost of CNMs and binders/adhesives/dispersants, we obtain a cost of \$0.80 and \$1.09 per m<sup>2</sup> of CNT coating (with sheet resistance of approximately 100 Ω/sq) for spray coating and screen printing respectively and \$4.24 per m<sup>2</sup> of screen-printed Gr coating. Taking into account that the price of CNMs continues to decrease, that often the sensors or heaters do not need to cover the whole surface (partial coating may be in the form of meanders, stripes, patches etc.), and that spray coating and screen printing are widely used inexpensive industrial techniques, we expect that such technology may find immediate application in industry.

### 3.4.3. Electrical connection

The final issue to mention here is the performance of electrical connections. In the experiments presented above, connections were made using commercial silver paint and metal wires. The mechanically unreliable silver paint could currently be replaced by carbon solder [40]. However, if metals in general are a concern in terms of environmental impact, they may be replaced by carbon-based adhesives and newly developed carbon nanotube based wires [41,42].

## 4. Conclusion

The above presented paper shows that CNMs may be easily integrated both with pure wood and WBMs, providing unexplored applications for these materials with the property of high electrical conductivity. The electrically-conductive surfaces may be used as sensors and heaters, enabling a wide range of new applications in the field of wood products. CNMs could be integrated with wood and wood-based products by coating the WBM surface or by gluing inside of the engineered wood product so as to keep the visual qualities of WBMs. The paper considers the production of a range of sensors and heaters in relation to industrial techniques, dispersion composition and WBM qualities proposing the best possible solutions for specific applications. To simplify the comparisons and conclusions, most experiments in the paper were performed for one type of industrial grade CNT, although as demonstrated towards the end of this paper, the developed methods will be useful for other CNMs if specific qualities of the other materials are taken into account. Finally, it is shown that the proposed technology can be inexpensive and fully carbon-based.

## Declaration of Competing Interest

The authors declared that there is no Conflict of Interest.

## Acknowledgements

D. Ł. would like to thank the National Science Centre, Poland (project no. 2015/19/N/ST8/02184) and A. D. the Ministry of Science & Higher Education (Poland) for sponsoring the study. All authors are grateful to Dr Mukund Unavane for proofreading of the manuscript.

## Appendix A. Supplementary material

Supplementary data to this article can be found online at <https://doi.org/10.1016/j.compositesa.2019.105656>.

## References

- [1] Chen C, Li Y, Song J, Yang Z, Kuang Y, Hitz E, et al. Highly flexible and efficient solar steam generation device. *Adv Mater* 2017;29:1–8.
- [2] Zhu M, Song J, Li T, Gong A, Wang Y, Dai J, et al. Highly anisotropic, highly transparent wood composites. *Adv Mater* 2016;28:5181–7.
- [3] Aigbomian EP, Fan M. Development of wood-crete building materials from sawdust and waste paper. *Constr Build Mater* 2013;40:361–6.
- [4] Polle A, Janz D, Teichmann T, Lipka V. Poplar genetic engineering: promoting desirable wood characteristics and pest resistance. *Appl Microbiol Biotechnol* 2013;97:5669–79.
- [5] Goodman SM, Bura R, Dichiara AB. Facile impregnation of graphene into porous wood filters for the dynamic removal and recovery of dyes from aqueous solutions. *ACS Appl Nano Mater* 2018;1:5682–90.
- [6] Xiong GY, Suda Y, Wang DZ, Huang JY, Ren ZF. Effect of temperature, pressure, and gas ratio of methane to hydrogen on the synthesis of double-walled carbon nanotubes by chemical vapour deposition. *Nanotechnology* 2005;16:532–5.
- [7] Lee K, Yeoh W, Chai S, Ichikawa S, Lee K, Yeoh W, et al. Optimization of carbon nanotubes synthesis via methane decomposition over alumina-based catalyst optimization of carbon nanotubes synthesis via methane decomposition over alumina-based catalyst. *Fullerenes, Nanotub Carbon Nanostructures* 2010;18:273–84.
- [8] Bo Z, Yang Y, Chen J, Yu K, Cen K. Nanoscale Plasma-enhanced chemical vapor deposition synthesis of vertically oriented graphene nanosheets. *Nanoscale* 2013;5:5180–204.
- [9] Mahajan A, Kingon A, Kukovec A, Konya Z, Vilarinho PM. Studies on the thermal decomposition of multiwall carbon nanotubes under different atmospheres. *Mater Lett* 2013;90:165–8.
- [10] Parks A, Chandler T, Ho K, Burgess R, Ferguson P. Environmental biodegradability of [14 c ] single-walled carbon nanotubes by trametescolor and natural microbial cultures found in new. *Environ Toxicol Chem* 2015;34:247–51.
- [11] Chen M, Qin X, Zeng G. Biodegradation of carbon nanotubes, graphene, and their derivatives. *Trends Biotechnol* 2017;35:836–46.
- [12] Łukawski D, Lekawa-Raus A, Lisiecki F, Kozioł K, Dudkowiak A. Towards the development of superhydrophobic carbon nanomaterial coatings on wood. *Prog Org Coatings* 2018;125:23–31.
- [13] Wang X, Gu Y, Xiong Z, Cui Z, Zhang T. Silk-molded flexible, ultrasensitive, and highly stable electronic skin for monitoring human physiological signals. *Adv Mater* 2014;26:1336–42.
- [14] Han S, Alvi NUH, Granlőf L, Granberg H, Berggren M, Fabiano S, et al. A multi-parameter pressure–temperature–humidity sensor based on mixed ionic-electronic cellulose aerogels. *Adv Sci* 2019;6.
- [15] Qi H, Mäder E, Liu J. Unique water sensors based on carbon nanotube–cellulose composites. *Sensors Actuators B Chem* 2013;185:225–30.
- [16] Janas D, Kozioł KK. Rapid electrothermal response of high-temperature carbon nanotube film heaters. *Carbon* 2013;59:457–63.
- [17] Kang TJ, Kim T, Seo SM, Park YJ, Kim YH. Thickness-dependent thermal resistance of a transparent glass heater with a single-walled carbon nanotube coating. *Carbon* 2011;49:1087–93.
- [18] Park HK, Kim SM, Lee JS, Park JH, Hong YK, Hong CH, et al. Flexible plane heater: Graphite and carbon nanotube hybrid nanocomposite. *Synth Met* 2015;203:127–34.
- [19] Li D, Müller MB, Gilje S, Kaner RB, Wallace GG. 1012Processable aqueous dispersions of graphene nanosheets. *Nat Nanotechnol* 2008;3:101–5.
- [20] Kopyt P, Salski B, Zagrajek P, Janczak D, Sloma M, Jakubowska M, et al. Electric properties of graphene-based conductive layers from DC up to terahertz range. *IEEE Trans Terahertz Sci Technol* 2016;6:480–90.
- [21] Bezak T, Kusy M, Elias M, Kopceck M, Kebisek M, Spendla L. Identification of surface topography scanned by laser scanning confocal microscope. *Appl Mech Mater* 2014;693:329–34.
- [22] Milczarek G. Kraft lignin as dispersing agent for carbon nanotubes. *J Electroanal Chem* 2010;638:178–81.
- [23] Adsul MG, Rey DA, Gokhale DV. Combined strategy for the dispersion/dissolution of single walled carbon nanotubes and cellulose in water. *J Phys Chem* 2011;21:2054–6.
- [24] Perez E, Martin N. π–π Interactions in Carbon Nanostructures. *Chem Soc Rev* 2015;44:6425–33.
- [25] Goodman SM, Ferguson N, Dichiara AB. Lignin-assisted double acoustic irradiation for concentrated aqueous dispersions of carbon nanotubes. *RSC Adv* 2017;7:5488–96.
- [26] Trigueiro JPC, Silva GG, Pereira FV, Lavall RL. Layer-by-layer assembled films of multi-walled carbon nanotubes with chitosan and cellulose nanocrystals. *J Colloid Interface Sci* 2014;432:214–20.
- [27] Neitzert HC, Vertuccio L, Sorrentino A. Epoxy/MWCNT composite as temperature sensor and electrical heating element. *IEEE Trans Nanotechnol* 2011;10:688–93.
- [28] Mizuno K, Ishii J, Kishida H, Hayamizu Y, Yasuda S, Futaba DN, et al. A black body absorber from vertically aligned single-walled carbon nanotubes. *Proc Natl Acad Sci U S A* 2009;106:6044–7.
- [29] Lekawa-Raus A, Kurzepa L, Kozłowski G, Hopkins SC, Wozniak M, et al. Influence of atmospheric water vapour on electrical performance of carbon nanotube fibres. *Carbon* 2015;87:18–28.
- [30] Stando G, Łukawski D, Lisiecki F, Janas D. Intrinsic hydrophilic character of carbon nanotube networks. *Appl Surf Sci* 2019;463.
- [31] Lekawa-Raus A, Walczak K, Kozłowski G, Hopkins SC, Wozniak M, Glowacki BA, et al. Low temperature electrical transport in modified carbon nanotube fibres. *Ser Mater* 2015;106:34–7.
- [32] Bulmer JS, Lekawa-Raus A, Rickel DG, Balakirev FF, Kozioł KK. Extreme magnetot-

- transport of bulk carbon nanotubes in sorted electronic concentrations and aligned high performance fiber. *Sci Rep* 2017;7:1–13.
- [33] Slobodian P, Riha P, Benlikaya R, Svoboda P, Petras D. A flexible multifunctional sensor based on carbon nanotube/polyurethane composite. *IEEE Sens J* 2013;13:4045–8.
- [34] Mohanty S, Misra A. Carbon nanotube based multifunctional flame sensor. *Sensors Actuators, B Chem* 2014;192:594–600.
- [35] Huang J, Yang X, Her SC, Liang YM. Carbon nanotube/graphene nanoplatelet hybrid film as a flexible multifunctional sensor. *Sensors (Switzerland)* 2019;19..
- [36] Janczak D, Peplowski A, Wroblewski G, Gorski L, Zwierkowska E, Jakubowska M. Investigations of printed flexible pH sensing materials based on graphene platelets and submicron RuO<sub>2</sub> powders. *J Sensors* 2017;2017..
- [37] Pepowski A, Janczak D, Ziolkowski R, Malinowska E, Jakubowska M. Graphene nanoplatelets for screen-printed nonenzymatic voltammetric H<sub>2</sub>O<sub>2</sub> sensors. *Sens Lett* 2017;15:779–84.
- [38] Li K. On determining density and specific heat of New Zealand medium density fibreboard. *Procedia Eng* 2013;62:769–77.
- [39] Czajkowski Ł, Olek W. Thermal properties of wood-based panels : specific heat determination. *Wood Sci Technol* 2016;50:537–45.
- [40] Burda M, Lekawa-Raus A, Gruszczyk A, Koziol KKK. Soldering of carbon materials using transition metal rich alloys. *ACS Nano* 2015;9:8099–107.
- [41] Lekawa-Raus A, Patmore J, Kurzepa L, Bulmer J, Koziol K. Electrical properties of carbon nanotube based fibers and their future use in electrical wiring. *Adv Funct Mater* 2014;24:3661–82.
- [42] Lekawa-Raus A, Gizewski T, Patmore J, Kurzepa L, Koziol KK. Electrical transport in carbon nanotube fibres. *Scr Mater* 2017;131:112–8.

Supporting information for:

**Preparation and applications of electrically conductive wood layered composites**

*Damian Łukawski<sup>a</sup>, Alina Dudkowiak<sup>a</sup>, Daniel Janczak<sup>b</sup>, Agnieszka Lekawa-Raus<sup>b\*</sup>*

*<sup>a</sup>Poznan University of Technology, Faculty of Technical Physics, 60-965 Poznan, Poland.*

*<sup>b</sup>Warsaw University of Technology, Faculty of Mechatronics, 02-525 Warsaw, Poland.*

*\*e-mail: [alekawa@mchtr.pw.edu.pl](mailto:alekawa@mchtr.pw.edu.pl)*

## 1. Morphology of selected wood based materials (WBM)s

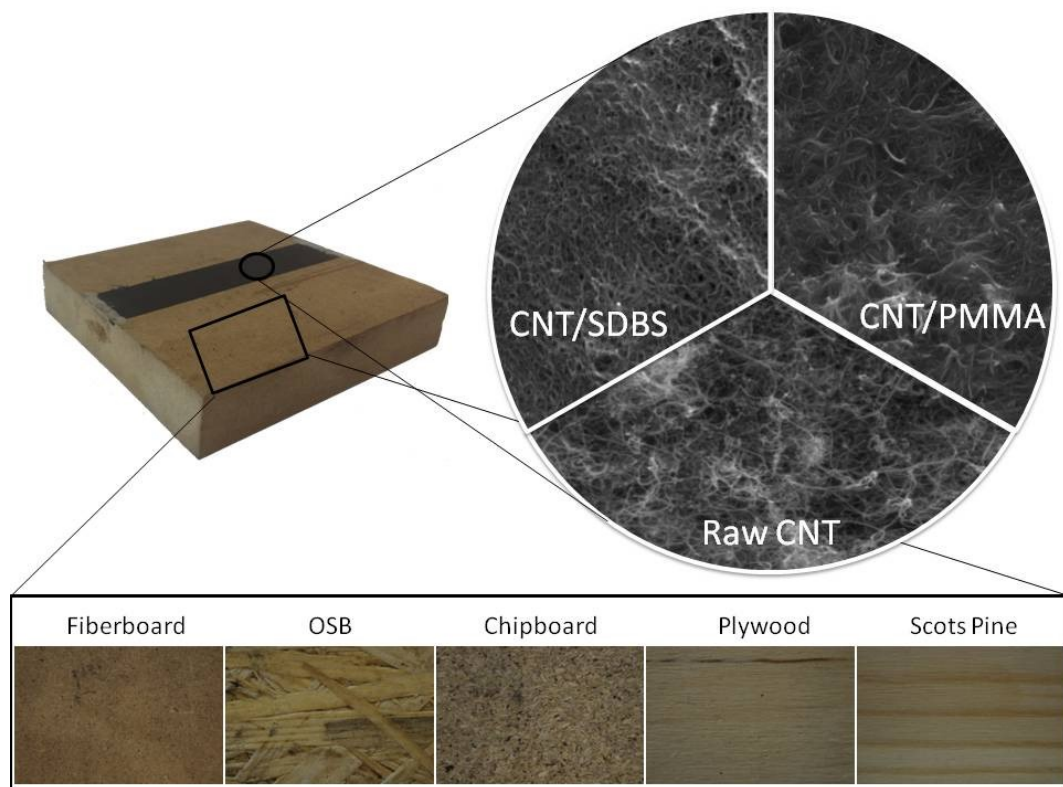


Figure S1 Various wood materials presented in the work and SEM image of three types of CNT-based coatings.

The fluorescent microscopy images were taken by Zeiss Laser Scanning Microscope (LSM) 510, using a mercury lamp HXP 120 and a filter set 38. Each image was taken with the exposure time of 300 ms.

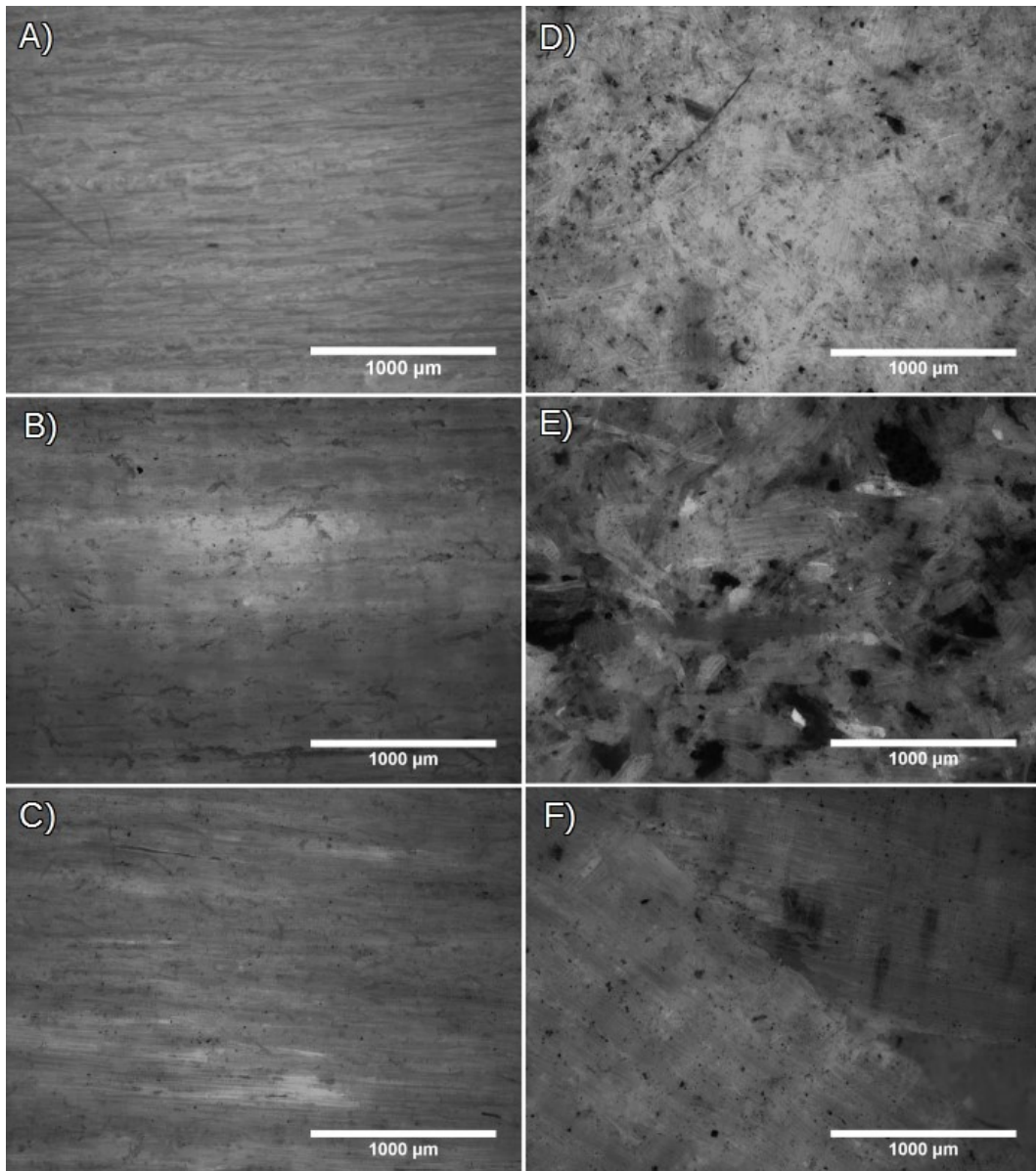


Figure S2 Fluorescence microscopy image of investigated wood based materials (A-balsa wood, B-Scots pine, C-plywood, D-fiberboard, E-chipboard, F-OSB)

The z-profile of wood based materials was measured by Zeiss LSM 510, using argon laser (458 nm) and EC Epiplan-Nefluar 10 × lens.

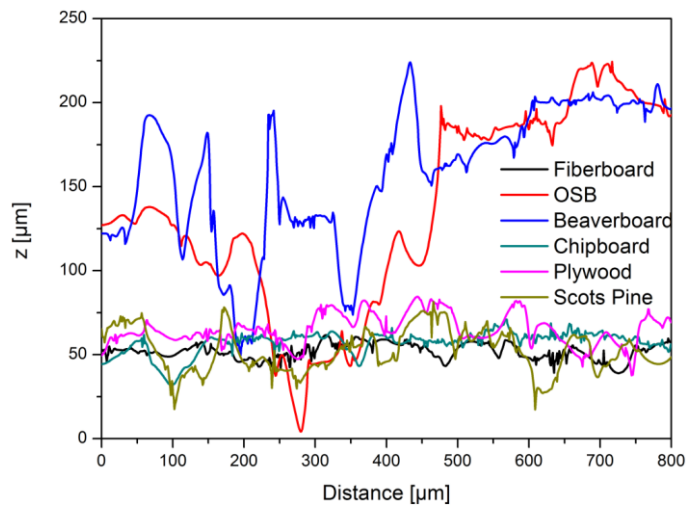


Figure S3 Z-profile of various types of wood

Table S1 Roughness of various WBM

<b>WBMs</b>	<b>Roughness <math>R_{sa}</math> (<math>\mu\text{m}</math>)</b>
fiberboard	4.87
OSB	33.41
beaverboard	32.95
chipboard	6.87
Scots pine	9.75
plywood	9.28

The CNT coatings were heated by applying increasing current (1mA/s) until reached temperature equal 80°C. The electrical resistance was measured before ( $R_0$ ) and after ( $R_i$ ) heating. Afterwards, samples were left in ambient conditions for 3 months. The resistance was measured and the selected samples were heated by applying constant current for 10 min and 20 min.

Table S2  $R_0$  and  $R_i/R_0$  after 3 months in air, after heating with constant current, where  $R_0$ - initial resistance,  $R_p$ - resistance after preheating,  $R_1$ - resistance after exposure to ambient conditions for 3 months,  $R_2$ - resistance after 10 min heating (approx. 4 W),  $R_3$ - resistance after 20 min heating (approx. 4 W).

Coating	$R_0$	$R_p/R_0$	$R_1/R_p$	$R_2/R_1$	$R_3/R_1$
CNT/PMMA	( $\Omega$ )			current 120 mA	current 120 mA
fiberboard	380±52	0.93	1,03	0,97	0,96
OSB	440±92	0.96	1,05	0,95	0,95
chipboard	378±52	0.99	1.03	0,95	0,97
plwood	206±33	0.96	1,02	0,96	0,95
Scots pine	448±72	0.91	0,97	0,95	0,94
<b>average</b>	370	0.95	1,00	0,96	0,95
Spray				current 90 mA	current 90 mA
fiberboard	616±78	1.00	1,07	0,99	1,02
OSB	590±70	1.01	1,11	0,99	1,08
chipboard	616±53	1.00	1,08	1,01	1,00
plwood	580±130	1.04	1,19	1,00	1,06
Scots pine	412±52	0.99	1,10	1,01	1,03
<b>average</b>	560	1.01	1,11	1,00	1,04

Table S3 The parameters of three types of CNT-based electroconductive layers: raw CNT, CNT/SDBS and CNT/PMMA.

	Deposition	Layer uniformity	Transparency	$\Delta R^1$ (%)	Wetting
raw CNT	Spray coating	Limited	Semi-transparent to black	(9±4)	Superhydrophobic
CNT/SDBS	Spray coating	Very good	Semi-transparent to black	(27±5)	Superhydrophilic
CNT/PMMA	Screen printing	Very good	Black	(3±4)	Hydrophilic, Impermeable to water

<sup>1</sup>Resistance change in CNT/wood composite after applying adhesive

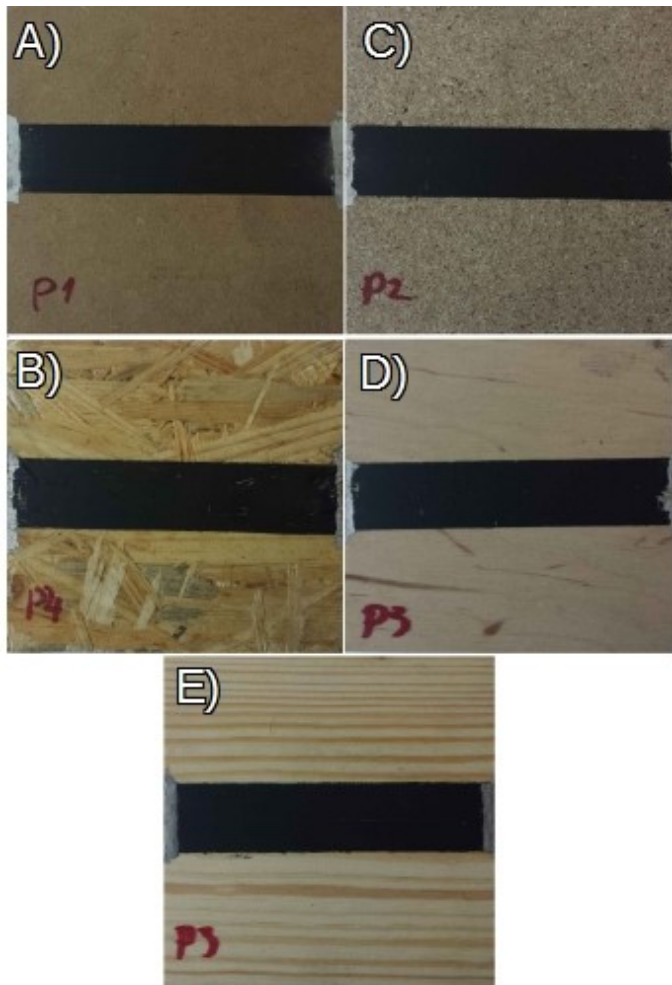


Figure S4 CNT/PMMA on various types of WBMs (A-fiberboard, B-OSB, C-chipboard, D-plywood, E-Scots pine)



Figure S5 CNT/PMMA patterned with various shapes

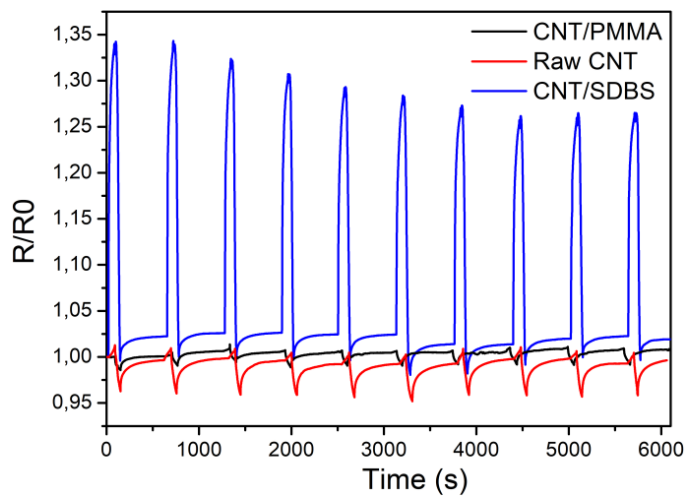


Figure S6 Response in resistance of CNT/SDBS 0.1 ml of water after liquid deposition onto 20 cm<sup>2</sup> sensor, heating with halogen lamp, after each cycle.

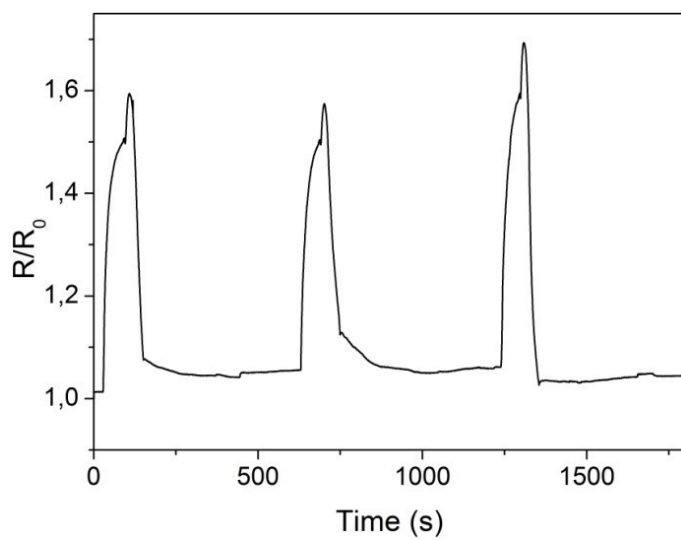


Figure S7 Response in resistance of CNT/SDBS 0.1 ml of water after liquid deposition onto 4 cm<sup>2</sup> sensor, heating with halogen lamp.

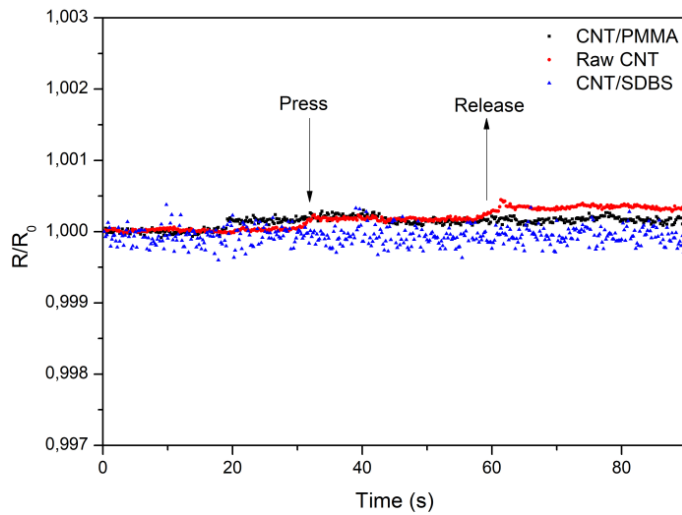


Figure S8 Electrical response of raw CNT, CNT/SDBS and CNT/PMMA coatings after applying 1kg weight.

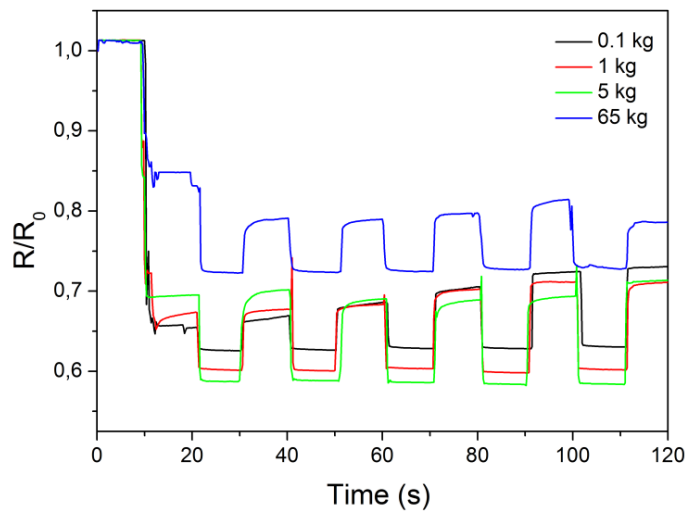


Figure S9 Operation of raw CNT stress sensor on Scots pine.

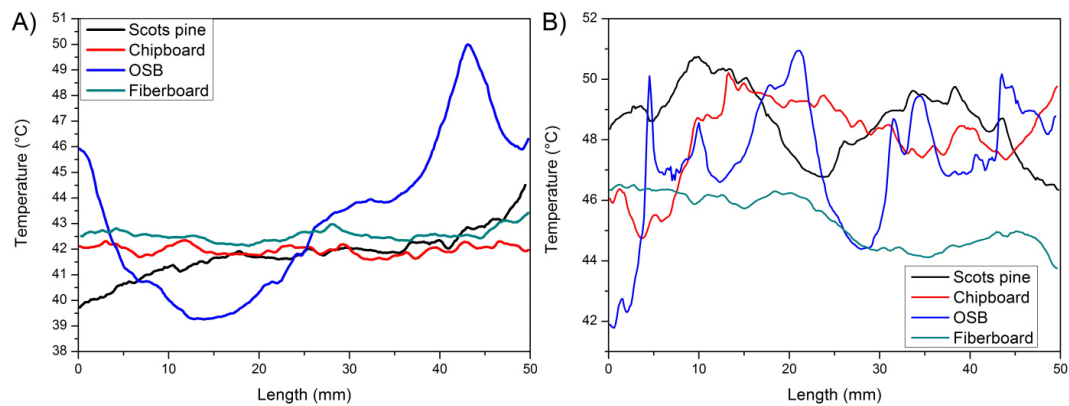


Figure S10 Longitudinal profile of temperature for A) CNT/PMMA and B) raw CNT heaters obtained from thermal camera images after 10 min Joule heating with 1 W.

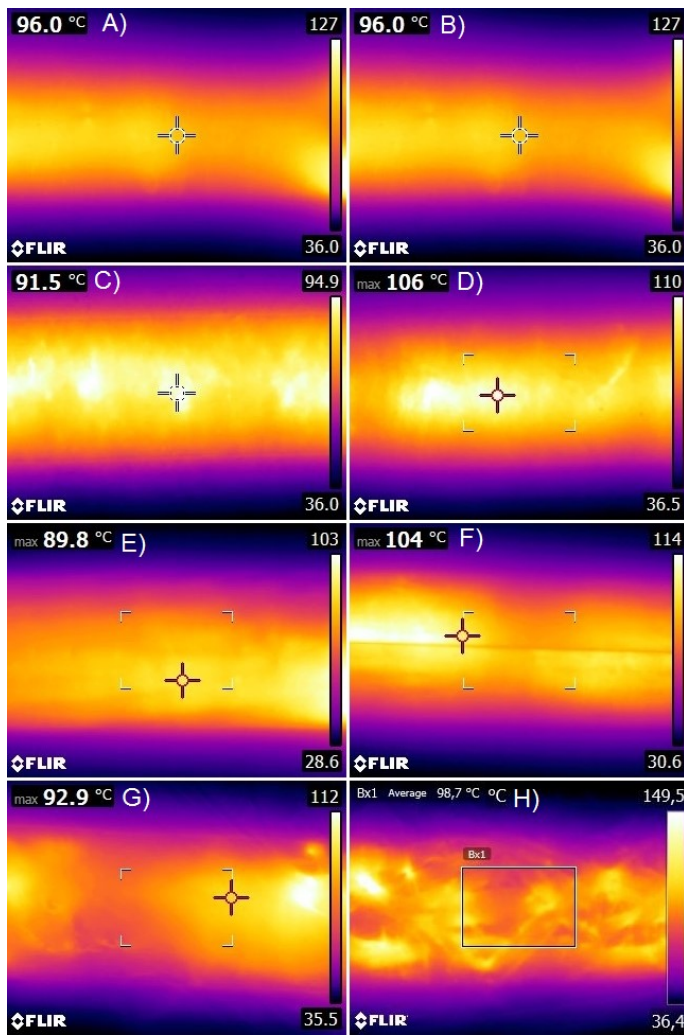


Figure S11 Thermal camera images of CNT heaters after 10 min heating with 4 W for CNT/PMMA: A) fiberboard, C) chipboard, E) Scots Pine, F) OSB and of raw CNT heaters: B) fiberboard, D) chipboard, F) Scots pine, H) OSB.

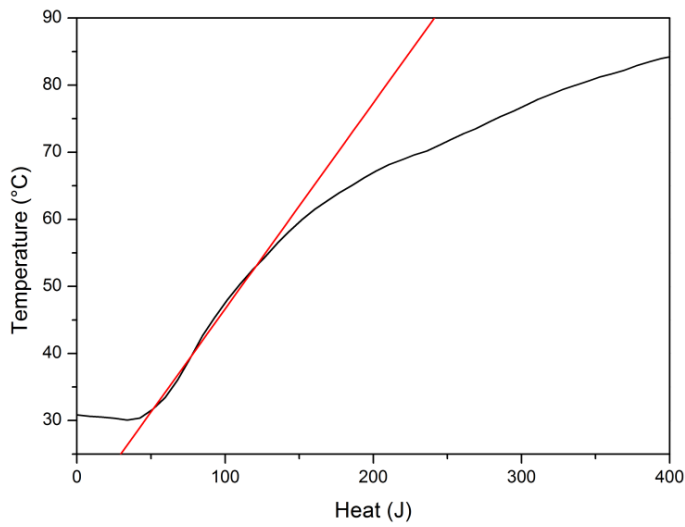


Figure S12 Heating CNT/PMMA on fiberboard using high power (9 W).

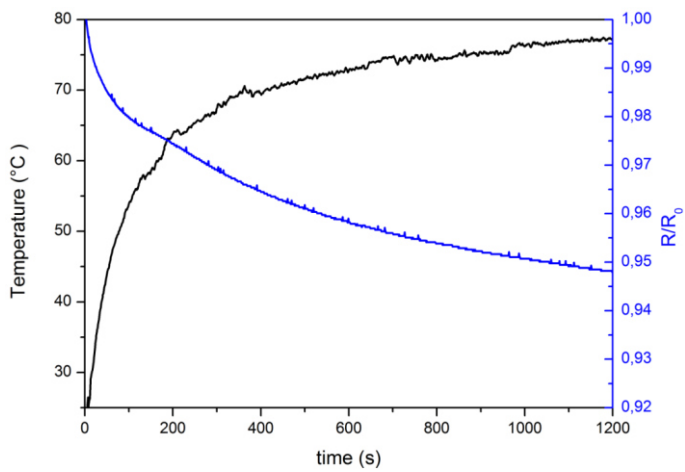


Figure S13 Temperature and resistance during 20 min heating with constant current ( $I=120$  mA,  $R_0=268$   $\Omega$ ) CNT/PMMA onto fiberboard during Joule heating

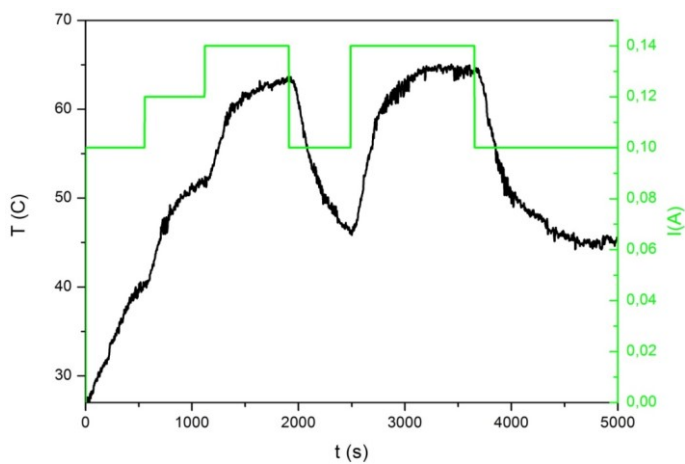


Figure S14 Electrothermal response of CNT/PMMA heater and temperature across fiberboard (7.3 mm thick) measured by pyrometer

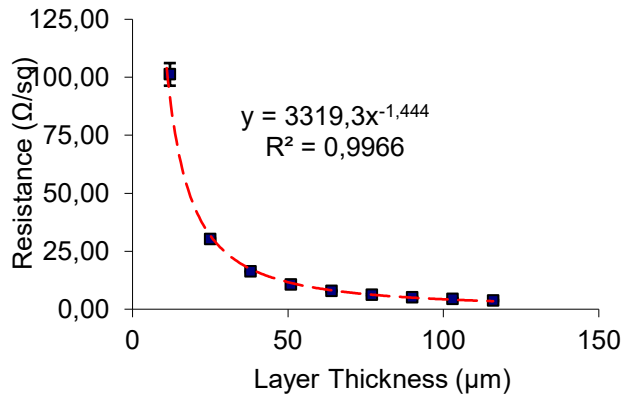


Figure S15 Sheet resistance of GNP/PMMA in function of layer thickness.